

Fine-mapping, Novel Loci Identification, and SNP Association Transferability in a
Genome-Wide Association Study of QRS Duration in African Americans

Daniel S. Evans^{1*}, Christy L. Avery², Mike A. Nalls³, Guo Li⁴, John Barnard⁵, Erin N. Smith⁶, Toshiko Tanaka⁷, Anne M. Butler², Sarah G. Buxbaum^{8,9}, Alvaro Alonso¹⁰, Dan E. Arking¹¹, Gerald S. Berenson¹², Joshua C. Bis^{4,13}, Steven Buyske¹⁴, Cara L. Carty¹⁵, Wei Chen¹⁶, Mina K. Chung^{17,18,19}, Steven R. Cummings¹, Rajat Deo²⁰, Charles B. Eaton²¹, Ervin R. Fox²², Susan R. Heckbert^{4,13,23}, Gerardo Heiss², Lucia A. Hindorf²⁴, Wen-Chi Hsueh²⁵, Aaron Isaacs^{26,27}, Yalda Jamshidi²⁸, Kathleen F. Kerr²⁹, Felix Liu³⁰, Yongmei Liu³¹, Kurt K. Lohman³¹, Jared W. Magnani³², Joseph F. Maher³³, Reena Mehra³⁴, Yan A. Meng³⁵, Solomon K. Musani³⁶, Christopher Newton-Cheh^{35,37}, Kari E. North^{2,38}, Bruce M. Psaty^{4,13,23,39}, Susan Redline⁴⁰, Jerome I. Rotter⁴¹, Renate B. Schnabel⁴², Nicholas J. Schork⁴³, Ralph V. Shohet⁴⁴, Andrew B. Singleton³, Jonathan D. Smith⁴⁵, Elsayed Z. Soliman⁴⁶, Sathanur R. Srinivasan¹⁶, Herman A. Taylor, Jr.³³, David R. Van Wagoner¹⁸, James G. Wilson⁴⁷, Taylor Young³⁵, Zhu-Ming Zhang⁴⁶, Alan B. Zonderman⁴⁸, Michele K. Evans⁴⁸, Luigi Ferrucci⁷, Sarah S. Murray⁴⁹, Gregory J. Tranah¹, Eric A. Whitsel^{2,50}, Alex P. Reiner^{4,15}, CHARGE QRS Consortium⁵¹, Nona Sotoodehnia^{13,52*}.

- ¹ California Pacific Medical Center Research Institute, San Francisco, CA, USA
- ² Department of Epidemiology, Gillings School of Global Public Health, University of North Carolina, Chapel Hill, NC, USA
- ³ Laboratory of Neurogenetics, National Institute on Aging, National Institutes of Health, Bethesda, MD, USA
- ⁴ Department of Epidemiology, University of Washington, Seattle, WA, USA
- ⁵ Department of Quantitative Health Sciences, Lerner Research Institute, Cleveland Clinic, Cleveland, OH, USA
- ⁶ Department of Pediatrics and Rady Children's Hospital, University of California at San Diego, School of Medicine, La Jolla, CA, USA
- ⁷ Translational Gerontology Branch, National Institute on Aging, National Institutes of Health, Baltimore, MD, USA
- ⁸ Jackson Heart Study, Jackson State University, Jackson, MS, USA
- ⁹ Department of Epidemiology and Biostatistics, Jackson State University School of Health Sciences, Jackson, MS, USA
- ¹⁰ Department of Epidemiology, Rollins School of Public Health, Emory University, Atlanta, GA, USA
- ¹¹ McKusick-Nathans Institute of Genetic Medicine, Johns Hopkins University School of Medicine, Baltimore, MD, USA
- ¹² Department of Medicine and Cardiology, Tulane University, New Orleans, LA, USA
- ¹³ Cardiovascular Health Research Unit, Department of Epidemiology, University of Washington, Seattle, WA, USA

¹⁴ Department of Statistics and Biostatistics and Department of Genetics, Rutgers University, Piscataway, NJ, USA

¹⁵ Division of Public Health Sciences, Fred Hutchinson Cancer Research Center, Seattle, WA, USA

¹⁶ Department of Epidemiology, Tulane University, New Orleans, LA, USA

¹⁷ Department of Cardiovascular Medicine, Heart and Vascular Institute, Cleveland Clinic, Cleveland, OH, USA

¹⁸ Department of Molecular Cardiology, Lerner Research Institute, Cleveland Clinic, Cleveland, OH, USA

¹⁹ Cleveland Clinic Lerner College of Medicine of Case Western Reserve University, Cleveland, OH, USA

²⁰ Division of Cardiovascular Medicine, University of Pennsylvania, Philadelphia, PA, USA

²¹ Departments of Family Medicine and Epidemiology, Alpert Medical School, Brown University, Providence, RI, USA

²² Department of Medicine, Division of Cardiovascular Disease, University of Mississippi Medical Center, Jackson, MS, USA

²³ Group Health Research Institute, Group Health Cooperative, Seattle, WA, USA

²⁴ National Institutes of Health, National Human Genome Research Institute, Office of Population Genomics, Bethesda, MD, USA

²⁵ Phoenix Epidemiology and Clinical Research Branch, National Institute of Diabetes and Digestive and Kidney Diseases, National Institutes of Health, Phoenix, AZ

²⁶ Genetic Epidemiology Unit, Department of Epidemiology, Erasmus University Medical Center, Rotterdam, the Netherlands

²⁷ CARIM School for Cardiovascular Diseases, Maastricht Centre for Systems Biology (MaCSBio), Dept. of Biochemistry, Maastricht University, Maastricht, the Netherlands

²⁸ Cardiogenetics Lab, Institute of Cardiovascular and Cell Sciences, St George's University of London, UK

²⁹ Department of Biostatistics, School of Public Health, University of Washington, Seattle, WA, USA

³⁰ Department of Epidemiology and Biostatistics, University of California, San Francisco, CA, USA

³¹ Department of Epidemiology and Prevention, Division of Public Health Sciences, Wake Forest University, Winston-Salem, NC, USA

³¹ Department of Epidemiology and Prevention, Division of Public Health Sciences, Wake Forest University, Winston-Salem, NC, USA

³² Department of Medicine, Division of Cardiology, University of Pittsburgh Medical Center Heart and Vascular Institute, University of Pittsburgh, Pittsburgh, PA, USA

³³ Department of Medicine, University of Mississippi Medical Center, Jackson, MS, USA

³⁴ Department of Medicine, Case Western Reserve University School of Medicine, Cleveland, OH, USA

³⁵ Program for Medical and Population Genetics, Broad Institute of Harvard and Massachusetts Institute of Technology, Cambridge, MA, USA

³⁶ Jackson Heart Study, University of Mississippi Medical Center, Jackson, MS, USA

³⁷ Cardiovascular Research Center and Center for Human Genetic Research, Massachusetts General Hospital and Harvard Medical School, Boston, MA, USA

³⁸ Carolina Center for Genome Sciences, University of North Carolina, Chapel Hill, NC, USA

- ³⁹ Departments of Medicine and Health Services, University of Washington, Seattle, WA, USA
- ⁴⁰ Department of Medicine, Division of Sleep Medicine, Brigham and Women's Hospital, Harvard Medical School, Boston, MA, USA
- ⁴¹ Institute for Translational Genomics and Population Sciences, Los Angeles Biomedical Research Institute and Departments of Medicine and Pediatrics, Harbor-UCLA Medical Center, Torrance, CA, USA
- ⁴² University Heart Center Hamburg and German Center for Cardiovascular Research, Hamburg, Germany
- ⁴³ J. Craig Venter Institute, San Diego, CA, USA
- ⁴⁴ Center for Cardiovascular Research, John A. Burns School of Medicine, University of Hawaii, Honolulu, HI, USA
- ⁴⁵ Department of Cellular and Molecular Medicine, Cleveland Clinic, Cleveland, OH, USA
- ⁴⁶ Epidemiological Cardiology Research Center (EPICARE), Department of Epidemiology and Prevention, Division of Public Health Sciences, Wake Forest School of Medicine, Winston-Salem, NC, USA
- ⁴⁷ Department of Physiology and Biophysics, University of Mississippi Medical Center, Jackson, MS, USA
- ⁴⁸ Laboratory of Epidemiology and Population Science, National Institute on Aging, National Institutes of Health, Baltimore, MD, USA
- ⁴⁹ Department of Pathology, University of California San Diego, La Jolla, CA, USA
- ⁵⁰ Department of Medicine, School of Medicine, University of North Carolina, Chapel Hill, NC, USA
- ⁵¹ Membership of the CHARGE QRS Consortium is provided in the acknowledgements

⁵² Division of Cardiology, Department of Medicine, University of Washington, Seattle, WA,
USA

The authors wish it to be known that, in their opinion, the first three authors should be regarded as joint First Authors.

* Corresponding authors

Daniel S. Evans

Mission Hall: Global Health & Clinical Sciences Building

550 16th Street, 2nd floor, Box #0560

San Francisco, CA 94158-2549

Telephone: 415-476-6090

Fax: 415-514-8150

Email: devans@psg.ucsf.edu

Nona Sotoodehnia

Metropolitan Park East Tower

1730 Minor Ave, Suite 1360

Seattle, WA 98101

Telephone: 206-221-7775

Fax: 206-221-2662

Email: nsotoo@u.washington.edu

Abstract

The electrocardiographic QRS duration, a measure of ventricular depolarization and conduction, is associated with cardiovascular mortality. While genome-wide association studies (GWAS) have identified single nucleotide polymorphisms (SNPs) associated with QRS duration at 22 loci among those of European descent, the genetic architecture of QRS duration in non-European populations is largely unknown. We therefore performed a GWAS meta-analysis of QRS duration in 13,031 African Americans from ten cohorts and a transethnic GWAS meta-analysis with additional results from populations of European descent. In the African American GWAS, a single genome-wide significant SNP association was identified (rs3922844, $P=4 \times 10^{-14}$) in intron 16 of *SCN5A*, a voltage-gated cardiac sodium channel gene. The QRS-prolonging rs3922844 C allele was also associated with decreased *SCN5A* RNA expression in human atrial tissue ($P=1.1 \times 10^{-4}$). High density genotyping revealed that the *SCN5A* association region in African Americans was confined to intron 16. Transethnic GWAS meta-analysis identified novel SNP associations on chromosome 18 in *MYL12A* (rs1662342, $P=4.9 \times 10^{-8}$) and chromosome 1 near *CDIE* and *SPTAI1* (rs7547997, $P=7.9 \times 10^{-9}$). The 22 QRS loci previously identified in populations of European descent were enriched for significant SNP associations with QRS duration in African Americans ($P=9.9 \times 10^{-7}$), and index SNP associations in or near *SCN5A*, *SCN10A*, *CDKN1A*, *NFIA*, *HAND1*, *TBX5*, and *SETBP1* replicated in African Americans. In summary, rs3922844 was associated with QRS duration and *SCN5A* expression, two novel QRS loci were identified using transethnic meta-analysis, and a significant proportion of QRS-SNP associations discovered in populations of European descent were transferable to African Americans when adequate power was achieved.

Introduction

The QRS duration, measured by the surface electrocardiogram (ECG), reflects depolarization and conduction of the electrical signal throughout the ventricular myocardium. Longer QRS duration is associated with an increased risk of cardiovascular (CV) mortality in Caucasians and all-cause mortality in African Americans from study populations unselected for specific CV disorders (1, 2). Among patients hospitalized for heart failure with reduced left ventricular ejection fraction, prolonged QRS duration (≥ 120 milliseconds) is associated with post-discharge all-cause mortality (3). The QRS duration has been reported to be shorter in African Americans compared to Caucasians, even after taking into account cardiovascular risk factors and coronary heart disease (4-6).

Prior genome-wide association studies (GWAS) of QRS duration performed in populations of European descent have identified 22 independent QRS loci (7, 8). The genetic architecture of QRS duration among African Americans, by contrast, is largely unknown. Expanding GWAS to populations of African descent holds the potential to refine association regions due to shorter-range linkage disequilibrium (LD) and to discover novel genetic associations given the presence of population-specific allele frequencies (9, 10). We therefore performed a GWAS meta-analysis of QRS duration in a total of 13,031 African Americans from 10 cohort studies in order to: (1) fine-map the QRS association regions previously identified among those of European descent; (2) discover novel QRS loci through a meta-analysis of results from African American cohorts as well as a transethnic meta-analysis; (3) determine whether SNP associations with QRS duration discovered in populations of European descent are transferable to African Americans.

Results

GWAS meta-analysis of QRS duration in African Americans

We conducted a meta-analysis of 2,955,816 autosomal SNPs in 13,031 African Americans from 10 GWAS of QRS duration (S1 and S2 Tables), with little evidence of genomic inflation in the individual cohorts (S1-S10 Figs. and S1 Table) or the meta-analysis (S11 Fig., $\lambda = 1.027$). European genetic ancestry percentage was similar across the cohorts (S2 Table) and was not significantly associated with QRS duration (S3 Table).

A single SNP, rs3922844 (MAF = 0.42), in intron 16 of the cardiac sodium channel gene *SCN5A*, was associated with QRS duration among African Americans at the genome-wide significance threshold ($\beta \pm SE = 0.94 \text{ ms} \pm 0.12 \text{ ms}$, $P = 4 \times 10^{-14}$) (Table 1, Fig. 1 and S12 Fig.). Adjustment for local ancestry minimally altered the association (Table 1). We fine-mapped the *SCN5A-SCN10A* region surrounding this signal by examining SNPs genotyped using the MetaboChip array in ARIC and WHI PAGE participants and imputed in the WHI SHARE participants (11). In the meta-analysis of the three cohorts, a second SNP in intron 16 of *SCN5A*, rs12635898, was in high LD with rs3922844 (HapMap YRI: $r^2 = 0.93$, Table 2) and was similarly associated with QRS duration (Table 2). Furthermore, LD was low (1000 Genomes AFR population $r^2 = 0.03$) between rs3922844 and rs7626962, an *SCN5A* missense mutation (S1103Y) associated with cardiac conduction and arrhythmias that is common in African Americans but rare in populations of European descent (12-15).

While the most significant SNP associations reported from previous GWAS of QRS interval among other ethnic groups are similarly located on chromosome 3 at the *SCN5A* / *SCN10A* locus, the SNP association region is broad, spanning approximately 300 kb, and

multiple independent signals have been identified (Fig. 1) (7, 8, 16). By contrast, the genome-wide association among African Americans points to a single SNP (Fig. 1). The rs3922844-QRS association discovered in African American cohorts replicated in cohorts of European ancestry ($P = 2 \times 10^{-13}$) (Table 4), but this variant was not in high LD with other *SCN5A* or *SCN10A* index SNPs among European ancestry individuals (Table 4).

SNP functional annotation and association with *SCN5A* expression in human cardiac tissue

Functional annotation indicated that rs3922844 and variants in LD (1000 Genomes AFR population $r^2 \geq 0.2$) overlapped and were near regulatory genomic features. These variants altered transcription factor binding motifs and overlapped with DNase I hypersensitive sites (DHS) (S4 Table). In multiple cell types, rs3922844 was located near a cluster of transcription factor binding events and a peak of Histone H3 Lysine 4 mono-methylation, a marker of putative enhancers (S13 Fig.). Rs3922844 and variants in LD overlapped with DHS and enhancer histone marks in fetal heart tissue based on data from the Roadmap Epigenomics Mapping Consortium (S4 Table and S14 Fig.).

We next assessed the functional relevance of rs3922844 by examining its association with *SCN5A* RNA expression levels in human cardiac tissue. The rs3922844 C allele associated with longer QRS duration was also associated with lower *SCN5A* RNA expression in left atrial appendage samples from 289 individuals of European ancestry ($\beta \pm SE$ (units are RNA levels on \log_2 scale) = -0.11 ± 0.03 , $P = 1.6 \times 10^{-3}$) and 40 individuals of African ancestry ($\beta \pm SE = -0.29 \pm 0.11$, $P = 0.013$), as well as in the meta-analysis across the two ethnic groups ($\beta \pm SE = -0.13 \pm 0.03$, $P = 1.1 \times 10^{-4}$, Fig. 2).

Transethnic meta-analysis of QRS duration

QRS duration GWAS results from 13,031 African Americans (reported above) and from 40,407 European-ancestry individuals in the previously reported CHARGE analysis (8) were meta-analyzed, with little evidence of genomic inflation ($\lambda = 1.018$, S15 Fig.). In addition to the previously identified QRS loci (S16 Fig., S5 Table), the transethnic meta-analysis identified SNPs at two novel loci associated with cardiac ventricular conduction: an intronic SNP (rs1662342, $P = 4.9 \times 10^{-8}$) in a myosin light chain regulatory gene, *MYL12A*, on chromosome 18, and an intergenic SNP (rs7547997, $P = 7.9 \times 10^{-9}$) near *CDIE* on chromosome 1 (Table 3, Figs. 3 and 4). For both SNPs, the coded allele frequency was higher in African Americans than individuals of European ancestry (Table 3), indicating that the addition of African American participants may have provided greater gains in power for these two SNPs than the addition of an equivalent number of individuals of European ancestry.

We examined whether rs1662342 or rs7547997 were eQTLs in human left atrial appendage tissue. While the rs1662342 A allele was nominally associated with higher *MYL12A* RNA levels in the meta-analysis of results from 289 individuals of European ancestry and 40 individuals of African ancestry ($\beta \pm SE = 0.08 \pm 0.04$, $P = 0.03$), the association was not significant after correction for multiple testing. Gene expression for only two genes (*CDIC* and *CDIE*) was detected within 250 kb upstream and downstream of rs7547997, and this SNP was not significantly associated with expression of either of these genes ($P > 0.05$).

Gene set enrichment and transferability of QRS-associated loci and SNPs

A gene set enrichment analysis (GSEA) revealed that genes identified from the 22 European-descent QRS loci were enriched for significant SNP associations in the African American QRS meta-analysis results, suggesting the transferability of QRS associations at the gene-set level between the two population groups. Gene-based P-values for 9 of the 22 QRS loci were in the top 95th percentile of all gene scores genome-wide in African Americans, whereas only one would be expected by chance, and the 22 QRS loci were significantly enriched for significant QRS-SNP associations in African Americans compared with randomly sampled gene sets (GSEA empirical $P = 9.9 \times 10^{-7}$). Importantly, the direction of the association was the same for all index SNPs at the 22 previously identified QRS loci in both ethnic groups, further supporting the transferability of associations between those of European and African ancestry (Tables 4 and 5, S6 Table).

SNP association transferability at *SCN5A/SCN10A* locus

The most significant SNP associations reported from previous GWAS of QRS interval among other ethnic groups are similarly located on chromosome 3 at the *SCN5A/SCN10A* locus, and multiple independent signals have been identified (Fig. 1) (7, 8, 16). The coded allele frequencies for all *SCN5A/SCN10A* European-ancestry index SNPs were lower among African Americans than individuals of European ancestry, which along with the smaller sample size among the African Americans we examined, reduces power to replicate (Table 4). Of the 4 independent European descent QRS index SNPs with adequate power ($\geq 80\%$) to replicate among African Americans, 2 were significant, including the top SNP-QRS association among individuals of European ancestry, rs6801957 ($P = 8 \times 10^{-4}$ among African Americans, Table 4).

The absence of genome-wide significant QRS associations among SNPs within *SCN10A* in African Americans does not appear to be due to a difference in the MAF distribution of *SCN10A* SNPs between populations of European and African descent (S7 Table). Compared to populations of European descent (S17 Fig.), LD was reduced and haplotypes were shorter in the *SCN10A* region in populations of African descent (S18 and S19 Figs.), which could impact the ability for assayed SNPs to tag potential non-genotyped causal variants.

SNP association transferability at the remaining known QRS loci

At the remaining 21 QRS loci (7, 8), there was adequate power ($\geq 80\%$) to replicate European-ancestry index SNPs at 8 loci, and index SNPs at 4 of these 8 loci replicated in African Americans at the multiple-testing corrected significance threshold of $P = 0.002$ (*CDKN1A*, *NF1A*, *HAND1*, and *TBX5*, Table 5, binomial test $P = 4 \times 10^{-4}$). Of the 13 loci where there was not adequate power to replicate, a European-ancestry index SNP at one locus replicated in African Americans (*SETBP1*, S6 Table). At the more liberal replication significance threshold of 0.05, European-ancestry index SNPs at 5 of the 8 loci with adequate power replicated (binomial test $P = 2 \times 10^{-5}$), and index SNPs at 7 of the 13 loci without adequate power replicated (binomial test $P = 1 \times 10^{-6}$) (Table 5 and S6 Table).

We next expanded our characterization of each of the 22 European-ancestry QRS loci to identify the most significant SNP association with QRS duration among African Americans (African-American index SNPs) and to determine the LD between European and African-ancestry index SNPs. Other than *SCN5A*, two other loci (*TBX5* and *NF1A*) contained African-ancestry index SNPs that passed the significance threshold for discovery ($P \leq 1.4 \times 10^{-5}$) within

the 22 QRS loci (Table 5). The African-ancestry index SNP associations in *TBX5* (rs7312625) and *NFIA* (rs2207791) replicated at the genome-wide significance level in populations of European descent (Table 5). For both loci, our results did not provide evidence for allelic heterogeneity, as the African-ancestry index SNPs were in moderate LD with the European-ancestry index SNPs (HapMap ASW $r^2 \geq 0.65$, HapMap CEU $r^2 \geq 0.5$) (Table 5, S20 and S21 Figs.).

Fine-mapping intervals based on Bayes factors and the resulting posterior probabilities generated from a transethnic meta-analysis with MANTRA (17) were constructed at the 22 QRS loci previously identified in populations of European descent and the two new QRS loci reported here. At each locus, the 95% credible set (CS) defines the genomic boundary that contains the smallest set of SNPs accounting for 95% of the posterior probability (S8 Table). Other than the loci at which the 95% CS contained a single SNP, the largest percentage decrease from the genome-wide significant interval discovered in European populations to the 95% CS in the transethnic meta-analysis was at the *TBX5* locus (S20 Fig.).

Discussion

Our genetic association study of cardiac ventricular conduction among African Americans identified variants in a putative transcriptional regulatory region within intron 16 of the cardiac sodium channel *SCN5A* that were associated with QRS duration and *SCN5A* RNA levels. Furthermore, two novel loci associated with cardiac ventricular depolarization and conduction were identified through a transethnic GWAS meta-analysis. Finally, our study demonstrated the transferability of QRS-SNP associations between populations of European and African-descent by both gene-set enrichment analysis as well as direct evaluation of top QRS-SNP associations.

Our GWAS meta-analysis with additional fine-mapping identified two SNPs in high LD (rs3922844 and rs12635898, HapMap YRI: $r^2 = 0.93$) in intron 16 of the cardiac sodium channel *SCN5A* gene associated with QRS duration among African Americans. *SCN5A* encodes the pore-forming α subunit of the cardiac voltage-gated sodium channel $Na_v1.5$, and opening of the $Na_v1.5$ channel drives rapid membrane depolarization during the cardiac action potential (18). Common and rare *SCN5A* genetic variants have been associated with cardiac depolarization, conduction, and repolarization (7, 8, 19). The most significantly associated SNP identified in this study (rs3922844) has been previously shown to associate with atrioventricular conduction (PR interval) among African Americans that included a subset of the same cohorts as this study (20, 21), similar to other SNPs at this locus where variants that prolong PR interval also prolong QRS duration.

Functional annotation indicated that rs3922844 and other intronic variants in LD overlapped with a putative intronic transcriptional regulatory region. While functional intronic enhancers have not been identified in *SCN5A*, transcriptional enhancers are commonly found

within intronic regions (22). Consistent with rs3922844's overlap with putative transcriptional regulatory features, we found that rs3922844 was associated with *SCN5A* expression in human atrial tissue. The rs3922844 C allele associated with longer QRS duration was also associated with lower *SCN5A* RNA expression in human cardiac tissue, supporting the hypothesis that fewer available Na_v1.5 channels would lead to subtly slower depolarization and conduction in cardiac tissue. It is intriguing that both genome-wide significant SNPs were located within intron 16 of *SCN5A*, which is immediately adjacent to an alternative splicing event that skips exons 17 and 18, resulting in the production of the non-functional Na_v1.5b isoform that contains a partial deletion of the sixth transmembrane spanning segment of the DII domain and a deletion of a large segment of the intracellular DII-DIII linker (18). While the array-based expression data in our eQTL study did not enable our examination of specific transcript isoforms, future studies could investigate this potential molecular consequence that could lead to an increased production of non-functional transcripts that would further reduce the number of functional Na_v1.5 voltage-gated sodium channels.

Using a transethnic meta-analysis approach, two novel QRS loci were identified: one in the gene *MYL12A* on chromosome 18 (rs1662342) and one in an intergenic region on chromosome one (rs7547997) near a cluster of five *CDI* genes. For both SNPs, the higher allele frequency in African Americans combined with the 13,031 additional sample size increased power to find associations in the transethnic meta-analysis.

While the association between intronic SNP rs1662342 and *MYL12A* gene expression did not pass multiple test correction, the nominal significance of the association provided suggestive evidence that rs1662342 could be associated with *MYL12A* gene expression. *MYL12A* encodes the myosin regulatory light chain that binds to a variety of myosin heavy chain IIs (MHC IIs) in

multiple cell types (23). *MYL12A* is expressed in the heart and cardiac myocytes in humans (24). Knockdown of *MYL12A* in mouse fibroblasts resulted in a significant reduction in cellular contractility, a disruption of cellular structure and morphology, and a decrease in non-muscle MHC II expression (23). The most significant SNP associations with RR interval in populations of European descent were located in *MYH6*, the α -heavy chain subunit of cardiac myosin (7, 25), and the associations replicated in African Americans (26). Our results suggest that genetic variation in a different component of myosin, myosin regulatory light chain, may play a role in QRS duration.

The candidate gene for the second novel QRS locus is not as obvious, as rs7547997 was not associated with gene expression of nearby genes in our eQTL study. SNP rs7547997 is located within an intergenic region on chromosome one near a cluster of five *CDI* genes, which mediate lipid and glycolipid antigen presentation to T cells (27) and near a cluster of 15 olfactory receptor genes (28). *SPTAI1*, which encodes α -spectrin, is located 240 kb from rs7547997, but measures of *SPTAI1* RNA did not pass quality filters in our eQTL study and rs7547997's association with *SPTAI1* gene expression could not be determined. Spectrin, a tetramer composed of α - β dimers, acts as an actin crosslinking and molecular scaffold protein that regulates cell shape and membrane protein localization (29). Spectrin binds ankyrin-G, and ankyrin-G is required for $\text{Na}_v1.5$ membrane targeting and excitability (29). The E1053K *SCN5A* variant disrupts the ankyrin-G/ $\text{Na}_v1.5$ binding interaction and results in Brugada Syndrome (30). In mouse cardiomyocytes, β -spectrin co-localizes with ankyrin-G and $\text{Na}_v1.5$ (31). β -spectrin also targets CaMKII to $\text{Na}_v1.5$ where CaMKII regulates $\text{Na}_v1.5$ by phosphorylation (31). While *SPTAI1* might be an attractive candidate gene, further studies are needed to identify causal gene(s) and variant(s) in the novel QRS association region identified on chromosome one.

Our transethnic meta-analysis results provide evidence that a large proportion of SNP and loci associations with QRS duration are shared between populations of European and African descent. Gene-set enrichment analysis revealed that the 22 previously reported European-descent QRS-associated loci were enriched for significant QRS-SNP associations among African Americans compared with randomly selected gene sets matched for gene set characteristics such as gene size and LD properties, which provided evidence for replication at the gene-set level. Where the power for replication was adequate, half of the European-descent index SNPs were also associated with QRS duration among African Americans. Even among the SNPs where power was inadequate, the majority were at least nominally associated with QRS duration among African Americans. Furthermore, the direction of association for all European-ancestry index SNPs was the same in both ethnic groups. While these results taken together provide evidence for the transferability of QRS genetic associations from one ethnic group to another, there are some exceptions. There are SNPs associated with QRS duration among those of European descent, for instance rs9851724 near *SCN10A* (Table 4) and rs4687718 in *TKT* (Table 5), where despite adequate power, no evidence for association was identified among African Americans.

In addition to replication sample size and population-specific allele frequencies, SNP associations could fail to replicate across continental ancestry groups for several reasons, including: (1) population-specific causal variants, (2) population-specific LD between assayed SNPs and causal variants, and (3) interactions between SNPs and population-specific non-genetic factors (9, 32). In a systematic survey of SNPs identified through GWAS (GWAS SNPs), the allele frequency and LD with nearby SNPs differed significantly between population groups for a number of GWAS SNPs, suggesting that at least some GWAS SNPs identified in European populations might not generalize to other populations (10). In addition, it has been

posited that rare variants, which are more likely to be population-specific (33-36), can create synthetic associations with common variants identified in GWAS, which would result in the lack of transferability of GWAS findings across populations (37). Others have argued that synthetic associations might exist, but they are unlikely to account for most GWAS results (38, 39). While a direct test of the synthetic association hypothesis requires a comprehensive collection of rare and common variants, our GWAS in African Americans provides an opportunity to test a prediction from the synthetic association hypothesis that SNP associations would not generalize across populations.

Well-powered studies for a limited number of traits and diseases have provided evidence that a majority of GWAS SNPs discovered in populations of European descent generalize to multiple populations (40-43). For instance, a high proportion of SNP associations with blood lipids discovered in populations of European descent generalized to populations of non-European descent (44, 45), but allelic heterogeneity was observed at some loci (45, 46). A recent systematic examination of GWAS SNP replication across populations found that 45.8% of GWAS SNPs initially identified in populations of European descent replicated in East Asian populations, and the percentage increased to 76.5% when replication attempts were limited to those that achieved sufficient power (47). The same study found that only 7 of 73 (9.6%) SNP associations replicated in populations of African descent, and the replication percentage only increased to 20% among the 25 replication attempts that achieved sufficient power (47). In an analysis of five traits and diseases in the Population Architecture Using Genomics and Epidemiology (PAGE) study, a consortium of multi-ancestry population-based studies, a significant proportion of GWAS SNPs discovered in European populations replicated in populations of non-European descent (43). However, the effect estimates in non-European

populations tended to be closer to the null, especially in African Americans (43). Our analysis of SNP associations with QRS duration is consistent with findings from other traits; namely, SNP associations generalize at most loci but not all. GWAS of ECG traits other than QRS duration have been conducted in African Americans, and SNP association transferability has been found (13, 20, 21, 26, 48, 49). In two large meta-analyses, the proportion of SNP associations that replicated in African Americans was 7 of 13 for RR interval and 10 of 22 for QT interval at $\alpha = 0.05$ (26, 48). While Dickson et al. predicted that synthetic associations would be inconsistent across populations (37), results from our study and others indicate that a majority of SNP associations do generalize across populations. Continuing to perform well-powered GWAS in African Americans should reveal whether SNP associations for a variety of traits and conditions are transferable.

In conclusion, by conducting a GWAS meta-analysis of QRS duration in African Americans, we refined the *SCN5A* association region to a single intron, and the associated SNP rs3922844 was also associated with reduced *SCN5A* expression in human atrial tissue in individuals of African and European ancestry. Two novel genome-wide significant SNP associations in or near intriguing candidate genes (*MYL12A* and *SPTAI1*) were identified using transethnic meta-analysis. In addition, the high proportion of QRS associations that were transferable between populations of European and African-descent indicated that, at many of the associated loci, common genetic variation shared across populations contributes to QRS duration.

Materials and Methods

Study samples and ECG recordings

The following ten cohorts with African American participants contributed to this study (in order of decreasing sample size): the Women's Health Initiative (WHI), the Atherosclerosis Risk in Communities (ARIC) study, the Jackson Heart Study (JHS), the Multi-Ethnic Study of Atherosclerosis (MESA), the Health, Aging, and Body Composition Study (Health ABC), the Healthy Aging in Neighborhoods of Diversity across the Life Span study (HANDLS), the Cardiovascular Health Study (CHS), the Cleveland Family Study (CFS), the Baltimore Longitudinal Study on Aging (BLSA) study, and the Bogalusa Heart Study (BHS). Detailed descriptions of the study samples and ECG recording methods are provided in S1 Text. The European-descent participants and cohorts that contributed to this analysis have been previously described (8). The study was approved by the Institutional Review Board at all participating institutions. All individuals included in this analysis provided written informed consent.

Genotyping and genotype imputation

Cohorts used Affymetrix or Illumina SNP genotyping arrays and applied quality control filters to samples and SNPs (S1 Table). Participants unlikely to be of African descent based on principal component analysis were excluded from the analysis (S1 text). Genotype imputation was performed using MACH or Beagle software. Individual studies performed genotype imputation using reference haplotypes that consisted of either a mixture of phased haplotype data from HapMap 2 YRI and CEU in a 1:1 ratio or a combination of HapMap 2 YRI and CEU in a 1:1 ratio and HapMap 3 YRI, CEU, and ASW in a 1:1:1 ratio (S1 Table). Detailed descriptions

of genotyping methods, quality control steps, and imputation methods can be found in S1 Text and S1 Table.

Genome-wide association analysis among African Americans

Study participants were excluded from analysis based on the following criteria: missing covariates, younger than 18 years of age, atrial fibrillation on the ECG, history of heart failure or myocardial infarction, QRS duration ≥ 120 ms, Wolff-Parkinson-White pattern, pacemaker or defibrillator implant, or use of class I and III antiarrhythmic medications. Genetic association analysis was performed in each cohort using linear regression models with the following covariates: age, sex, study site (if multiple sites were present), BMI, height, and principal components derived from principal component analysis (PCA) of genotype data (50) (S1 Text). The exclusion criteria and covariate adjustment we applied were the same as those applied in a previous GWAS of QRS duration in populations of European descent (8), which facilitated comparisons of results between the two studies. In addition to adjustment for global genetic ancestry estimates, the genome-wide significant SNP association was additionally adjusted for local genetic ancestry estimates (see below for local ancestry estimation details). GWAS in ARIC, JHS, MESA, and CFS were performed as part of the Candidate gene Association Resource (CARE) using QRS standardized residuals adjusted for the covariates mentioned above (51, 52). All cohorts except for CFS performed GWAS using PLINK, R, MACH2QTL, or Merlin (S1 Table and S1 Text). The family-based CFS study performed GWAS using linear mixed models to account for relatedness (52, 53). A subcohort of JHS was family-based, but previous analyses determined that the use of methods accounting for family structure had

minimal influence on effect estimates, so linear regression was used as in previous studies (52). Imputed allele dosages were modeled with an additive mode of inheritance. When available, results from directly genotyped SNP data were used in preference over those from imputed SNP data. Detailed descriptions of cohort-specific GWAS analytic methods can be found in S1 Text.

Prior to meta-analysis, GWAS results from each cohort were filtered to remove SNPs with minor allele frequency (MAF) < 0.01 or imputation quality scores < 0.3. Effect estimates and their standard errors estimated from cohorts that used QRS standardized residuals as the phenotype (ARIC, JHS, MESA, and CFS) were transformed back to units of milliseconds by multiplying by the study-specific standard deviation of the residuals. Cohort-specific GWAS results were combined using fixed effect meta-analysis with inverse variance weights as implemented in METAL (54). SNPs that were non-autosomal or were only present in a single study were excluded from analysis. Genomic control was applied to the results from each cohort prior to meta-analysis and to the results of the meta-analysis (double GC-correction) (S1 Table) (55). To maintain an experiment-wide type I error rate of 0.05, a genome-wide significance threshold of 2.5×10^{-8} was pre-specified based on a Bonferroni correction for the 2 million independent common variants estimated to exist in genomes of individuals of African ancestry (56). Heterogeneity across samples was assessed using Cochran's X^2 test of heterogeneity with 9 degrees of freedom (57) and the I^2 statistic (58). A transethnic GWAS meta-analysis of QRS duration was performed using fixed-effect inverse variance weighted meta-analysis to combine the double GC-corrected African American GWAS meta-analysis results with the double GC-corrected European ancestry CHARGE GWAS meta-analysis results (8).

Global and local genetic ancestry was estimated in ARIC, JHS, MESA, and CFS cohorts using ANCESTRYMAP (59) and HAPMIX (60) as previously described (52). For the WHI

cohort, global ancestry was estimated using Frappe (61) and local ancestry was estimated using SABRE (62). For the HANDLS and Health ABC cohorts, STRUCTURE (63) was used to estimate global ancestry, as previously described for the Health ABC cohort (64), and LAMP (65) was used to estimate local ancestry. Additional details of global and local ancestry estimation can be found in S1 Text. Linear regression was used to estimate the association between global genetic ancestry estimates and QRS duration.

Variant annotation was performed using HaploReg (66), which leveraged data from the 1000 Genomes Project (36), ENCODE (67), and the Roadmap Epigenomics Mapping Consortium (68).

Genome-wide SNP results from the GWAS in African Americans and the transethnic GWAS will be made available through the dbGaP CHARGE summary results site under dbGaP accession phs000930.

Gene set enrichment analysis

A gene set enrichment analysis (GSEA) was performed using MAGENTA version 2.4 (69) on the QC-filtered double GC-corrected African American GWAS meta-analysis results. Briefly, MAGENTA assigns a gene score based on the most significant SNP association in the gene region, corrects for potential gene score confounders (e.g., gene size and number of independent SNPs), and determines the proportion of gene scores in the gene set above a specified percentile cut-off (i.e., the leading edge fraction). The construction of gene scores from the minimum QRS-SNP association P-value for each gene region enabled a gene score to be significant in the presence of allelic heterogeneity, i.e., different SNPs that are the most

significantly associated with QRS duration at each locus in populations of European and African descent. Significance of the gene set's leading edge fraction was determined using an empirical null distribution of 10,000 leading edge fractions from randomly sampled gene sets matched to the user-defined gene set by gene score confounder characteristics. To enable MAGENTA to calculate the number of SNPs per gene for populations of African descent, we generated a genome-wide list of SNP positions after SNPs in high LD (pairwise genotypic correlation $r^2 \geq 0.8$) were removed by applying PLINK's LD pruning function to HapMap phase 2 YRI genotype data using sliding windows of 50 SNPs moving by 5 SNP increments (70).

The candidate gene set was created using the gene closest to the index SNP from the GWAS of QRS duration previously conducted by the CHARGE consortium (8), the largest GWAS of QRS duration, and included: *SCN5A*, *SCN10A*, *CDKN1A*, *PLN*, *NFIA*, *HAND1*, *TBX20*, *SIPA1L1*, *TBX5*, *TBX3*, *VTG1A*, *SETBP1*, *STRN*, *TKT*, *CRIM1*, *CDKN2C*, *PRKCA*, *IGFBP3*, *CASQ2*, *KLF12*, *LRIG1*, *DKK1*, and *GOSR2*. *SCN5A* and *SCN10A* were individually included in our gene set because the previously published CHARGE GWAS of QRS duration determined that SNP associations in these adjacent genes were independent (8).

Locus-specific replication and regional association analysis

The 30 European ancestry index SNPs (EA index SNPs) from the 22 previously reported EA QRS loci that were examined for replication in African Americans were 3 *SCN10A* SNPs, 3 *SCN5A* SNPs, 1 *EXOG* SNP, 2 *CDKN1A* SNPs, 2 *TBX5* SNPs, and a single SNP from each of the other 19 previously reported loci (7, 8, 16). To account for the 30 examined SNPs, a significance threshold of 0.002 was adopted. The following parameters were used in power

calculations for the 30 SNP replication analysis: $\alpha = 0.002$, African American sample size = 13,031, African American QRS duration mean \pm SD = 89.23 ± 9.70 ms (weighted average and pooled SD across the 10 COGENT/CARE cohorts), the previously reported SNP effect size, and the SNP coded allele frequency in populations of African descent (weighted average across the 10 COGENT/CARE cohorts).

In the analysis of the genomic region surrounding each of the European-ancestry index SNPs, each region was defined as the genomic interval encompassing all SNPs with QRS association P-values $\leq 5 \times 10^{-8}$ from the largest GWAS meta-analysis conducted in individuals of European ancestry (8), and then extending the genomic interval boundaries by 100 kb in both directions. To set the significance threshold, the number of independent SNPs in these 22 regions was determined from HapMap phase 2 YRI SNP genotype data using the same LD pruning procedure that was described for our GSEA method. For the 22 previously reported QRS loci, 3,526 independent SNPs were identified and a Bonferroni-based significance threshold of 1.4×10^{-5} was adopted.

At each of the 22 previously identified QRS loci, the most significant SNP association in African Americans (AA index SNP) was also examined in GWAS results from populations of European descent (8). Power to replicate African-ancestry index SNP associations in populations of European descent was calculated using the following parameters: $\alpha = 0.002$, sample size of individuals with European ancestry = 40,407, QRS duration mean \pm SD from individuals of European ancestry = 88.32 ± 10.13 ms (estimated from 2,845 CHS subjects of European ancestry after application of exclusion factors described above), African-ancestry index SNP effect size, and the previously reported SNP coded allele frequency in populations of European descent (8). All power calculations were performed using QUANTO (71).

Regional association plots were created using LocusZoom (72), customized to separately plot recombination rates estimated from African Americans (73) and HapMap CEU individuals. For S17-S19 Figs., LD plots were created using Haploview and LD blocks were estimated using 95% confidence bounds on D prime (74, 75).

95% credible set construction

Regions used to construct credible sets (CS) at the 22 QRS loci discovered in populations of European descent were defined as genomic intervals encompassing all SNPs with QRS association P-values $\leq 5 \times 10^{-8}$ reported by Sotoodehnia et al. (8), and then extending those genomic intervals by 100 kb in both directions. At the two new QRS loci reported here, intervals 100 kb upstream and downstream of the transethnic index SNP were used as regions for CS construction. Transethnic meta-analysis of fixed-effects meta-analysis results from populations of European descent (8) and African Americans was performed using MANTRA (17). As previously described (76) and in the context of a transethnic meta-analysis (77), for n SNPs in a region, a Bayes factor (BF_i) was estimated for each SNP $_i$ using MANTRA, and the posterior probability for SNP $_i$ is equal to

$$\frac{BF_i}{\sum_{i=1}^n BF_i}$$

SNPs with high posterior probabilities are more likely to be associated with a trait than SNPs with low posterior probabilities. SNPs at each region were ranked by their posterior probabilities in decreasing order, and the 95% CS consisted of the smallest set of ranked SNPs for which the

cumulative sum of their posterior probabilities reached 0.95. The genomic interval of a 95% CS was the range of the positions of the SNPs in the CS.

MetaboChip analysis of *SCN5A-SCN10A* gene region

To more comprehensively evaluate genetic variation in the *SCN5A-SCN10A* genomic region, we examined SNP associations using the MetaboChip, a high-density custom Illumina iSelect array that includes SNPs from the 1000 Genomes Project (11, 78). In the *SCN5A-SCN10A* region (NCBI build 36 positions 38,490,026 - 38,818,967), 654 MetaboChip SNPs were directly genotyped and passed QC filters (SNP and sample call rate > 90%, concordance among blind duplicates > 98%, HWE P-value > 0.001, MAF > 0.01) in ARIC and WHI-PAGE participants. MetaboChip SNPs were imputed in WHI-SHARE participants using genome-wide genotype data (Affymetrix 6.0 SNP array), as previously described (79).

Gene expression analysis in human atrial tissue

Human left atrial appendage and pulmonary vein trimming tissues were obtained with written informed consent from 289 European-ancestry and 40 African-ancestry patients undergoing cardiac surgery. Use of discarded surgical tissue was approved by the Institutional Review Board of the Cleveland Clinic. Total RNA was extracted using TRIzol. Genome-wide RNA levels were measured using Illumina HT12 v.3 and v.4 expression arrays. RNA expression levels were background corrected, log₂-transformed, quantile normalized, and batch adjusted. Genome-wide SNPs were genotyped in these subjects using Illumina Hap550 and Hap610

arrays, and multidimensional scaling (MDS) was performed. SNP association with RNA levels was determined separately for each racial group using linear regression with SNPs coded as dosages and additive adjustment for sex, tissue location, MDS dimensions, and surrogate variables, which were included to reduce expression heterogeneity and improve power to detect eQTLs (80). Effect estimates were expressed on the \log_2 -transformed RNA scale. Analysis was performed using expression probes detected in at least 10% of samples within 250 kb of the query SNP. Nine eQTLs were examined: rs3922844 and *SCN5A*, rs1662342 and probes in *MYL12A*, *TGIF1* (2 probes), *LPIN2* (2 probes), and *MYOM1*, and rs7547997 and probes in *CDIC* and *CDIE*, and an eQTL P-value < 0.006 ($0.05/9$) was deemed significant. *SCN5A* exonic locations are expressed relative to the longest isoform, NM_198056.2, which contains 28 exons.

Acknowledgements

The authors wish to acknowledge the contributions of the involved research institutions, study investigators, field staff, and study participants of WHI, ARIC, JHS, MESA, Health ABC, HANDLS, CHS, CFS, BLSA, and BHS.

This work was supported by the National Institutes of Health [R01 HL088456 to N.S., R01 HL116747 to N.S., R01 HL111089 to N.S., R01 HL091244 to N.S., K99 HL098458 to C.L.A., 5T32CA009330-30 to A.M.B., R01 ES017794 to E.A.W., P20MD006899 to S.G.B., and U24AG051129 to D.S.E.], the Laughlin Family [to N.S.], and the German Research Foundation [SCHNA 1149/3-1 to R.B.S.].

As part of the National Heart, Lung, and Blood Institute (NHLBI)-sponsored Candidate gene Association Resource (CARE) project, the ARIC, JHS, MESA, and CFS studies contributed parent study data, ancillary study data, and DNA samples through the Broad Institute of Harvard and MIT (N01-HC-65226) to create a genotype/phenotype database for wide dissemination to the biomedical research community.

Atherosclerosis Risk in Communities (ARIC): The ARIC study is carried out as a collaborative study supported by National Heart, Lung, and Blood Institute contracts to the University of North Carolina at Chapel Hill (N01-HC-55015), Baylor Medical College (N01-HC-55016), University of Mississippi Medical Center (N01-HC-55021), University of Minnesota (N01-HC-55019), Johns Hopkins University (N01-HC-55020), University of Texas, Houston (N01-HC-55022), and University of North Carolina, Forsyth County (N01-HC-55018).

Cleveland Family Study (CFS): Case Western Reserve University (NIH HL 46380, M01RR00080).

Jackson Heart Study (JHS): The Jackson Heart Study is supported by contracts HHSN268201300046C, HHSN268201300047C, HHSN268201300048C, HHSN268201300049C, HHSN268201300050C from the National Heart, Lung, and Blood Institute and the National Institute on Minority Health and Health Disparities.

Multi-Ethnic Study of Atherosclerosis (MESA): University of Washington (N01-HC-95159), Regents of the University of California (N01-HC-95160), Columbia University (N01-HC-95161), Johns Hopkins University (N01-HC-95162, N01-HC-95168), University of Minnesota (N01-HC95163), Northwestern University (N01-HC-95164), Wake Forest University (N01-HC-95165), University of Vermont (N01-HC-95166), New England Medical Center (N01-HC-95167), Harbor-UCLA Research and Education Institute (N01-HC-95169), Cedars-Sinai Medical Center (R01-HL-071205), and University of Virginia (subcontract to R01-HL-071205).

Health, Aging, and Body Composition Study (Health ABC): The Health ABC study was supported by NIA contracts N01AG62101, N01AG62103, and N01AG62106. The genome-wide association study was funded by NIA grant 1R01AG032098-01A1 to Wake Forest University Health Sciences and genotyping services were provided by the Center for Inherited Disease Research (CIDR). CIDR is fully funded through a federal contract from the National Institutes of Health to The Johns Hopkins University, contract number HHSN268200782096C. This research was supported in part by the Intramural Research Program of the NIH, National Institute on Aging.

Healthy Aging in Neighborhoods of Diversity across the Life Span Study (HANDLS): The HANDLS study was in part supported by the intramural research program of the National Institute on Aging and the National Center for Minority Health and Health Disparities, National Institutes of Health. This research was supported by the Intramural Research Program of the

NIH, National Institute on Aging and the National Center on Minority Health and Health Disparities (contract # Z01-AG000513 and human subjects protocol # 2009-149). Data analyses for the HANDLS study utilized the high-performance computational capabilities of the Biowulf Linux cluster at the National Institutes of Health, Bethesda, Md. (<http://biowulf.nih.gov>).

Women's Health Initiative (WHI): The WHI program is funded by the National Heart, Lung, and Blood Institute, National Institutes of Health, U.S. Department of Health and Human Services through contracts HHSN268201100046C, HHSN268201100001C, HHSN268201100002C, HHSN268201100003C, HHSN268201100004C, and HHSN271201100004C. This manuscript was prepared in collaboration with investigators of the WHI, and has been reviewed and/or approved by the Women's Health Initiative (WHI). WHI investigators are listed at http://www.whiscience.org/publications/WHI_investigators_shortlist.pdf. Funding for WHI SHARe genotyping was provided by NHLBI Contract N02-HL-64278.

Cardiovascular Health Study (CHS): This CHS research was supported by NHLBI contracts HHSN268201200036C, HHSN268200800007C, N01HC55222, N01HC85079, N01HC85080, N01HC85081, N01HC85082, N01HC85083, N01HC85086, HHSN268200960009C; and NHLBI grants HL080295, HL087652, HL105756, HL103612, HL120393, and HL085251 with additional contribution from the National Institute of Neurological Disorders and Stroke (NINDS). Additional support was provided through AG023629 from the National Institute on Aging (NIA). A full list of principal CHS investigators and institutions can be found at CHS-NHLBI.org/. The provision of genotyping data was supported in part by the National Center for Advancing Translational Sciences, CTSI grant UL1TR000124, and the National Institute of Diabetes and Digestive and Kidney Disease

Diabetes Research Center (DRC) grant DK063491 to the Southern California Diabetes Endocrinology Research Center. The content is solely the responsibility of the authors and does not necessarily represent the official views of the National Institutes of Health.

Baltimore Longitudinal Study of Aging (BLSA): The BLSA was supported in part by the Intramural Research Program of the NIH, National Institute on Aging. A portion of that support was through a R&D contract with MedStar Research Institute.

Bogalusa Heart Study (BHS): BHS is supported by grants R01ES021724 from National Institute of Environmental Health Science and R01AG016592 from the National Institute on Aging. Analysis performed at STSI/TSRI was supported by U54 NS056883 and Scripps Genomic Medicine.

The Population Architecture Using Genomics and Epidemiology (PAGE) program is funded by the National Human Genome Research Institute (NHGRI), supported by U01HG007416 (CALiCo), U01HG007417 (ISMMS), U01HG007397 (MEC), U01HG007376 (WHI), and U01HG007419 (Coordinating Center). The contents of this paper are solely the responsibility of the authors and do not necessarily represent the official views of the NIH. The complete list of PAGE members can be found at <http://www.pagestudy.org>. Assistance with data management, data integration, data dissemination, genotype imputation, ancestry deconvolution, and general study coordination was provided by the PAGE Coordinating Center (U01HG007419). The PAGE consortium thanks the staff and participants of all PAGE studies for their important contributions.

Funding for the atrial tissue eQTL study was provided by NIH 5R01HL090620, NIH 5R01HL111314, Fondation Leducq CVD-07-03, European North American Atrial Fibrillation Research Alliance.

The funders had no role in study design, data collection and analysis, decision to publish, or preparation of the manuscript.

The authors would also like to acknowledge the generous sharing of QRS GWAS results from the CHARGE consortium. The following individuals are members of the CHARGE QRS Consortium: Nona Sotoodehnia, Aaron Isaacs, Paul I.W. de Bakker, Marcus Dörr, Christopher Newton-Cheh, Ilja M. Nolte, Pim van der Harst, Martina Müller, Mark Eijgelsheim, Alvaro Alonso, Andrew A. Hicks, Sandosh Padmanabhan, Caroline Hayward, Albert Vernon Smith, Ozren Polasek, Steven Giovannone, Jingyuan Fu, Jared W. Magnani, Kristin D. Marciante, Arne Pfeufer, Sina A. Gharib, Alexander Teumer, Man Li, Joshua C. Bis, Fernando Rivadeneira, Thor Aspelund, Anna Köttgen, Toby Johnson, Kenneth Rice, Mark P.S. Sie, Amanda Ying Wang, Norman Klopp, Christian Fuchsberger, Sarah H. Wild, Irene Mateo Leach, Karol Estrada, Uwe Völker, Alan F. Wright, Folkert W. Asselbergs, Jiaxiang Qu, Aravinda Chakravarti, Moritz F. Sinner, Jan A. Kors, Astrid Petersmann, Tamara B. Harris, Elsayed Z. Soliman, Patricia B. Munroe, Bruce M. Psaty, Ben A. Oostra, L. Adrienne Cupples, Siegfried Perz, Rudolf A. de Boer, André G. Uitterlinden, Henry Völzke, Timothy D. Spector, Fang-Yu Liu, Eric Boerwinkle, Anna F. Dominiczak, Jerome I. Rotter, Gé van Herpen, Daniel Levy, H.-Erich Wichmann, Wiek H. van Gilst, Jacqueline C.M. Witteman, Heyo K. Kroemer, W.H. Linda Kao, Susan R. Heckbert, Thomas Meitinger, Albert Hofman, Harry Campbell, Aaron R. Folsom, Dirk J. van Veldhuisen, Christine Schwienbacher, Christopher J. O'Donnell, Claudia Beu Volpato, Mark J. Caulfield, John M. Connell, Lenore Launer, Xiaowen Lu, Lude Franke, Rudolf S.N. Fehrmann, Gerard te Meerman, Harry J.M. Groen, Rinse K. Weersma, Leonard H. van den Berg, Cisca Wijmenga, Roel A. Ophoff, Gerjan Navis, Igor Rudan, Harold Snieder, James F. Wilson, Peter P. Pramstaller, David S. Siscovick, Thomas J. Wang, Vilundur Gudnason, Cornelia M. van

Duijn, Stephan B. Felix, Glenn I. Fishman, Yalda Jamshidi, Bruno H Ch Stricker, Nilesh J. Samani, Stefan Käab, Dan E. Arking.

Conflict of Interest Statement

Bruce M. Psaty serves on the DSMB of a clinical trial funded by the manufacturer (Zoll LifeCor) and on the Steering Committee of the Yale Open Data Access Project funded by Johnson & Johnson. Anne M. Butler has received investigator-initiated support from Amgen and AstraZeneca.

References

- 1 Badheka, A.O., Singh, V., Patel, N.J., Deshmukh, A., Shah, N., Chothani, A., Mehta, K., Grover, P., Savani, G.T., Gupta, S. *et al.* (2013) QRS duration on electrocardiography and cardiovascular mortality (from the National Health and Nutrition Examination Survey-III). *Am. J. Cardiol.*, **112**, 671-677.
- 2 Mentz, R.J., Greiner, M.A., DeVore, A.D., Dunlay, S.M., Choudhary, G., Ahmad, T., Khazanie, P., Randolph, T.C., Griswold, M.E., Eapen, Z.J. *et al.* (2015) Ventricular conduction and long-term heart failure outcomes and mortality in African Americans: insights from the Jackson Heart Study. *Circulation. Heart failure*, **8**, 243-251.
- 3 Wang, N.C., Maggioni, A.P., Konstam, M.A., Zannad, F., Krasa, H.B., Burnett, J.C., Jr., Grinfeld, L., Swedberg, K., Udelson, J.E., Cook, T. *et al.* (2008) Clinical implications of QRS duration in patients hospitalized with worsening heart failure and reduced left ventricular ejection fraction. *JAMA*, **299**, 2656-2666.
- 4 Vitelli, L.L., Crow, R.S., Shahar, E., Hutchinson, R.G., Rautaharju, P.M. and Folsom, A.R. (1998) Electrocardiographic findings in a healthy biracial population. Atherosclerosis Risk in Communities (ARIC) Study Investigators. *Am. J. Cardiol.*, **81**, 453-459.
- 5 Rautaharju, P.M., Prineas, R.J., Kadish, A., Larson, J.C., Hsia, J. and Lund, B. (2006) Normal standards for QT and QT subintervals derived from a large ethnically diverse population of women aged 50 to 79 years (the Women's Health Initiative [WHI]). *Am. J. Cardiol.*, **97**, 730-737.
- 6 Walsh, J.A., 3rd, Prineas, R., Daviglus, M.L., Ning, H., Liu, K., Lewis, C.E., Sidney, S., Schreiner, P.J., Iribarren, C. and Lloyd-Jones, D.M. (2010) Prevalence of electrocardiographic

abnormalities in a middle-aged, biracial population: Coronary Artery Risk Development in Young Adults study. *J. Electrocardiol.*, **43**, 385 e381-389.

7 Holm, H., Gudbjartsson, D.F., Arnar, D.O., Thorleifsson, G., Thorgeirsson, G., Stefansdottir, H., Gudjonsson, S.A., Jonasdottir, A., Mathiesen, E.B., Njolstad, I. *et al.* (2010) Several common variants modulate heart rate, PR interval and QRS duration. *Nat. Genet.*, **42**, 117-122.

8 Sotoodehnia, N., Isaacs, A., de Bakker, P.I., Dorr, M., Newton-Cheh, C., Nolte, I.M., van der Harst, P., Muller, M., Eijgelsheim, M., Alonso, A. *et al.* (2010) Common variants in 22 loci are associated with QRS duration and cardiac ventricular conduction. *Nat. Genet.*, **42**, 1068-1076.

9 Rosenberg, N.A., Huang, L., Jewett, E.M., Szpiech, Z.A., Jankovic, I. and Boehnke, M. (2010) Genome-wide association studies in diverse populations. *Nat. Rev. Genet.*, **11**, 356-366.

10 Casto, A.M. and Feldman, M.W. (2011) Genome-wide association study SNPs in the human genome diversity project populations: does selection affect unlinked SNPs with shared trait associations? *PLoS Genet.*, **7**, e1001266.

11 Matise, T.C., Ambite, J.L., Buyske, S., Carlson, C.S., Cole, S.A., Crawford, D.C., Haiman, C.A., Heiss, G., Kooperberg, C., Marchand, L.L. *et al.* (2011) The Next PAGE in understanding complex traits: design for the analysis of Population Architecture Using Genetics and Epidemiology (PAGE) Study. *Am. J. Epidemiol.*, **174**, 849-859.

12 Splawski, I., Timothy, K.W., Tateyama, M., Clancy, C.E., Malhotra, A., Beggs, A.H., Cappuccio, F.P., Sagnella, G.A., Kass, R.S. and Keating, M.T. (2002) Variant of SCN5A sodium channel implicated in risk of cardiac arrhythmia. *Science*, **297**, 1333-1336.

- 13 Jeff, J.M., Brown-Gentry, K., Buxbaum, S.G., Sarpong, D.F., Taylor, H.A., George, A.L., Jr., Roden, D.M. and Crawford, D.C. (2011) SCN5A variation is associated with electrocardiographic traits in the Jackson Heart Study. *Circ. Cardiovasc. Genet.*, **4**, 139-144.
- 14 Magnani, J.W., Brody, J.A., Prins, B.P., Arking, D.E., Lin, H., Yin, X., Liu, C.T., Morrison, A.C., Zhang, F., Spector, T.D. *et al.* (2014) Sequencing of SCN5A identifies rare and common variants associated with cardiac conduction: Cohorts for Heart and Aging Research in Genomic Epidemiology (CHARGE) Consortium. *Circ. Cardiovasc. Genet.*, **7**, 365-373.
- 15 Ilkhanoff, L., Arking, D.E., Lemaitre, R.N., Alonso, A., Chen, L.Y., Durda, P., Hesselson, S.E., Kerr, K.F., Magnani, J.W., Marcus, G.M. *et al.* (2014) A common SCN5A variant is associated with PR interval and atrial fibrillation among African Americans. *J. Cardiovasc. Electrophysiol.*, **25**, 1150-1157.
- 16 Chambers, J.C., Zhao, J., Terracciano, C.M., Bezzina, C.R., Zhang, W., Kaba, R., Navaratnarajah, M., Lotlikar, A., Sehmi, J.S., Kooner, M.K. *et al.* (2010) Genetic variation in SCN10A influences cardiac conduction. *Nat. Genet.*, **42**, 149-152.
- 17 Morris, A.P. (2011) Transethnic meta-analysis of genomewide association studies. *Genet. Epidemiol.*, **35**, 809-822.
- 18 Schroeter, A., Walzik, S., Blechschmidt, S., Haufe, V., Benndorf, K. and Zimmer, T. (2010) Structure and function of splice variants of the cardiac voltage-gated sodium channel Na(v)1.5. *J. Mol. Cell. Cardiol.*, **49**, 16-24.
- 19 Zimmer, T. and Surber, R. (2008) SCN5A channelopathies--an update on mutations and mechanisms. *Prog. Biophys. Mol. Biol.*, **98**, 120-136.

- 20 Smith, J.G., Magnani, J.W., Palmer, C., Meng, Y.A., Soliman, E.Z., Musani, S.K., Kerr, K.F., Schnabel, R.B., Lubitz, S.A., Sotoodehnia, N. *et al.* (2011) Genome-wide association studies of the PR interval in African Americans. *PLoS Genet.*, **7**, e1001304.
- 21 Butler, A.M., Yin, X., Evans, D.S., Nalls, M.A., Smith, E.N., Tanaka, T., Li, G., Buxbaum, S.G., Whitsel, E.A., Alonso, A. *et al.* (2012) Novel loci associated with PR interval in a genome-wide association study of 10 African American cohorts. *Circ. Cardiovasc. Genet.*, **5**, 639-646.
- 22 Stadhouders, R., van den Heuvel, A., Kolovos, P., Jorna, R., Leslie, K., Grosveld, F. and Soler, E. (2012) Transcription regulation by distal enhancers: who's in the loop? *Transcription*, **3**, 181-186.
- 23 Park, I., Han, C., Jin, S., Lee, B., Choi, H., Kwon, J.T., Kim, D., Kim, J., Lifirsu, E., Park, W.J. *et al.* (2011) Myosin regulatory light chains are required to maintain the stability of myosin II and cellular integrity. *Biochem. J.*, **434**, 171-180.
- 24 Su, A.I., Wiltshire, T., Batalov, S., Lapp, H., Ching, K.A., Block, D., Zhang, J., Soden, R., Hayakawa, M., Kreiman, G. *et al.* (2004) A gene atlas of the mouse and human protein-encoding transcriptomes. *Proc. Natl. Acad. Sci. U S A*, **101**, 6062-6067.
- 25 Eijgelsheim, M., Newton-Cheh, C., Sotoodehnia, N., de Bakker, P.I., Muller, M., Morrison, A.C., Smith, A.V., Isaacs, A., Sanna, S., Dorr, M. *et al.* (2010) Genome-wide association analysis identifies multiple loci related to resting heart rate. *Hum. Mol. Genet.*, **19**, 3885-3894.
- 26 Deo, R., Nalls, M.A., Avery, C.L., Smith, J.G., Evans, D.S., Keller, M.F., Butler, A.M., Buxbaum, S.G., Li, G., Miguel Quibrera, P. *et al.* (2013) Common genetic variation near the

connexin-43 gene is associated with resting heart rate in African Americans: a genome-wide association study of 13,372 participants. *Heart Rhythm*, **10**, 401-408.

27 Cohen, N.R., Garg, S. and Brenner, M.B. (2009) Antigen Presentation by CD1 Lipids, T Cells, and NKT Cells in Microbial Immunity. *Adv. Immunol.*, **102**, 1-94.

28 Malnic, B., Godfrey, P.A. and Buck, L.B. (2004) The human olfactory receptor gene family. *Proc. Natl. Acad. Sci. U S A*, **101**, 2584-2589.

29 Smith, S., Curran, J., Hund, T.J. and Mohler, P.J. (2012) Defects in cytoskeletal signaling pathways, arrhythmia, and sudden cardiac death. *Front. Physiol.*, **3**, 122.

30 Mohler, P.J., Rivolta, I., Napolitano, C., LeMaillet, G., Lambert, S., Priori, S.G. and Bennett, V. (2004) Nav1.5 E1053K mutation causing Brugada syndrome blocks binding to ankyrin-G and expression of Nav1.5 on the surface of cardiomyocytes. *Proc. Natl. Acad. Sci. U S A*, **101**, 17533-17538.

31 Hund, T.J., Koval, O.M., Li, J., Wright, P.J., Qian, L., Snyder, J.S., Gudmundsson, H., Kline, C.F., Davidson, N.P., Cardona, N. *et al.* (2010) A beta(IV)-spectrin/CaMKII signaling complex is essential for membrane excitability in mice. *J. Clin. Invest.*, **120**, 3508-3519.

32 Teo, Y.Y., Small, K.S. and Kwiatkowski, D.P. (2010) Methodological challenges of genome-wide association analysis in Africa. *Nat. Rev. Genet.*, **11**, 149-160.

33 Gravel, S., Henn, B.M., Gutenkunst, R.N., Indap, A.R., Marth, G.T., Clark, A.G., Yu, F., Gibbs, R.A. and Bustamante, C.D. (2011) Demographic history and rare allele sharing among human populations. *Proc. Natl. Acad. Sci. U S A*, **108**, 11983-11988.

34 Tennessen, J.A., Bigham, A.W., O'Connor, T.D., Fu, W., Kenny, E.E., Gravel, S., McGee, S., Do, R., Liu, X., Jun, G. *et al.* (2012) Evolution and functional impact of rare coding variation from deep sequencing of human exomes. *Science*, **337**, 64-69.

- 35 Fu, W., O'Connor, T.D., Jun, G., Kang, H.M., Abecasis, G., Leal, S.M., Gabriel, S., Rieder, M.J., Altshuler, D., Shendure, J. *et al.* (2013) Analysis of 6,515 exomes reveals the recent origin of most human protein-coding variants. *Nature*, **493**, 216-220.
- 36 Abecasis, G.R., Auton, A., Brooks, L.D., DePristo, M.A., Durbin, R.M., Handsaker, R.E., Kang, H.M., Marth, G.T. and McVean, G.A. (2012) An integrated map of genetic variation from 1,092 human genomes. *Nature*, **491**, 56-65.
- 37 Dickson, S.P., Wang, K., Krantz, I., Hakonarson, H. and Goldstein, D.B. (2010) Rare variants create synthetic genome-wide associations. *PLoS Biol.*, **8**, e1000294.
- 38 Anderson, C.A., Soranzo, N., Zeggini, E. and Barrett, J.C. (2011) Synthetic associations are unlikely to account for many common disease genome-wide association signals. *PLoS Biol.*, **9**, e1000580.
- 39 Wray, N.R., Purcell, S.M. and Visscher, P.M. (2011) Synthetic associations created by rare variants do not explain most GWAS results. *PLoS Biol.*, **9**, e1000579.
- 40 Waters, K.M., Stram, D.O., Hassanein, M.T., Le Marchand, L., Wilkens, L.R., Maskarinec, G., Monroe, K.R., Kolonel, L.N., Altshuler, D., Henderson, B.E. *et al.* (2010) Consistent association of type 2 diabetes risk variants found in europeans in diverse racial and ethnic groups. *PLoS Genet.*, **6**.
- 41 Haiman, C.A., Chen, G.K., Blot, W.J., Strom, S.S., Berndt, S.I., Kittles, R.A., Rybicki, B.A., Isaacs, W.B., Ingles, S.A., Stanford, J.L. *et al.* (2011) Characterizing genetic risk at known prostate cancer susceptibility loci in African Americans. *PLoS Genet.*, **7**, e1001387.
- 42 Chen, F., Chen, G.K., Millikan, R.C., John, E.M., Ambrosone, C.B., Bernstein, L., Zheng, W., Hu, J.J., Ziegler, R.G., Deming, S.L. *et al.* (2011) Fine-mapping of breast cancer

susceptibility loci characterizes genetic risk in African Americans. *Hum. Mol. Genet.*, **20**, 4491-4503.

43 Carlson, C.S., Matise, T.C., North, K.E., Haiman, C.A., Fesinmeyer, M.D., Buyske, S., Schumacher, F.R., Peters, U., Franceschini, N., Ritchie, M.D. *et al.* (2013) Generalization and dilution of association results from European GWAS in populations of non-European ancestry: the PAGE study. *PLoS Biol.*, **11**, e1001661.

44 Dumitrescu, L., Carty, C.L., Taylor, K., Schumacher, F.R., Hindorff, L.A., Ambite, J.L., Anderson, G., Best, L.G., Brown-Gentry, K., Buzkova, P. *et al.* (2011) Genetic determinants of lipid traits in diverse populations from the population architecture using genomics and epidemiology (PAGE) study. *PLoS Genet.*, **7**, e1002138.

45 Coram, M.A., Duan, Q., Hoffmann, T.J., Thornton, T., Knowles, J.W., Johnson, N.A., Ochs-Balcom, H.M., Donlon, T.A., Martin, L.W., Eaton, C.B. *et al.* (2013) Genome-wide characterization of shared and distinct genetic components that influence blood lipid levels in ethnically diverse human populations. *Am. J. Hum. Genet.*, **92**, 904-916.

46 Wu, Y., Waite, L.L., Jackson, A.U., Sheu, W.H., Buyske, S., Absher, D., Arnett, D.K., Boerwinkle, E., Bonnycastle, L.L., Carty, C.L. *et al.* (2013) Trans-ethnic fine-mapping of lipid loci identifies population-specific signals and allelic heterogeneity that increases the trait variance explained. *PLoS Genet.*, **9**, e1003379.

47 Marigorta, U.M. and Navarro, A. (2013) High Trans-ethnic Replicability of GWAS Results Implies Common Causal Variants. *PLoS Genet.*, **9**, e1003566.

48 Smith, J.G., Avery, C.L., Evans, D.S., Nalls, M.A., Meng, Y.A., Smith, E.N., Palmer, C., Tanaka, T., Mehra, R., Butler, A.M. *et al.* (2012) Impact of ancestry and common genetic variants on QT interval in African Americans. *Circ. Cardiovasc. Genet.*, **5**, 647-655.

- 49 Jeff, J.M., Ritchie, M.D., Denny, J.C., Kho, A.N., Ramirez, A.H., Crosslin, D., Armstrong, L., Basford, M.A., Wolf, W.A., Pacheco, J.A. *et al.* (2013) Generalization of variants identified by genome-wide association studies for electrocardiographic traits in African Americans. *Ann. Hum. Genet.*, **77**, 321-332.
- 50 Price, A.L., Patterson, N.J., Plenge, R.M., Weinblatt, M.E., Shadick, N.A. and Reich, D. (2006) Principal components analysis corrects for stratification in genome-wide association studies. *Nat. Genet.*, **38**, 904-909.
- 51 Musunuru, K., Lettre, G., Young, T., Farlow, D.N., Pirruccello, J.P., Ejebe, K.G., Keating, B.J., Yang, Q., Chen, M.H., Lapchyk, N. *et al.* (2010) Candidate gene association resource (CARE): design, methods, and proof of concept. *Circ. Cardiovasc. Genet.*, **3**, 267-275.
- 52 Lettre, G., Palmer, C.D., Young, T., Ejebe, K.G., Allayee, H., Benjamin, E.J., Bennett, F., Bowden, D.W., Chakravarti, A., Dreisbach, A. *et al.* (2011) Genome-wide association study of coronary heart disease and its risk factors in 8,090 African Americans: the NHLBI CARE Project. *PLoS Genet.*, **7**, e1001300.
- 53 Chen, M.H. and Yang, Q. (2010) GWAF: an R package for genome-wide association analyses with family data. *Bioinformatics*, **26**, 580-581.
- 54 Willer, C.J., Li, Y. and Abecasis, G.R. (2010) METAL: fast and efficient meta-analysis of genomewide association scans. *Bioinformatics*, **26**, 2190-2191.
- 55 Devlin, B. and Roeder, K. (1999) Genomic control for association studies. *Biometrics*, **55**, 997-1004.
- 56 Pe'er, I., Yelensky, R., Altshuler, D. and Daly, M.J. (2008) Estimation of the multiple testing burden for genomewide association studies of nearly all common variants. *Genet. Epidemiol.*, **32**, 381-385.

- 57 Whitehead, A. and Whitehead, J. (1991) A general parametric approach to the meta-analysis of randomized clinical trials. *Stat. Med.*, **10**, 1665-1677.
- 58 Higgins, J.P. and Thompson, S.G. (2002) Quantifying heterogeneity in a meta-analysis. *Stat. Med.*, **21**, 1539-1558.
- 59 Patterson, N., Hattangadi, N., Lane, B., Lohmueller, K.E., Hafler, D.A., Oksenberg, J.R., Hauser, S.L., Smith, M.W., O'Brien, S.J., Altshuler, D. *et al.* (2004) Methods for high-density admixture mapping of disease genes. *Am. J. Hum. Genet.*, **74**, 979-1000.
- 60 Price, A.L., Tandon, A., Patterson, N., Barnes, K.C., Rafaels, N., Ruczinski, I., Beaty, T.H., Mathias, R., Reich, D. and Myers, S. (2009) Sensitive detection of chromosomal segments of distinct ancestry in admixed populations. *PLoS Genet.*, **5**, e1000519.
- 61 Tang, H., Peng, J., Wang, P. and Risch, N.J. (2005) Estimation of individual admixture: analytical and study design considerations. *Genet. Epidemiol.*, **28**, 289-301.
- 62 Tang, H., Coram, M., Wang, P., Zhu, X. and Risch, N. (2006) Reconstructing genetic ancestry blocks in admixed individuals. *Am. J. Hum. Genet.*, **79**, 1-12.
- 63 Pritchard, J.K., Stephens, M. and Donnelly, P. (2000) Inference of population structure using multilocus genotype data. *Genetics*, **155**, 945-959.
- 64 Nalls, M.A., Wilson, J.G., Patterson, N.J., Tandon, A., Zmuda, J.M., Huntsman, S., Garcia, M., Hu, D., Li, R., Beamer, B.A. *et al.* (2008) Admixture mapping of white cell count: genetic locus responsible for lower white blood cell count in the Health ABC and Jackson Heart studies. *Am. J. Hum. Genet.*, **82**, 81-87.
- 65 Pasaniuc, B., Sankararaman, S., Kimmel, G. and Halperin, E. (2009) Inference of locus-specific ancestry in closely related populations. *Bioinformatics*, **25**, i213-221.

- 66 Ward, L.D. and Kellis, M. (2012) HaploReg: a resource for exploring chromatin states, conservation, and regulatory motif alterations within sets of genetically linked variants. *Nucleic Acids Res.*, **40**, D930-934.
- 67 Dunham, I., Kundaje, A., Aldred, S.F., Collins, P.J., Davis, C.A., Doyle, F., Epstein, C.B., Frietze, S., Harrow, J., Kaul, R. *et al.* (2012) An integrated encyclopedia of DNA elements in the human genome. *Nature*, **489**, 57-74.
- 68 Bernstein, B.E., Stamatoyannopoulos, J.A., Costello, J.F., Ren, B., Milosavljevic, A., Meissner, A., Kellis, M., Marra, M.A., Beaudet, A.L., Ecker, J.R. *et al.* (2010) The NIH Roadmap Epigenomics Mapping Consortium. *Nat. Biotechnol.*, **28**, 1045-1048.
- 69 Segre, A.V., Groop, L., Mootha, V.K., Daly, M.J. and Altshuler, D. (2010) Common inherited variation in mitochondrial genes is not enriched for associations with type 2 diabetes or related glycemic traits. *PLoS Genet.*, **6**, e1001058.
- 70 Purcell, S., Neale, B., Todd-Brown, K., Thomas, L., Ferreira, M.A., Bender, D., Maller, J., Sklar, P., de Bakker, P.I., Daly, M.J. *et al.* (2007) PLINK: a tool set for whole-genome association and population-based linkage analyses. *Am. J. Hum. Genet.*, **81**, 559-575.
- 71 Gauderman, W.J. (2002) Sample size calculations for matched case-control studies of gene-environment interaction. *Statistics in Medicine*, **21**, 35-50.
- 72 Pruim, R.J., Welch, R.P., Sanna, S., Teslovich, T.M., Chines, P.S., Gliedt, T.P., Boehnke, M., Abecasis, G.R. and Willer, C.J. (2010) LocusZoom: regional visualization of genome-wide association scan results. *Bioinformatics*, **26**, 2336-2337.
- 73 Hinch, A.G., Tandon, A., Patterson, N., Song, Y., Rohland, N., Palmer, C.D., Chen, G.K., Wang, K., Buxbaum, S.G., Akylbekova, E.L. *et al.* (2011) The landscape of recombination in African Americans. *Nature*, **476**, 170-175.

- 74 Barrett, J.C., Fry, B., Maller, J. and Daly, M.J. (2005) Haploview: analysis and visualization of LD and haplotype maps. *Bioinformatics*, **21**, 263-265.
- 75 Gabriel, S.B., Schaffner, S.F., Nguyen, H., Moore, J.M., Roy, J., Blumenstiel, B., Higgins, J., DeFelice, M., Lochner, A., Faggart, M. *et al.* (2002) The structure of haplotype blocks in the human genome. *Science*, **296**, 2225-2229.
- 76 Wellcome Trust Case Control, C., Maller, J.B., McVean, G., Byrnes, J., Vukcevic, D., Palin, K., Su, Z., Howson, J.M., Auton, A., Myers, S. *et al.* (2012) Bayesian refinement of association signals for 14 loci in 3 common diseases. *Nat. Genet.*, **44**, 1294-1301.
- 77 Asimit, J.L., Hatzikotoulas, K., McCarthy, M., Morris, A.P. and Zeggini, E. (2016) Trans-ethnic study design approaches for fine-mapping. *Eur. J. Hum. Genet.*, in press.
- 78 (2010) A map of human genome variation from population-scale sequencing. *Nature*, **467**, 1061-1073.
- 79 Liu, E.Y., Buyske, S., Aragaki, A.K., Peters, U., Boerwinkle, E., Carlson, C., Carty, C., Crawford, D.C., Haessler, J., Hindorff, L.A. *et al.* (2012) Genotype imputation of Metabochip SNPs using a study-specific reference panel of ~4,000 haplotypes in African Americans from the Women's Health Initiative. *Genet. Epidemiol.*, **36**, 107-117.
- 80 Leek, J.T. and Storey, J.D. (2007) Capturing heterogeneity in gene expression studies by surrogate variable analysis. *PLoS Genet.*, **3**, 1724-1735.

Legends to Figures

Fig 1. Regional association plot at *SCN5A/SCN10A* locus. African American SNP association meta-analysis results are plotted in the top panel, and meta-analysis results from cohorts of European ancestry are plotted in the bottom panel. The AA index SNP (rs3922844) is designated by a red diamond in both panels. The LD (r^2) shown is relative to the AA index SNP and is based on HapMap YRI in the top panel and HapMap CEU in the bottom panel. Gray circles are SNPs without HapMap LD data. The X-axis marks the chromosomal position. Recombination rates estimated from African Americans and HapMap CEU individuals are shown in the top and bottom panels, respectively. The dashed horizontal lines in the top and bottom panels mark the GWAS significance level in African Americans (2.5×10^{-8}) and populations of European descent (5.0×10^{-8}), respectively.

Fig 2. Association between rs3922844 genotype and *SCN5A* expression in human atrial tissue. Box plots display data from individuals of African ancestry (A) and European ancestry (B). Plotted along the Y-axis are RNA levels adjusted for covariates. The bottom and top of each box indicates the 25th and 75th percentiles, and the band within the box is the median. Whiskers extend to the most extreme value or the most extreme value within 1.5*interquartile range (IQR), whichever value is closer to the median. The fitted regression line is shown in blue.

Fig 3. Regional association plot of transethnic meta-analysis results at *MYL12A* locus. Transethnic meta-analysis SNP association results are plotted in the top panel, meta-analysis results from cohorts of European ancestry are plotted in the middle panel, and African American

SNP association meta-analysis results are plotted in the bottom panel. The transethnic index SNP (rs1662342) is designated by a red diamond in all panels. The LD (r^2) shown is relative to the index SNP and is based on HapMap CEU in the top and middle panels and is based on HapMap YRI in the bottom panel. Gray circles are SNPs without HapMap LD data. The X-axis marks the chromosomal position. Recombination rates averaged across HapMap populations, in HapMap CEU individuals, and in African Americans are shown in the top panel, middle panel, and bottom panel, respectively. The dashed horizontal line in the top and middle panels marks the GWAS significance level for European ancestry (5.0×10^{-8}) and in the bottom panel marks the GWAS significance level for African Americans (2.5×10^{-8}).

Fig 4. Regional association plot of transethnic meta-analysis results at chromosome 1q23.1.

Transethnic meta-analysis SNP association results are plotted in the top panel, meta-analysis results from cohorts of European ancestry are plotted in the middle panel, and African American SNP association meta-analysis results are plotted in the bottom panel. The transethnic index SNP (rs7547997) is designated by a red diamond in all panels. The LD (r^2) shown is relative to the index SNP and is based on HapMap CEU in the top and middle panels and is based on HapMap YRI in the bottom panel. Gray circles are SNPs without HapMap LD data. The X-axis marks the chromosomal position. Recombination rates averaged across HapMap populations, in HapMap CEU individuals, and in African Americans are shown in the top panel, middle panel, and bottom panel, respectively. The dashed horizontal line in the top and middle panels marks the GWAS significance level for European ancestry (5.0×10^{-8}) and in the bottom panel marks the GWAS significance level for African Americans (2.5×10^{-8}).

Table 1. Association results for rs3922844 with and without adjustment for local ancestry estimates.

Study	Assay (G/T) ^a	CAF ^b	N	Adjusted for global ancestry ^d		Adjusted for local ancestry ^{d,e}	
				$\beta \pm SE_{GC}$	P_{GC}	$\beta \pm SE_{GC}$	P_{GC}
WHI	I	0.42	4012	0.86 ± 0.21	6x10 ⁻⁵	0.90 ± 0.23	3x10 ⁻⁵
ARIC	I	0.41	2372	0.61 ± 0.28	0.03	0.68 ± 0.29	0.02
JHS	I	0.40	1918	1.41 ± 0.32	1x10 ⁻⁵	1.40 ± 0.33	2x10 ⁻⁵
MESA	I	0.43	1554	1.02 ± 0.36	0.005	1.17 ± 0.38	0.002
Health ABC	G	0.43	993	0.98 ± 0.47	0.04	0.99 ± 0.50	0.05
HANDLS	G	0.41	945	0.96 ± 0.43	0.03	0.85 ± 0.45	0.06
CHS	G	0.44	621	0.84 ± 0.56	0.13	ND	ND
CFS	I	0.39	315	0.16 ± 0.80	0.84	0.21 ± 0.82	0.80
BLSA	G	0.44	153	3.27 ± 0.99	9x10 ⁻⁴	ND	ND
BHS	G	0.42	147	-1.14 ± 1.27	0.37	ND	ND
Meta-analysis							
All studies		0.42	12,877	0.94 ± 0.12	4x10 ⁻¹⁴	-	-
LA studies ^c		0.42	12,109	0.91 ± 0.13	3x10 ⁻¹³	0.95 ± 0.13	7x10 ⁻¹³

^a G = directly genotyped SNP, I = imputed SNP.

^b Coded allele frequency. C and T are the coded and non-coded alleles for rs3922844, respectively. CAF for the meta-analysis is the weighted average across the 10 cohorts.

^c Studies with local ancestry (LA) estimates: WHI, ARIC, JHS, MESA, Health ABC, HANDLS, and CFS.

^d β and SE expressed in units of milliseconds.

^e ND = not determined.

Table 2. Association results from dense SNP genotyping study at the *SCN5A* locus.

SNP	Position ^a	Coded/ Reference allele (CAF)	ARIC		WHI PAGE		WHI SHARE		Meta-analysis	rs3922844 LD (r ²) ^c
			n	$\beta \pm SE^b$ (<i>P</i>)	n	$\beta \pm SE^b$ (<i>P</i>)	n	$\beta \pm SE^b$ (<i>P</i>)	$\beta \pm SE^b$ (<i>P</i>)	
rs12635898	38,601,069	A/C (0.30)	2911	1.03 ± 0.34 (0.002)	725	1.18 ± 0.52 (0.02)	3283	1.04 ± 0.24 (2x10 ⁻⁵)	1.05 ± 0.19 (1x10 ⁻⁸)	0.93

^a Position based on NCBI reference sequence build 36.

^b β and SE expressed in units of milliseconds.

^c LD estimates between rs12635898 and rs3922844 based on rs12635898 genotype data from unrelated YRI samples on MetaboChip arrays used in the PAGE study and rs3922844 genotype data from unrelated YRI samples downloaded from HapMap phase 2 data.

1 **Table 3. Novel genome-wide significant SNP associations from transethnic meta-analysis.**

SNP	Chr	Position ^a	Nearby Genes	SNP Annotation	European ancestry			African ancestry			Meta-analysis		
					CA (Freq) ^b	$\beta \pm SE_{GC}$ (P_{GC}) ^c	I^2 ^d	CA (Freq) ^b	$\beta \pm SE_{GC}$ (P_{GC}) ^c	I^2 ^d	CA (Freq) ^b	$\beta \pm SE_{GC}$ (P_{GC}) ^c	I^2 ^d
rs1662342	18	3,245,301	<i>MYL12A</i>	intron	A (0.14)	0.53 ± 0.10 (3.1×10^{-7})	34.7	A (0.21)	0.35 ± 0.16 (0.03)	16.6	A (0.16)	0.47 ± 0.09 (4.9×10^{-8})	0.0
rs7547997	1	156,607,897	<i>CDIE,</i> <i>OR10T2,</i> <i>SPTAI</i>	intergenic	A (0.16)	0.48 ± 0.10 (1.0×10^{-6})	0.0	A (0.59)	0.38 ± 0.12 (1.5×10^{-3})	18.8	A (0.33)	0.44 ± 0.08 (7.9×10^{-9})	0.0

2

3 ^a Position based on NCBI reference sequence build 36.

4 ^b CA = coded effect allele. Freq = frequency.

5 ^c β and SE expressed in units of milliseconds.

6 ^d Heterogeneity I^2 statistics bolded if the Cochran's X^2 P-value ≤ 0.05 .

1 **Table 4. SNP association transferability at the *SCN5A/SCN10A* locus.**

Index SNP/ annotation	Nearest gene	Chr (Position) ^h	Discovery population (Ref)	European ancestry				African ancestry				rs3922844 LD (r ²) ^d		
				CA (Freq) ^a	$\beta \pm SE_{GC}$ (P_{GC}) ^e	I ² ^f	Power ^b	CA (Freq) ^a	$\beta \pm SE_{GC}$ (P_{GC}) ^e	I ² ^f	Power ^c	CEU	YRI	ASW
rs6801957/ intron	<i>SCN10A</i>	3 (38,742,319)	EA (8)	T (0.41)	0.77 ± 0.07 (1x10⁻²⁸)	45.3	-	T (0.17)	0.54 ± 0.16 (8x10⁻⁴)	0.0	0.95	0.00	0.01	ND
rs6795970/ missense	<i>SCN10A</i>	3 (38,741,679)	EA/Asian (7,16)	A (0.40)	0.75 ± 0.07 (5x10⁻²⁷)	44.8	-	A (0.10)	0.44 ± 0.20 (0.03)	0.0	0.73	0.01	0.01	0.03
rs9851724/ intergenic	<i>SCN10A</i>	3 (38,694,939)	EA (8)	C (0.33)	-0.66 ± 0.07 (2x10⁻²⁰)	57.1	-	C (0.16)	-0.30 ± 0.16 (0.06)	7.2	0.82	0.00	0.01	0.01
rs11710077/ intron	<i>SCN5A</i>	3 (38,632,903)	EA (8)	T (0.21)	-0.84 ± 0.09 (6x10⁻²²)	23.8	-	T (0.11)	-0.87 ± 0.19 (7x10⁻⁶)	0.0	0.90	0.15	0.04	0.09
rs11708996/ intron	<i>SCN5A</i>	3 (38,608,927)	EA (8)	C (0.16)	0.79 ± 0.10 (1x10⁻¹⁶)	0.0	-	C (0.04)	0.86 ± 0.80 (0.28)	0.0	0.29	0.10	ND	ND
rs10865879/ intergenic	<i>SCN5A</i>	3 (38,552,366)	EA (8)	C (0.26)	0.78 ± 0.08 (3x10⁻²³)	53.6	-	C (0.18)	0.46 ± 0.15 (3x10⁻³)	0.0	0.97	0.00	0.01	ND
rs2051211/ intron	<i>EXOG</i>	3 (38,534,753)	EA (8)	G (0.26)	-0.44 ± 0.08 (2x10⁻⁸)	0.0	-	G (0.18)	-0.41 ± 0.15 (7x10⁻³)	0.0	0.38	0.20	0.00	0.05
rs3922844/ intron	<i>SCN5A</i>	3 (38,599,257)	AA	C (0.69)	0.56 ± 0.08 (2x10⁻¹³)	23.7	0.99	C (0.42)	0.94 ± 0.12 (4x10⁻¹⁴)	10.6	-	-	-	-

- 2
- 3 ^a CA = coded effect allele. Freq = frequency.
- 4 ^b Power to detect effect size reported in COGENT/CARe results using the coded effect allele frequency and trait variance as observed in European samples and
- 5 keeping $\alpha=0.002$ adjusting for 22 SNPs.
- 6 ^c Power to detect effect size reported in European discovery population using the effect allele frequency and trait variance as observed in African-American
- 7 samples and keeping $\alpha=0.002$ adjusting for 30 SNPs.
- 8 ^d LD between index SNP and rs3922844. ND indicates the SNP was not genotyped in the HapMap population or was monomorphic.
- 9 ^e In non-African ancestry discovery rows, significance was based on the genome-wide discovery threshold and P-values $\leq 5.0 \times 10^{-8}$ were bolded. In the African
- 10 ancestry discovery row, significance was based on the replication threshold and P-values ≤ 0.002 were bolded. β and SE expressed in units of milliseconds.
- 11 ^f Heterogeneity I² statistics bolded if the Cochran's χ^2 P-value ≤ 0.05 .
- 12 ^g In non-African ancestry discovery rows, significance was based on replication of the 30 previously identified SNPs and P-values ≤ 0.002 were bolded. In the
- 13 African ancestry discovery row, significance was based on genome-wide discovery and P-values $\leq 2.5 \times 10^{-8}$ were bolded. β and SE expressed in units of
- 14 milliseconds.
- 15 ^h Position based on NCBI reference sequence build 36.

1 **Table 5. SNP replication results with adequate power from GWAS in African Americans.**

Index SNP/ annotation	Nearby gene	Chr (Position) ^h	Discovery population (Ref)	European ancestry				African ancestry				LD (r ²) ^d		
				CA (Freq) ^a	$\beta \pm SE_{GC}$ (P_{GC}) ^c	I ² ^f	Power ^b	CA (Freq) ^a	$\beta \pm SE_{GC}$ (P_{GC}) ^g	I ² ^f	Power ^c	CEU	YRI	ASW
rs9470361/ intergenic	<i>CDKN1A</i>	6 (36,731,357)	EA (8)	A (0.25)	0.87 ± 0.08 (3x10⁻²⁷)	14.6	-	A (0.31)	0.43 ± 0.13 (1x10⁻³)	17.1	0.99	0.95	0.91	ND
rs1321311/ intergenic	<i>CDKN1A</i>	6 (36,730,878)	EA (7)	A (0.21)	0.94 ± 0.15 (3x10⁻¹⁰)	ND	-	A (0.39)	0.40 ± 0.12 (1x10⁻³)	0.0	0.99	0.95	0.70	ND
rs7756236/ intergenic	<i>CDKN1A</i>	6 (36,735,031)	AA	G (0.26)	0.83 ± 0.08 (2x10⁻²⁶)	34.3	0.99	G (0.30)	0.53 ± 0.13 (4x10 ⁻⁵)	3.0	-	-	-	-
rs11153730/ intergenic	<i>PLN</i>	6 (118,774,215)	EA (8)	C (0.49)	0.59 ± 0.07 (1x10⁻¹⁸)	5.3	-	C (0.29)	0.32 ± 0.13 (0.02)	0.0	0.91	0.92	0.27	ND
rs4307206/ intron	<i>PLN</i>	6 (118,920,013)	AA	A (0.45)	0.54 ± 0.07 (5x10⁻¹⁶)	14.4	0.99	A (0.21)	0.52 ± 0.15 (4x10 ⁻⁴)	0.0	-	-	-	-
rs9436640/ intron	<i>NF1A</i>	1 (61,646,265)	EA (8)	G (0.46)	-0.59 ± 0.07 (5x10⁻¹⁸)	51.2	-	G (0.37)	-0.51 ± 0.12 (2x10⁻⁵)	0.0	0.95	0.54	0.53	0.69
rs2207791/ intron	<i>NF1A</i>	1 (61,667,490)	AA	G (0.48)	-0.59 ± 0.07 (1x10⁻¹⁷)	44.5	0.99	G (0.31)	-0.62 ± 0.13 (1x10⁻⁶)	6.7	-	-	-	-
rs13165478/ intergenic	<i>HAND1</i>	5 (153,849,233)	EA (8)	A (0.36)	-0.55 ± 0.07 (7x10⁻¹⁴)	64.6	-	A (0.53)	-0.45 ± 0.14 (1x10⁻³)	0.0	0.93	1.00	1.00	ND
rs13185595/ intergenic	<i>HAND1</i>	5 (153,852,363)	AA	G (0.63)	0.56 ± 0.07 (9x10⁻¹⁴)	64.8	0.99	G (0.47)	0.44 ± 0.13 (5x10 ⁻⁴)	0.0	-	-	-	-
rs883079/ 3' UTR	<i>TBX5</i>	12 (113,277,623)	EA (8)	G (0.25)	0.49 ± 0.08 (1x10⁻¹⁰)	8.3	-	G (0.33)	0.60 ± 0.13 (1x10⁻⁶)	0.0	0.76	0.90	0.92	0.75
rs3825214/ intron	<i>TBX5</i>	12 (113,279,826)	EA (7)	G (0.22)	1.06 ± 0.15 (3x10⁻¹³)	ND	-	G (0.25)	0.49 ± 0.14 (3x10⁻⁴)	0.0	0.99	0.71	0.36	0.65
rs7312625/ intron	<i>TBX5</i>	12 (113,284,357)	AA	G (0.28)	0.46 ± 0.08 (1x10⁻⁹)	15.9	0.99	G (0.29)	0.66 ± 0.13 (7x10⁻⁷)	0.0	-	-	-	-
rs7342028/ intron	<i>VTG1A</i>	10 (114,469,252)	EA (8)	T (0.27)	0.48 ± 0.08 (5x10⁻¹⁰)	0.0	-	T (0.54)	0.18 ± 0.12 (0.12)	0.0	0.81	1.0	0.44	0.46
rs7907361/ intron	<i>VTG1A</i>	10 (114,458,127)	AA	G (0.74)	-0.47 ± 0.08 (1x10⁻⁹)	0.0	0.96	G (0.47)	-0.39 ± 0.12 (9x10 ⁻⁴)	23.8	-	-	-	-
rs4687718/ intron	<i>TKT</i>	3 (53,257,343)	EA (8)	A (0.14)	-0.63 ± 0.11 (6x10⁻⁹)	0.0	-	A (0.53)	-0.06 ± 0.12 (0.64)	0.0	0.98	ND	0.05	0.02
rs9311496/ intron	<i>TKT</i>	3 (53,347,118)	AA	A (0.001)	0.46 ± 4.49 (0.92)	0.0	0.00	A (0.06)	-0.48 ± 0.26 (0.06)	0.0	-	-	-	-
rs17391905/ intron	<i>CDKN2C</i>	1	EA	G	-1.35 ± 0.23	4.0	-	G	-0.12 ± 0.26	0.0	0.99	0.13	0.02	ND

intergenic	(51,318,728)	(8)	(0.05)	(9x10⁻⁹)				(0.07)	(0.65)				
rs11205809/ <i>CDKN2C</i>	1	AA	A	0.11 ± 0.10	6.6	0.90		A	0.42 ± 0.12	0.0	-	-	-
intergenic	(51,273,357)		(0.84)	(0.25)				(0.48)	(8x10 ⁻⁴)				

^a CA = coded effect allele. Freq = frequency.

^b Power to detect effect size reported in COGENT/CARe results using the effect allele frequency and trait variance as observed in European samples and keeping $\alpha=0.002$ adjusting for 22 SNPs.

^c Power to detect effect size reported in European discovery population using the effect allele frequency and trait variance as observed in African-American samples and keeping $\alpha=0.002$ adjusting for 30 SNPs.

^d LD between AA and EA index SNPs. ND indicates the SNP was not genotyped in the HapMap population or was monomorphic.

^e In non-African ancestry discovery rows, significance was based on the genome-wide discovery threshold and P-values $\leq 5.0 \times 10^{-8}$ were bolded. In African ancestry discovery rows, significance was based on the replication threshold and P-values ≤ 0.002 were bolded. β and SE expressed in units of milliseconds.

^f Heterogeneity I^2 statistics bolded if the Cochran's X^2 P-value ≤ 0.05 .

^g In non-African ancestry discovery rows, significance was based on replication of the 30 previously identified SNPs and P-values ≤ 0.002 were bolded. In African ancestry discovery rows, significance was based on discovery within the 22 loci and P-values $\leq 1.4 \times 10^{-5}$ were bolded. β and SE expressed in units of milliseconds.

^h Position based on NCBI reference sequence build 36.

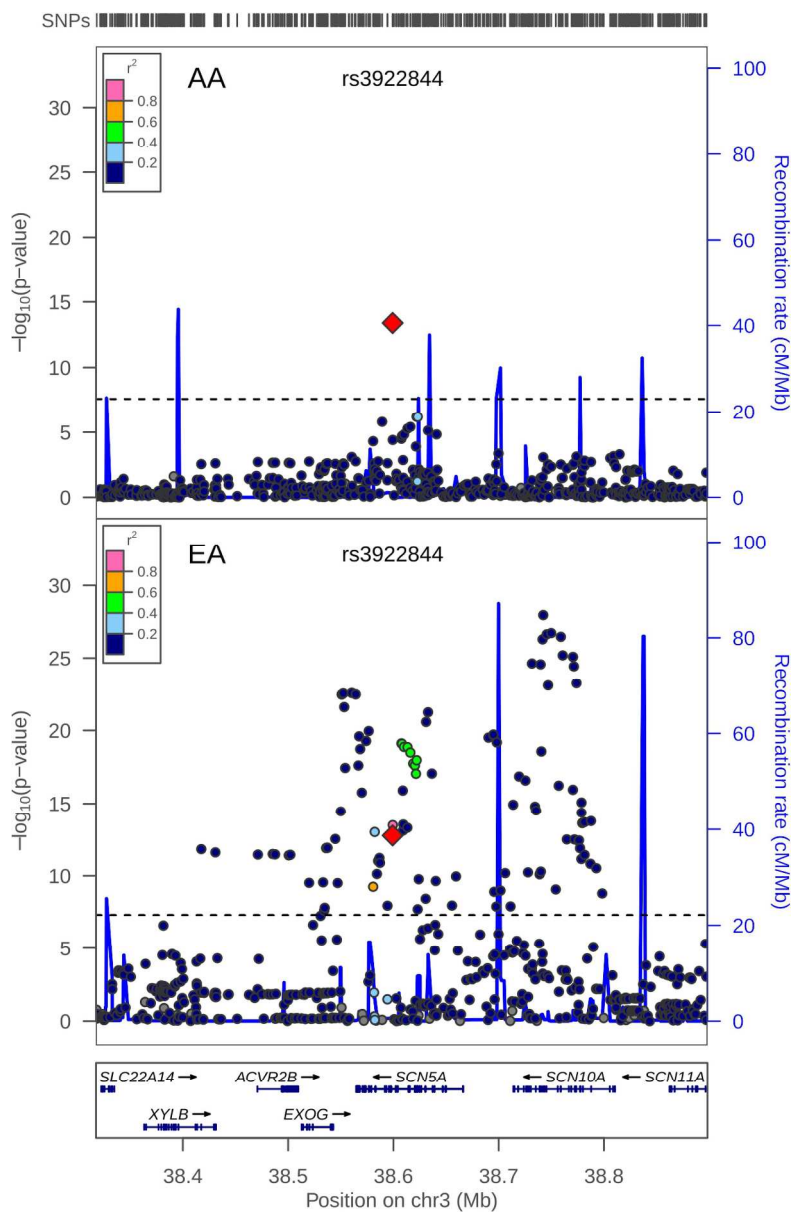


Fig 1. Regional association plot at SCN5A/SCN10A locus. African American SNP association meta-analysis results are plotted in the top panel, and meta-analysis results from cohorts of European ancestry are plotted in the bottom panel. The AA index SNP (rs3922844) is designated by a red diamond in both panels. The LD (r^2) shown is relative to the AA index SNP and is based on HapMap YRI in the top panel and HapMap CEU in the bottom panel. Gray circles are SNPs without HapMap LD data. The X-axis marks the chromosomal position. Recombination rates estimated from African Americans and HapMap CEU individuals are shown in the top and bottom panels, respectively. The dashed horizontal lines in the top and bottom panels mark the GWAS significance level in African Americans (2.5×10^{-8}) and populations of European descent (5.0×10^{-8}), respectively.

Fig. 1
177x272mm (300 x 300 DPI)

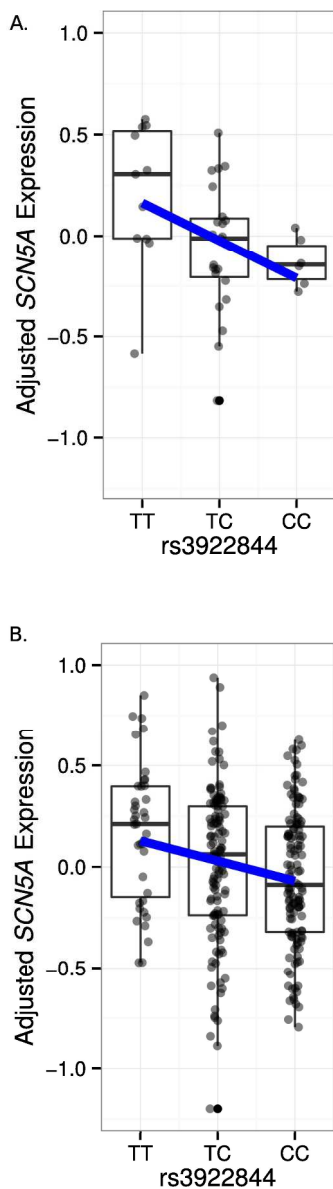


Fig 2. Association between rs3922844 genotype and SCN5A expression in human atrial tissue. Box plots display data from individuals of African ancestry (A) and European ancestry (B). Plotted along the Y-axis are RNA levels adjusted for covariates. The bottom and top of each box indicates the 25th and 75th percentiles, and the band within the box is the median. Whiskers extend to the most extreme value or the most extreme value within 1.5*interquartile range (IQR), whichever value is closer to the median. The fitted regression line is shown in blue.

Fig. 2

204x578mm (300 x 300 DPI)

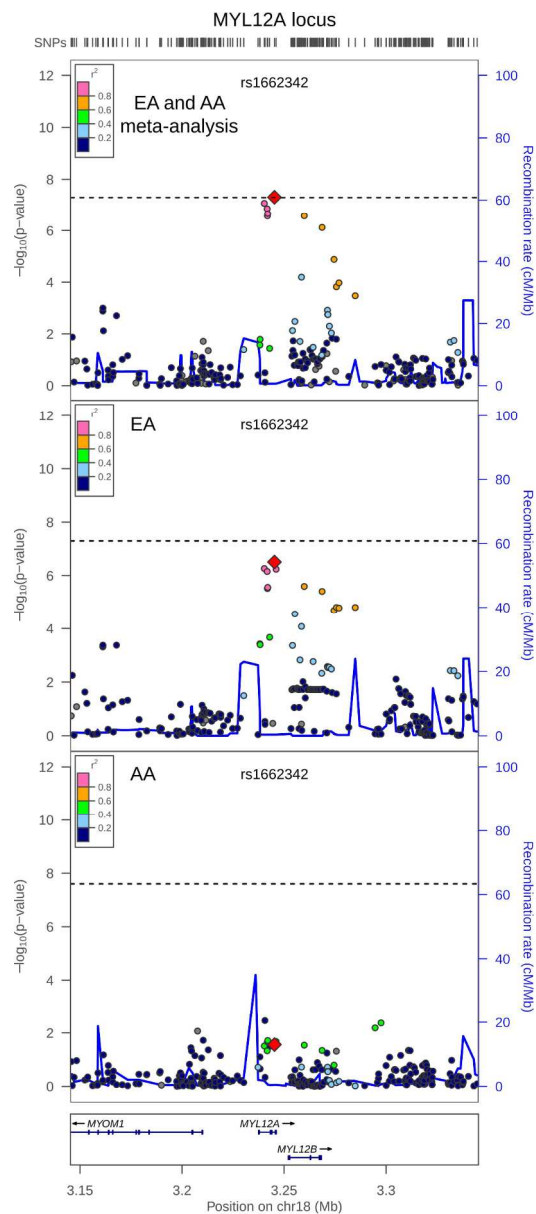


Fig 3. Regional association plot of transethnic meta-analysis results at MYL12A locus. Transethnic meta-analysis SNP association results are plotted in the top panel, meta-analysis results from cohorts of European ancestry are plotted in the middle panel, and African American SNP association meta-analysis results are plotted in the bottom panel. The transethnic index SNP (rs1662342) is designated by a red diamond in all panels. The LD (r^2) shown is relative to the index SNP and is based on HapMap CEU in the top and middle panels and is based on HapMap YRI in the bottom panel. Gray circles are SNPs without HapMap LD data. The X-axis marks the chromosomal position. Recombination rates averaged across HapMap populations, in HapMap CEU individuals, and in African Americans are shown in the top panel, middle panel, and bottom panel, respectively. The dashed horizontal line in the top and middle panels marks the GWAS significance level for European ancestry (5.0×10^{-8}) and in the bottom panel marks the GWAS significance level for African Americans (2.5×10^{-8}).

Fig. 3
222x512mm (300 x 300 DPI)

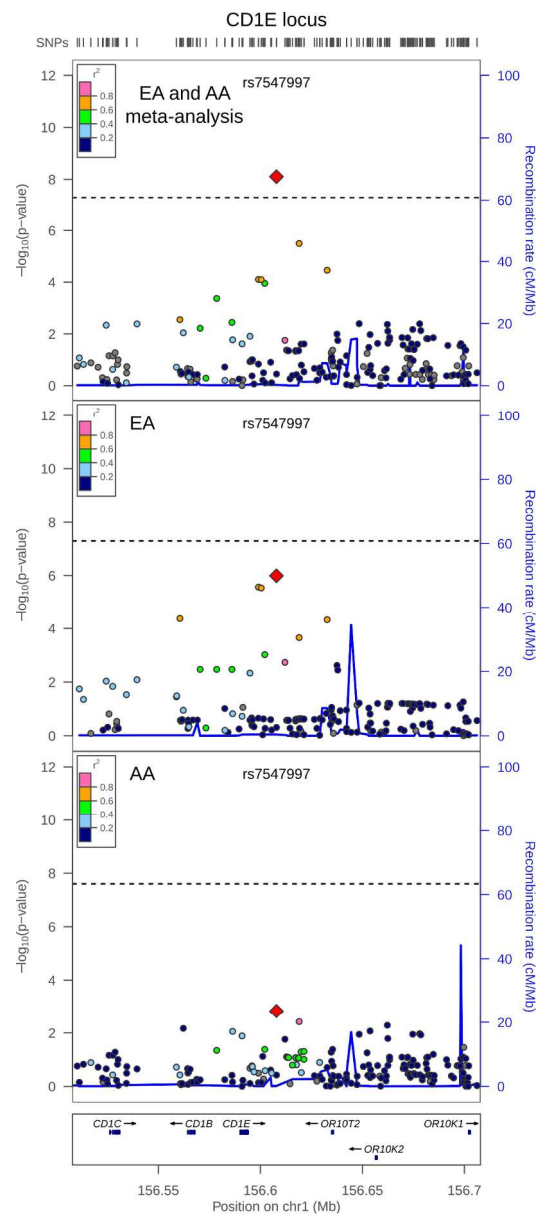


Fig 4. Regional association plot of transethnic meta-analysis results at chromosome 1q23.1. Transethnic meta-analysis SNP association results are plotted in the top panel, meta-analysis results from cohorts of European ancestry are plotted in the middle panel, and African American SNP association meta-analysis results are plotted in the bottom panel. The transethnic index SNP (rs7547997) is designated by a red diamond in all panels. The LD (r^2) shown is relative to the index SNP and is based on HapMap CEU in the top and middle panels and is based on HapMap YRI in the bottom panel. Gray circles are SNPs without HapMap LD data. The X-axis marks the chromosomal position. Recombination rates averaged across HapMap populations, in HapMap CEU individuals, and in African Americans are shown in the top panel, middle panel, and bottom panel, respectively. The dashed horizontal line in the top and middle panels marks the GWAS significance level for European ancestry (5.0×10^{-8}) and in the bottom panel marks the GWAS significance level for African Americans (2.5×10^{-8}).

Fig. 4
222x512mm (300 x 300 DPI)

Supplementary Material

Supplementary Tables

S1 Table. Genotyping, imputation, QC, and association methods of participating studies.

S2 Table. Study participant characteristics.

S3 Table. Association between QRS duration and European genetic ancestry.

S4 Table. Functional annotation of rs3922844 and variants in LD using data from ENCODE and Roadmap Epigenomics.

S5 Table. Most significant SNP associations from transethnic meta-analysis at 22 previously identified QRS loci.

S6 Table. SNP replication results without adequate power (Power < 0.8) from GWAS in African Americans.

S7 Table. Counts of SNPs in linkage equilibrium by MAF interval within the *SCN10A* region in populations of European and African descent.

S8 Table. 95% credible sets at genome-wide significant QRS loci.

Legends to Supplementary Figures

S1 Fig. QQ plot of P-values from WHI data unadjusted for genomic control.

S2 Fig. QQ plot of P-values from ARIC data unadjusted for genomic control.

S3 Fig. QQ plot of P-values from JHS data unadjusted for genomic control.

S4 Fig. QQ plot of P-values from MESA data unadjusted for genomic control.

S5 Fig. QQ plot of P-values from HABC data unadjusted for genomic control.

S6 Fig. QQ plot of P-values from HANDLS data unadjusted for genomic control.

S7 Fig. QQ plot of P-values from CHS data unadjusted for genomic control.

- S8 Fig. QQ plot of P-values from CFS data unadjusted for genomic control.**
- S9 Fig. QQ plot of P-values from BLSA data unadjusted for genomic control.**
- S10 Fig. QQ plot of P-values from BHS data unadjusted for genomic control.**
- S11 Fig. QQ plot of meta-analysis P-values from African Americans.**
- S12 Fig. Manhattan plot of GWAS meta-analysis in African Americans.**
- S13 Fig. Functional annotation of *SCN5A* region using ENCODE data.**
- S14 Fig. Functional annotation of *SCN5A* region using data from a Roadmap Epigenomics heart sample.**
- S15 Fig. QQ plot of transeethnic meta-analysis P-values.**
- S16 Fig. Manhattan plot of transeethnic meta-analysis results.**
- S17 Fig. LD plot of *SCN10A* based on HapMap phase II CEU.**
- S18 Fig. LD plot of *SCN10A* based on HapMap phase II YRI.**
- S19 Fig. LD plot of *SCN10A* based on HapMap phase III ASW.**
- S20 Fig. Regional association plot at *TBX5* locus.**
- S21 Fig. Regional association plot at *NF1A* locus.**

S1 Text.

Descriptions of cohorts and ECG recordings, and methods for genotyping, imputation, quality control, and association analysis.

S1 Table. Genotyping, imputation, QC, and association methods of participating studies.

Characteristic	WHI	ARIC	JHS	MESA	Health ABC	HANDLS	CHS	CFS	BLSA	BHS
Genotyping array	Affymetrix 6.0	Affymetrix 6.0	Affymetrix 6.0	Affymetrix 6.0	Illumina 1M	Illumina 1M ^a	Illumina HumanOmni 1-Quad	Affymetrix 6.0	Illumina 550K	Illumina Human610 and HumanCVD BeadChip
Genotype calling software	Birdseed	Birdseed	Birdseed	Birdseed	BeadStudio	BeadStudio	GenomeStudio	Birdseed	BeadStudio	BeadStudio
Sample call rate exclusion	<95%	<95%	<95%	<95%	<97%	≤95%	<97%	<95%	≤98.5%	<99%
SNP call rate exclusion	<95%	<90%	<90%	<90%	<97%	≤95%	<90%	<90%	≤99%	<90%
SNP MAF exclusion ^b	<1%	<1%	<1%	<1%	<1%	≤1%	None	<1%	≤1%	NA
SNP HWE P-value exclusion ^b	<10 ⁻⁶	NA	NA	NA	<10 ⁻⁶	≤10 ⁻⁷	<10 ⁻⁵	NA	≤10 ⁻⁴	NA
Genotyped autosomal SNPs passing QC	829,370	796,384	868,969	881,666	1,007,948	907,763	963,248	867,495	501,704	608,756
Imputation software	MACH v1.16	BEAGLE version 3.2.1	MACH v1.16	MACH v1.0.16	MACH v1.0.16					
GWAS software	PLINK, ProbABEL	PLINK	PLINK	PLINK	R	R, MACH2QTL	R	R	Merlin	PLINK
NCBI imputation build	36	36	36	36	36	36	36	36	36	36
HapMap Reference Panel	1:1 CEU:YRI phase II	1:1 CEU:YRI phase II and 1:1:1 ASW:CEU:YRI phase 3	1:1 CEU:YRI phase II	1:1 CEU:YRI phase II	1:1 CEU:YRI phase II					
Imputed autosomal SNPs passing QC	2,376,870	2,650,163	2,652,030	2,659,947	2,872,605	2,862,231	2,420,268	2,635,879	2,589,198	2,252,323
GC factor (λ)	1.014	1.003	1.085	1.010	1.012	0.991	1.041	1.142	0.980	1.056

^a Of the 1024 HANDLS participants, 709 participants were genotyped using Illumina 1M and 1M Duo arrays, and 315 participants were genotyped to the equivalent of the 1 million SNP level of coverage using a combination of Illumina 550K, 370K, 510S, and 240S arrays.

^b NA indicates no filter was applied.

S2 Table. Study participant characteristics.

Characteristic (units) ^a	WHI	ARIC	JHS	MESA	Health ABC	HANDLS	CHS	CFS	BLSA	BHS
N ^b	4012	2372	1918	1554	993	945	621	315	153	148
Age (years)	61.5 ± 6.8	53.1 ± 5.8	49.0 ± 11.6	62.0 ± 10.1	73.4 ± 2.9	48.6 ± 9.0	72.6 ± 5.6	39.2 ± 18.0	64.2 ± 11.3	35.4 ± 5.4
Female sex	100	63	61	56	58	56	65	59	63	57
BMI (kg/m ²)	31.6 ± 6.2	29.4 ± 5.9	32.3 ± 7.8	30.1 ± 5.9	28.5 ± 5.4	29.9 ± 8.1	28.4 ± 5.4	32.9 ± 9.5	28.3 ± 5.2	30.5 ± 7.6
Height (cm)	162.6 ± 6.1	167.9 ± 8.9	169.7 ± 9.4	168.2 ± 9.5	165.0 ± 9.5	169.8 ± 9.2	164.2 ± 9.1	166.7 ± 12.3	168.1 ± 8.9	168.6 ± 8.8
QRS duration (ms)	85.3 ± 9.1	94.8 ± 9.4	91.8 ± 9.9	91.1 ± 10.0	88.0 ± 11.1	86.5 ± 9.7	87.8 ± 10.5	89.3 ± 10.3	86.4 ± 8.8	88.4 ± 10.0
European ancestry ^c	0.17 (0.10,0.27)	0.15 (0.11,0.22)	0.16 (0.12, 0.21)	0.19 (0.12, 0.30)	0.19 (0.12, 0.28)	0.16 (0.11, 0.22)	ND	0.18 (0.13, 0.26)	ND	ND

^a Female sex presented as a percentage, percent European ancestry presented as the median (1st, 3rd quartiles), and all other characteristics presented as mean ± standard deviation.

^b Number of participants with ECG and genome-wide genotype data after phenotypic exclusions.

^c ND = not determined.

S3 Table. Association between QRS duration and European genetic ancestry.

Trait	WHI N = 4012 $\beta \pm SE$ (P-value)	ARIC N = 2372 $\beta \pm SE$ (P-value)	JHS N = 1917 $\beta \pm SE$ (P-value)	MESA N = 1554 $\beta \pm SE$ (P-value)	Health ABC N = 945 $\beta \pm SE$ (P-value)	HANDLS N = 945 $\beta \pm SE$ (P-value)	CFS N = 314 $\beta \pm SE$ (P-value)	Meta-analysis $\beta \pm SE$ (P-value)
QRS duration ^a	0.78 ± 1.06 (0.46)	-1.01 ± 1.70 (0.55)	1.19 ± 2.50 (0.63)	1.92 ± 1.74 (0.27)	0.76 ± 2.76 (0.78)	5.57 ± 3.39 (0.10)	7.47 ± 5.33 (0.16)	1.02 ± 0.71 (0.15)

^a Adjusted for age, sex, BMI, height, and study site (if applicable). β and SE expressed in units of milliseconds.

S4 Table. Functional annotation of rs3922844 and variants in LD using data from ENCODE and Roadmap Epigenomics.

rsID	Position (hg19)	LD (r ²) ^a	Tissues with DHS overlap ^b	Tissues with enhancer histone mark overlap ^c	Altered motifs
rs3922844	38624253	NA	hepatocytes, osteoblasts	fetal heart, fetal brain, liver, brain-germinal matrix and anterior caudate, neurosphere CC cortex derived and ganglionic derived	Myc_known3;Pou1f1_1; Pou2f2_known8; Pou5f1_disc2;TFE;XBP-1_1
rs3922843	38624343	0.24	hepatocytes	fetal heart, fetal brain, liver, brain-germinal matrix and anterior caudate, neurosphere CC cortex derived and ganglionic derived	BHLHE40_disc1;MZF1::1-4_3;SMC3_disc1;TATA_disc4
rs6772989	38623703	0.21	fibroblasts, medulloblastoma	fetal heart, fetal brain, liver, brain-germinal matrix and anterior caudate and mid-frontal lobe and angular gyrus, neurosphere CC cortex derived and ganglionic derived, H1-derived CD184+ endoderm	CHD2_disc3;EBF_disc2;ERalpha-a_disc4; Egr-1_disc6;Ets_disc9;NF-kappaB_disc2; NRSF_disc4;NRSF_disc9;Pax-5_known3;Pou2f2_disc2;SP1_disc3; TATA_disc7;TCF12_disc5; Znf143_disc3;Znf143_disc4
rs6773076	38623752	0.22	prostate adenocarcinoma (LNCap), fibroblasts, medulloblastoma	fetal heart, liver, brain-germinal matrix and anterior caudate and mid-frontal lobe and angular gyrus, neurosphere CC cortex derived and ganglionic derived, H1-derived CD184+ endoderm	None
rs9870213	38623284	0.26	chorion, pancreatic islets, primary tracheal epithelial cells	fetal heart, liver, brain-germinal matrix and anterior caudate and mid-frontal lobe and angular gyrus and hippocampus middle and substantia nigra and inferior temporal lobe, neurosphere CC cortex derived and ganglionic derived, skeletal muscle, ES cell	ERalpha-a_disc4;MZF1::1-4_2; Maf_known2;PLAG1;PPAR_2;Pbx3_disc2;Sin3Ak-20_disc6;VDR_2

^a LD calculated from 1000 genomes phase 1 AFR population

^b ENCODE narrow peaks of DNase I hypersensitive site

^c Enhancer defined from chromatin state segmentation using Roadmap Epigenomics data.

S5 Table. Most significant SNP associations from transethnic meta-analysis at 22 previously identified QRS loci.

Locus	Nearby gene	SNP	CA/RefA ^a	Transethnic meta-analysis ^b				European ancestry ^b			African ancestry ^b		
				β	SE _{GC}	P _{GC}	I ² ^d	CA Freq ^c	β	P _{GC}	CA Freq ^c	β	P _{GC}
1	<i>SCN10A</i>	rs6801957	t/c	0.73	0.06	1.8E-30	0	0.41	0.77	1.1E-28	0.17	0.54	8.4E-04
2	<i>CDKN1A</i>	rs7756236	a/g	-0.75	0.07	6.1E-29	21.8	0.74	-0.83	2.4E-26	0.70	-0.53	3.9E-05
3	<i>PLN</i>	rs11153730	t/c	-0.54	0.06	5.2E-19	9.7	0.51	-0.59	1.3E-18	0.71	-0.32	1.5E-02
4	<i>NFIA</i>	rs2207791	a/g	0.60	0.06	1.3E-22	0	0.52	0.59	1.2E-17	0.69	0.62	1.1E-06
5	<i>HAND1</i>	rs13185595	a/g	-0.53	0.06	3.9E-16	0	0.37	-0.56	8.8E-14	0.53	-0.44	5.2E-04
6	<i>TBX20</i>	rs1362212	a/g	0.68	0.09	1.3E-14	0	0.18	0.69	1.1E-13	0.05	0.61	2.6E-02
7	<i>SIPAIL1</i>	rs12127	t/c	0.50	0.07	6.4E-13	0	0.74	0.49	1.7E-10	0.84	0.55	6.7E-04
8	<i>TBX5</i>	rs883079	t/c	-0.52	0.07	2.0E-15	0	0.71	-0.49	1.3E-10	0.66	-0.60	1.5E-06
9	<i>TBX3</i>	rs3914956	a/t	0.41	0.07	1.4E-09	20.0	0.73	0.48	3.4E-10	0.78	0.17	0.24
10	<i>VTG1A</i>	rs7907361	c/g	0.45	0.07	6.3E-12	0	0.26	0.47	1.1E-09	0.53	0.39	9.3E-04
11	<i>SETBP1</i>	rs991014	t/c	0.43	0.06	1.2E-12	0	0.42	0.42	6.2E-10	0.25	0.50	2.9E-04
12	<i>STRN</i>	rs17020136	t/c	-0.48	0.08	1.8E-09	0	0.79	-0.51	1.9E-09	0.91	-0.27	0.21
13	<i>TKT</i>	rs4687718	a/g	-0.38	0.08	3.3E-06	75.1	0.14	-0.63	6.3E-09	0.53	-0.06	0.64
14	<i>CRIM1</i>	rs1523787	a/g	0.38	0.06	1.2E-10	0	0.40	0.39	9.7E-09	0.55	0.36	2.7E-03
15	<i>CDKN2C</i>	rs17391905	t/g	0.80	0.18	4.9E-06	75.3	0.95	1.35	8.7E-09	0.93	0.12	0.65
16	<i>PRKCA</i>	rs9912468	c/g	-0.38	0.06	1.4E-10	0	0.57	-0.39	1.1E-08	0.62	-0.37	2.8E-03
17	<i>IGFBP3</i>	rs7784776	a/g	-0.36	0.06	2.3E-09	0	0.57	-0.39	1.4E-08	0.59	-0.26	2.9E-02
18	<i>CASQ2</i>	rs10923445	t/c	0.39	0.07	8.0E-09	0	0.75	0.44	3.0E-08	0.73	0.25	0.06
19	<i>KLF12</i>	rs9573330	a/g	-0.40	0.06	4.0E-10	0	0.37	-0.40	4.5E-08	0.33	-0.40	2.0E-03
20	<i>LRIG1</i>	rs2242285	a/g	0.32	0.06	1.2E-07	0	0.42	0.37	4.8E-08	0.28	0.14	0.30
21	<i>DKK1</i>	rs1733724	a/g	0.48	0.09	7.3E-08	0	0.25	0.49	1.3E-07	0.05	0.46	0.23
22	<i>GOSR2</i>	rs17608766	t/c	-0.48	0.10	1.9E-06	11.3	0.84	-0.53	3.7E-07	0.97	0.32	0.48

^a CA = coded effect allele. RefA = reference allele.

^b β and/or SE expressed in units of milliseconds.

^c Freq = frequency.

^d Heterogeneity I² statistics bolded if the Cochran's X² P-value \leq 0.05.

S6 Table. SNP replication results without adequate power (Power < 0.8) from GWAS in African Americans.

Index SNP/ annotation	Nearby gene	Chr (Position) ^b	Discovery population (Ref)	European ancestry				African ancestry				LD (r ²) ^d		
				CA (Freq) ^a	$\beta \pm SE_{GC}$ (P_{GC}) ^e	I ² ^f	Power ^b	CA (Freq) [†]	$\beta \pm SE_{GC}$ (P_{GC}) ^g	I ² ^f	Power ^c	CEU	YRI	ASW
rs1362212/ intergenic	<i>TBX20</i>	7 (35,271,831)	EA [7]	A (0.18)	0.69 ± 0.09 (1x10⁻¹³)	0.0	-	A (0.05)	0.61 ± 0.27 (0.03)	28.2	0.27	0.01	0.01	ND
rs1364733/ intergenic	<i>TBX20</i>	7 (35,363,030)	AA	T (0.33)	0.32 ± 0.07 (8x10⁻⁶)	16.6	0.99	T (0.34)	0.45 ± 0.14 (8x10 ⁻⁴)	26.9	-	-	-	-
rs11848785/ intron	<i>SIPAIL1</i>	14 (71,127,108)	EA [7]	G (0.27)	-0.50 ± 0.08 (1x10⁻¹⁰)	0.0	-	G (0.08)	-0.61 ± 0.22 (5x10 ⁻³)	16.2	0.19	ND	ND	ND
rs11627918/ intron	<i>SIPAIL1</i>	14 (70,794,161)	AA	C (0.25)	-0.39 ± 0.08 (6x10⁻⁷)	0.0	0.99	C (0.25)	-0.49 ± 0.14 (3x10 ⁻⁴)	15.4	-	-	-	-
rs10850409/ intergenic	<i>TBX3</i>	12 (113,866,123)	EA [7]	A (0.27)	-0.49 ± 0.08 (3x10⁻¹⁰)	0.0	-	A (0.24)	-0.11 ± 0.15 (0.49)	15.5	0.64	0.09	0.00	ND
rs11067352/ intergenic	<i>TBX3</i>	12 (113,902,694)	AA	G (0.05)	-0.54 ± 0.22 (0.01)	31.2	0.99	G (0.02)	1.21 ± 0.52 (0.02)	0.0	-	-	-	-
rs991014/ intron	<i>SETBP1</i>	18 (40,693,884)	EA [7]	T (0.42)	0.42 ± 0.07 (6x10⁻¹⁰)	0.0	-	T (0.25)	0.50 ± 0.14 (3x10⁻⁴)	0.0	0.46	-	-	-
rs991014/ intron	<i>SETBP1</i>	18 (40,693,884)	AA	T (0.42)	0.42 ± 0.07 (6x10⁻¹⁰)	0.0	0.99	T (0.25)	0.50 ± 0.14 (3x10 ⁻⁴)	0.0	-	-	-	-
rs17020136/ intron	<i>STRN</i>	2 (37,101,519)	EA [7]	C (0.21)	0.51 ± 0.08 (2x10⁻⁹)	0.0	-	C (0.09)	0.27 ± 0.21 (0.21)	32.1	0.24	ND	ND	ND
rs1468810/ intron	<i>STRN</i>	2 (36,847,444)	AA	A (0.59)	0.01 ± 0.07 (0.92)	29.1	0.99	A (0.20)	-0.65 ± 0.17 (9x10 ⁻⁵)	0.0	-	-	-	-
rs7562790/ intron	<i>CRIMI</i>	2 (36,527,059)	EA [7]	G (0.40)	0.39 ± 0.07 (8x10⁻⁹)	0.0	-	G (0.59)	0.29 ± 0.12 (0.01)	0.7	0.53	0.14	0.27	0.29
rs17018693/ intron	<i>CRIMI</i>	2 (36,476,410)	AA	C (0.11)	0.32 ± 0.12 (0.007)	0.0	0.95	C (0.34)	0.53 ± 0.13 (2x10 ⁻⁵)	0.0	-	-	-	-
rs9912468/ intron	<i>PRKCA</i>	17 (61,748,819)	EA [7]	G (0.43)	0.39 ± 0.07 (1x10⁻⁸)	28.2	-	G (0.38)	0.37 ± 0.12 (3x10 ⁻³)	0.0	0.51	0.03	0.18	0.01
rs8178822/ 5'UTR	<i>PRKCA</i> / <i>APOH</i>	17 (61,655,991)	AA	T (0.07)	0.04 ± 0.13 (0.75)	10.8	0.97	T (0.07)	0.69 ± 0.22 (0.002)	0.0	-	-	-	-
rs7784776/ intergenic	<i>IGFBP3</i>	7 (46,586,670)	EA [7]	G (0.43)	0.39 ± 0.07 (1x10⁻⁸)	0.0	-	G (0.41)	0.26 ± 0.12 (0.03)	0.0	0.53	0.01	0.00	ND
rs856567/ intergenic	<i>IGFBP3</i>	7 (46,687,973)	AA	C (0.56)	-0.08 ± 0.07 (0.23)	0.0	0.80	C (0.44)	-0.28 ± 0.12 (0.02)	48.5	-	-	-	-

rs4074536/ missense	<i>CASQ2</i>	1 (116,112,490)	EA [7]	C (0.29)	-0.42 ± 0.07 (2×10^{-8})	0.5	-	C (0.44)	0.06 ± 0.12 (0.61)	0.0	0.54	0.02	0.03	ND
rs12083270/ intron	<i>CASQ2</i>	1 (116,087,211)	AA	A (0.002)	-2.02 ± 1.45 (0.16)	0.0	0.02	A (0.05)	0.79 ± 0.27 (0.003)	0.0	-	-	-	-
rs1886512/ intron	<i>KLF12</i>	13 (73,418,187)	EA [7]	A (0.37)	-0.40 ± 0.07 (4×10^{-8})	0.0	-	A (0.47)	-0.34 ± 0.12 (6×10^{-3})	0.0	0.58	0.74	0.66	ND
rs17061772/ intron	<i>KLF12</i>	13 (73,437,170)	AA	A (0.33)	-0.30 ± 0.07 (4×10^{-5})	0.0	0.98	A (0.35)	-0.39 ± 0.12 (0.002)	0.0	-	-	-	-
rs2242285/ intron	<i>LRIG1</i>	3 (66,514,292)	EA [7]	A (0.42)	0.37 ± 0.07 (5×10^{-8})	35.4	-	A (0.28)	0.14 ± 0.13 (0.30)	0.0	0.36	0.32	0.01	0.10
rs12633819/ intron	<i>LRIG1</i>	3 (66,530,997)	AA	G (0.36)	-0.28 ± 0.07 (1×10^{-4})	46.6	0.97	G (0.32)	-0.37 ± 0.13 (0.004)	2.0	-	-	-	-
rs1733724/ intergenic	<i>DKK1</i>	10 (53,893,983)	EA [7]	A (0.25)	0.49 ± 0.09 (1×10^{-7})	0.0	-	A (0.05)	0.46 ± 0.39 (0.23)	0.0	0.09	0.01	ND	ND
rs7092403/ intergenic	<i>DKK1</i>	10 (53,796,158)	AA	C (0.05)	0.14 ± 0.23 (0.54)	0.0	0.32	C (0.32)	-0.42 ± 0.15 (0.005)	0.0	-	-	-	-
rs17608766/ intron	<i>GOSR2</i>	17 (42,368,270)	EA [7]	C (0.16)	0.53 ± 0.10 (4×10^{-7})	13.8	-	C (0.03)	-0.32 ± 0.45 (0.48)	15.3	0.05	0.48	ND	ND
rs16941434/ intergenic	<i>GOSR2</i>	17 (42,424,057)	AA	T (0.21)	0.23 ± 0.08 (0.005)	19.0	0.99	T (0.07)	-0.58 ± 0.23 (0.01)	0.0	-	-	-	-

^a CA = coded effect allele. Freq = frequency.

^b Power to detect effect size reported in COGENT/CARe results using the effect allele frequency and trait variance as observed in European samples and keeping $\alpha=0.002$ adjusting for 22 SNPs.

^c Power to detect effect size reported in European discovery population using the effect allele frequency and trait variance as observed in African-American samples and keeping $\alpha=0.002$ adjusting for 30 SNPs.

^d LD between AA and EA index SNPs. ND indicates the SNP was not genotyped in the HapMap population or was monomorphic. For *SIPAIL1* and *SETBP1*, EA and AA index SNPs were greater than 250 kb apart and LD was not determined by HapMap.

^e In non-African ancestry discovery rows, significance was based on the genome-wide discovery threshold and P-values $\leq 5.0 \times 10^{-8}$ were bolded. In African ancestry discovery rows, significance was based on the replication threshold and P-values ≤ 0.002 were bolded. β and SE expressed in units of milliseconds.

^f Heterogeneity I^2 statistics bolded if the Cochran's X^2 P-value ≤ 0.05 .

^g In non-African ancestry discovery rows, significance was based on replication of the 30 previously identified SNPs and P-values ≤ 0.002 were bolded. In African ancestry discovery rows, significance was based on discovery within the 22 loci and P-values $\leq 1.4 \times 10^{-5}$ were bolded. β and SE expressed in units of milliseconds.

^h Position based on NCBI reference sequence build 36.

S7 Table. Counts of SNPs in linkage equilibrium by MAF interval within the *SCN10A* region in populations of European and African descent.

Population	MAF intervals					P-value ^a
	[0.01, 0.1]	(0.1, 0.2]	(0.2, 0.3]	(0.3, 0.4]	(0.4, 0.5]	
European ancestry	11	15	12	13	10	> 0.05
African ancestry	28	27	17	16	15	

^a Chi-squared test of independence, 2000 rounds of Monte-Carlo simulation.

S8 Table. 95% credible sets at genome-wide significant QRS loci.

Locus	Nearby gene	Interval of genome-wide significant SNPs in EA ^a			Transethnic 95% CS ^b		
		position start ^c	position end ^c	length ^d	position start ^c	position end ^c	length ^d
1	<i>SCN5A</i>	38417508	38798319	380811	38742319	38742319	0
2	<i>CDKN1A</i>	36721790	36778378	56588	36731357	36736931	5574
3	<i>PLN</i>	118663228	119134018	470790	118774215	119095055	320840
4	<i>NFIA</i>	61645834	61670555	24721	61667490	61670555	3065
5	<i>HAND1</i>	153849233	153852363	3130	153852363	153852363	0
6	<i>TBX20</i>	35200065	35320785	120720	35246929	35307511	60582
7	<i>SIPA1L1</i>	70818106	71232731	414625	70840238	71127108	286870
8	<i>TBX5</i>	113101891	113312090	210199	113274883	113291418	16535
9	<i>TBX3</i>	113828468	113866123	37655	113841386	113866123	24737
10	<i>VTG1A</i>	114447090	114506363	59273	114456833	114496282	39449
11	<i>SETBP1</i>	40641066	40693884	52818	40685242	40693884	8642
12	<i>STRN</i>	36921932	37101519	179587	36952843	37110890	158047
13	<i>TKT</i>	53257343	53257343	0	53257343	53257343	0
14	<i>CRMI</i>	36467811	36535123	67312	36497732	36535123	37391
15	<i>CDKN2C</i>	51114254	51530562	416308	51318728	51623389	304661
16	<i>PRKCA</i>	61734255	61748819	14564	61737476	61748819	11343
17	<i>IGFBP3</i>	46583301	46607425	24124	46583301	46607425	24124
18	<i>CASQ2</i>	116112341	116134634	22293	116102542	116126742	24200
19	<i>KLF12</i>	73411123	73418187	7064	73409992	73416211	6219
20	<i>LRIG1</i>	66514292	66514292	0	66502192	66516366	14174
21	<i>DKK1</i>	53893983	53893983	0	53893983	53893983	0
22	<i>GOSR2</i>	42368270	42368270	0	42368270	42368270	0
23	<i>MYL12A</i>	3245301	3245301	NA	3240326	3259893	19567
24	<i>SPTA1</i>	156607897	156607897	NA	156607897	156607897	0

^a EA = European Ancestry.^b CS = Credible Sets.^c Position based on NCBI reference sequence build 36.^d Length of 0 indicates a single SNP was genome-wide significant at the locus or a single SNP had a posterior probability $\geq 95\%$ at the locus. NA = not applicable; loci 23 and 24 were genome-wide significant in the transethnic meta-analysis only.

Legends to Supplementary Figures

S1 Fig. QQ plot of P-values from WHI data unadjusted for genomic control. The X-axis marks the expected quantiles, the left-hand Y-axis marks the observed quantiles, and the right-hand Y-axis marks the P-values corresponding to the observed quantiles. A line originating from the origin and having a slope of 1 is shown in red. The 95% probability bounds for each order statistic are shaded in gray.

S2 Fig. QQ plot of P-values from ARIC data unadjusted for genomic control. The X-axis marks the expected quantiles, the left-hand Y-axis marks the observed quantiles, and the right-hand Y-axis marks the P-values corresponding to the observed quantiles. A line originating from the origin and having a slope of 1 is shown in red. The 95% probability bounds for each order statistic are shaded in gray.

S3 Fig. QQ plot of P-values from JHS data unadjusted for genomic control. The X-axis marks the expected quantiles, the left-hand Y-axis marks the observed quantiles, and the right-hand Y-axis marks the P-values corresponding to the observed quantiles. A line originating from the origin and having a slope of 1 is shown in red. The 95% probability bounds for each order statistic are shaded in gray.

S4 Fig. QQ plot of P-values from MESA data unadjusted for genomic control. The X-axis marks the expected quantiles, the left-hand Y-axis marks the observed quantiles, and the right-hand Y-axis marks the P-values corresponding to the observed quantiles. A line originating from the origin and having a slope of 1 is shown in red. The 95% probability bounds for each order statistic are shaded in gray.

S5 Fig. QQ plot of P-values from HABC data unadjusted for genomic control. The X-axis marks the expected quantiles, the left-hand Y-axis marks the observed quantiles, and the right-

hand Y-axis marks the P-values corresponding to the observed quantiles. A line originating from the origin and having a slope of 1 is shown in red. The 95% probability bounds for each order statistic are shaded in gray.

S6 Fig. QQ plot of P-values from HANDLS data unadjusted for genomic control. The X-axis marks the expected quantiles, the left-hand Y-axis marks the observed quantiles, and the right-hand Y-axis marks the P-values corresponding to the observed quantiles. A line originating from the origin and having a slope of 1 is shown in red. The 95% probability bounds for each order statistic are shaded in gray.

S7 Fig. QQ plot of P-values from CHS data unadjusted for genomic control. The X-axis marks the expected quantiles, the left-hand Y-axis marks the observed quantiles, and the right-hand Y-axis marks the P-values corresponding to the observed quantiles. A line originating from the origin and having a slope of 1 is shown in red. The 95% probability bounds for each order statistic are shaded in gray.

S8 Fig. QQ plot of P-values from CFS data unadjusted for genomic control. The X-axis marks the expected quantiles, the left-hand Y-axis marks the observed quantiles, and the right-hand Y-axis marks the P-values corresponding to the observed quantiles. A line originating from the origin and having a slope of 1 is shown in red. The 95% probability bounds for each order statistic are shaded in gray.

S9 Fig. QQ plot of P-values from BLSA data unadjusted for genomic control. The X-axis marks the expected quantiles, the left-hand Y-axis marks the observed quantiles, and the right-hand Y-axis marks the P-values corresponding to the observed quantiles. A line originating from the origin and having a slope of 1 is shown in red. The 95% probability bounds for each order statistic are shaded in gray.

S10 Fig. QQ plot of P-values from BHS data unadjusted for genomic control. The X-axis marks the expected quantiles, the left-hand Y-axis marks the observed quantiles, and the right-hand Y-axis marks the P-values corresponding to the observed quantiles. A line originating from the origin and having a slope of 1 is shown in red. The 95% probability bounds for each order statistic are shaded in gray.

S11 Fig. QQ plot of meta-analysis P-values from African Americans. P-values adjusted for genomic control at the study level but not at the meta-analysis level. The X-axis marks the expected quantiles, the left-hand Y-axis marks the observed quantiles, and the right-hand Y-axis marks the P-values corresponding to the observed quantiles. A line originating from the origin and having a slope of 1 is shown in red. The 95% probability bounds for each order statistic are shaded in gray.

S12 Fig. Manhattan plot of GWAS meta-analysis in African Americans. Plotted P-values are genomic control-corrected at the level of the study and the meta-analysis. Red points mark the region harboring a genome-wide significant association ($P \leq 2.5 \times 10^{-8}$). Genome-wide significant SNP ID indicated.

S13 Fig. Functional annotation of *SCN5A* region using ENCODE data. Gene annotations from GENCODE version 19, and genomic coordinates based on hg 19. Location of rs3922844 indicated in red. Layered Histone H3 Lysine 4 mono-methylation from 7 ENCODE cell lines and transcription factor ChIP-Seq from 72 ENCODE cell lines.

S14 Fig. Functional annotation of *SCN5A* region using data from a Roadmap Epigenomics heart sample. Gene annotations from GENCODE version 7, and genomic coordinates based on hg 19. Location of rs3922844 indicated in red. DNase I hypersensitive sites (DHS) and Histone H3 Lysine 4 mono-methylation from the same male fetal heart donor (H-23524).

S15 Fig. QQ plot of transethnic meta-analysis P-values. P-values adjusted for genomic control at the study level but not at the meta-analysis level. The X-axis marks the expected quantiles, the left-hand Y-axis marks the observed quantiles, and the right-hand Y-axis marks the P-values corresponding to the observed quantiles. A line originating from the origin and having a slope of 1 is shown in red. The 95% probability bounds for each order statistic are shaded in gray.

S16 Fig. Manhattan plot of transethnic meta-analysis results. Plotted P-values are double genomic control-corrected. Red points mark regions harboring genome-wide significant associations ($P \leq 5 \times 10^{-8}$). Candidate genes are indicated at each genome-wide significant locus.

S17 Fig. LD plot of *SCN10A* based on HapMap phase II CEU. LD measured in r^2 is displayed.

S18 Fig. LD plot of *SCN10A* based on HapMap phase II YRI. LD measured in r^2 is displayed.

S19 Fig. LD plot of *SCN10A* based on HapMap phase III ASW. LD measured in r^2 is displayed.

S20 Fig. Regional association plot at *TBX5* locus. African American SNP association meta-analysis results are plotted in the top panel, and meta-analysis results from cohorts of European ancestry are plotted in the bottom panel. The AA index SNP (rs7312625) is designated by a red diamond in both panels. The LD (r^2) shown is relative to the AA index SNP and is based on HapMap YRI in the top panel and HapMap CEU in the bottom panel. Gray circles are SNPs without HapMap LD data. The X-axis marks the chromosomal position. Recombination rates estimated from African Americans and HapMap CEU individuals are shown in the top and bottom panels, respectively. The dashed horizontal line in the top panel marks the discovery

significance threshold for the 22 previously discovered loci (1.4×10^{-5}) and in the bottom panel marks the GWAS significance level (5.0×10^{-8}) for European ancestry.

S21 Fig. Regional association plot at *NF1A* locus. African American SNP association meta-analysis results are plotted in the top panel, and meta-analysis results from cohorts of European ancestry are plotted in the bottom panel. The AA index SNP (rs2207791) is designated by a red diamond in both panels. The LD (r^2) shown is relative to the AA index SNP and is based on HapMap YRI in the top panel and HapMap CEU in the bottom panel. Gray circles are SNPs without HapMap LD data. The X-axis marks the chromosomal position. Recombination rates estimated from African Americans and HapMap CEU individuals are shown in the top and bottom panels, respectively. The dashed horizontal line in the top panel marks the discovery significance threshold for the 22 previously discovered loci (1.4×10^{-5}) and in the bottom panel marks the GWAS significance level (5.0×10^{-8}) for European ancestry.

S1 Text

Fine-mapping, Novel Loci Identification, and SNP Association Transferability in a
Genome-Wide Association Study of QRS Duration in African Americans

Descriptions of cohorts and ECG recordings, and methods for genotyping, imputation, quality control, and association analysis.

Cohort descriptions

ARIC. The Atherosclerosis Risk in Communities (ARIC) study is a prospective population-based study of atherosclerosis and cardiovascular disease in 15,792 men and women between 45 and 64 years from four US communities, 4,314 of whom were self-reported black Americans from two of the four communities (Jackson, MS and Forsyth County, NC) (1). Electrocardiographic recordings used in the present study were performed at baseline examinations from 1987-1989. After exclusions, data on 2,372 black individuals with genotypes, information on all covariates and informed consent remained for analyses.

CFS. The Cleveland Family Study (CFS) is a family-based, longitudinal study designed to study the risk factors for sleep apnea (2). Participants were individuals with sleep apnea (probands), their family members, and neighborhood control families. The 632 African Americans with available DNA were genotyped as part of CARE. Electrocardiographic recordings used for the present study were performed at the final exam cycle conducted in a Clinical Research Unit from 2001-2006. After exclusions, 315 individuals remained for analyses.

JHS. The Jackson Heart Study (JHS) is a prospective, community-based study of the causes of the high prevalence of cardiovascular disease in African Americans that includes 5,301 self-reported African Americans recruited from 2000-2004 (3). The cohort comprises residents of the tri-county area (Hinds County, Rankin County, and Madison County) that contains Jackson, MS. The study includes a subsample of unrelated participants (35-84 years) and a nested family-based subcohort (≥ 21 years). Electrocardiographic recordings used in the present study and blood collection for DNA extraction were performed at baseline examinations from 2000-2004. Genotype data were available in 3,030 individuals, including 885 who were also included in the ARIC study. After exclusions, 1,918 individuals with ECG data and not included in ARIC were included in the present analysis.

MESA. The Multi-Ethnic Study of Atherosclerosis (MESA) is a population-based study of the characteristics of subclinical cardiovascular disease that included 6,814 individuals (28% African Americans) free from known cardiovascular disease between 45-84 years recruited from 6 field centers in the US (4). Electrocardiographic recordings used in the present study and blood sampling for DNA extraction were performed at baseline visits from 2000-2002. African Americans constituted 28% of the total sample, of whom 1,554 with genotype and phenotype data remained after exclusions.

WHI. The Women's Health Initiative (WHI) is a long-term national health study of the etiology and prevention of chronic diseases including heart disease, breast and colorectal cancer, and osteoporotic fractures in postmenopausal women. WHI enrolled 161,808 postmenopausal women in an Observational Study or a randomized Clinical Trial between 1993 and 1998 (5). African American clinical trial participants with baseline electrocardiographic recordings and GWAS data from the SNP Health Association Resource (SHARe) funded by the National Heart

Lung and Blood Institute, were included in this study. After exclusions, phenotype and genotype data were available from 4012 self-identified African Americans from SHARe. Additional genotype data were obtained from the PAGE Study which genotyped a subset of WHI African American participants using the MetaboChip array, and imputed MetaboChip genotypes for the non-overlapping African American SHARe participants.

Health ABC. The Health, Aging, and Body Composition Study (Health ABC) is an NIA-sponsored cohort study of the factors that contribute to incident disability and the decline in function of healthier older persons, with a particular emphasis on changes in body composition in old age. Between 4/15/97 and 6/5/98 the Health ABC study recruited 3,075 70-79 year old community-dwelling adults (41% African-American), who were initially free of disabilities related to mobility and activities of daily living. At baseline, all participants reported no difficulty walking a quarter of a mile or walking up 10 steps without resting. Electrocardiographic recordings used in the present study and blood samples used for DNA extraction were from the baseline visit from 1997 to 1998. After exclusions, phenotype and genotype data was available from 993 self-identified black participants.

HANDLS. The Healthy Aging in Neighborhoods of Diversity across the Life Span study (HANDLS) is an interdisciplinary, community-based, prospective longitudinal epidemiologic study examining the influences of race and socioeconomic status (SES) on the development of age-related health disparities among socioeconomically diverse African Americans and whites in Baltimore. This study investigates whether health disparities develop or persist due to differences in SES, differences in race, or their interaction. The HANDLS design is an area probability sample of Baltimore based on the 2000 Census. The study protocol facilitated our ability to recruit 3722 participants from Baltimore, MD. Electrocardiographic recordings used in

the present study were performed at the baseline visit. Genotyping focused on a subset of participants self-reporting as African American was undertaken at the Laboratory of Neurogenetics, National Institute on Aging, National Institutes of Health. In the larger genotyping effort, a small set of self-reported European ancestry samples were included. This research was supported by the Intramural Research Program of the NIH, National Institute on Aging and the National Center on Minority Health and Health Disparities. After exclusions, phenotype and genotype data was available from 945 self-identified African American subjects.

CHS. The Cardiovascular Health Study (CHS) is a population-based cohort study of risk factors for CHD and stroke in adults ≥ 65 years conducted across four field centers (6). The original predominantly Caucasian cohort of 5,201 persons was recruited in 1989-1990 from random samples of the Medicare eligibility lists. Subsequently, an additional predominantly African-American cohort of 687 persons was enrolled for a total sample of 5,888. DNA was extracted from blood samples drawn on all participants at their baseline examination in 1989-90. Electrocardiographic recordings used in the present study were performed at the baseline visit. After exclusions, phenotype and genotype data was available from 621 self-identified African American subjects.

BLSA. The Baltimore longitudinal study on Aging (BLSA) study is a population-based study aimed to evaluate contributors of healthy aging in the older population residing predominantly in the Baltimore-Washington DC area (7). Starting in 1958, participants are examined every one to four years depending on their age. Currently there are approximately 1100 active participants enrolled in the study. A resting 12-lead ECG was performed on all participants (8). Blood samples were collected for DNA extraction, and genome-wide genotyping was completed for 1231 subjects. After exclusions, phenotype and genotype data was available

from 153 self-identified African American subjects. The BLSA has continuing approval from the Institutional Review Board (IRB) of Medstar Research Institute.

BHS. The Bogalusa Heart Study (BHS) began in 1973 as a long term study of the early natural history of cardiovascular disease in a semirural parish of Bogalusa, Louisiana. Between 1973 and 2008, 9 cross-sectional surveys of children aged 4-17 years and 10 cross-sectional surveys of adults aged 18-48 years, who had been previously examined as children, were conducted for CVD risk factor examinations in Bogalusa, Louisiana (9). In the ongoing Longitudinal Aging Study funded by NIH and NIA since 2000, there were 1,202 subjects who have been examined 4-14 times from childhood to adulthood and had DNA available for GWA genotyping. A standard resting, 12 lead electrocardiogram was performed on all participants. After exclusions, phenotype and genotype data was available from 148 self-identified African American subjects.

ECG recordings

Ten-second, resting, standard 12-lead electrocardiograms were recorded using the Marquette MAC PC (ARIC, JHS, CHS, BHS, WHI, Health ABC), MAC6 (CFS), MAC1200 (MESA), MAC5000 (BLSA), and MAC5500 (HANDLS) (GE Healthcare, Milwaukee, WI, USA). QRS duration was measured electronically using the Marquette 12SL algorithm (ARIC, CFS, MESA, BHS, BLSA, CHS, WHI, Health ABC, and HANDLS) and the MC MEANS algorithm (JHS).

Genotyping, imputation, quality control, and association analysis

CARe. Genotyping and imputation methods and the quality control steps for ARIC, JHS, MESA, and CFS have been previously described and are summarized in Table S1 (10). ARIC,

JHS, MESA, and CFS were genotyped as part of the Candidate gene Association Resource (CARE) (10, 11).

WHI. Sample selection and genotyping: 8515 self-identified African American and 3642 self-identified Hispanic subjects from WHI, who had consented to genetic research were selected for WHI SHARe (n=12157). DNA was extracted by the Specimen Processing Laboratory at the Fred Hutchinson Cancer research Center (FHCRC) using specimens that were collected at the time of enrollment of the subjects in WHI. Specimens were stored at -80C degrees. Genotyping was done at Affymetrix Inc. on the Affymetrix 6.0 array, using 2 ug DNA at a concentration of 100 ng/ul. 2% (238) additional samples were genotyped as blind duplicates.

Genotype cleaning: When needed, multiple attempts were made to genotype samples. Approximately 1% of samples could not be genotyped (n=99). We first removed samples that had call rates below 95% (n=16), that were duplicates of subjects other than monozygotic twins (n=34), or that had a Y-chromosome (n=1). SNPs that were located on the Y chromosome or were Affymetrix QC probes (not intended for analysis) were excluded (n=3280). We also flagged SNPs that had call rates (calculated separately for African Americans and Hispanics) below 95% and concordance rates below 98%, leaving us 871,309 unflagged SNPs. We were left with 12,008 unique subjects (8421 African Americans and 3587 Hispanics), with an average call rate of 99.8% over the unflagged SNPs. We analyzed 188 pairs of blind duplicate samples. The overall concordance rate was 99.8% (range 94.5-100% over samples, 98.3%-100% over samples with call rate >98%, 98.1-100%% over unflagged SNPs).

Relatedness: We computed IBD coefficients between all pairs of 12,008 subjects using a random subset of 100,000 SNPs from autosomal chromosomes using the method of moments

approach to a three parameter identity-by-descent model (12). Based on these coefficients we identified pairs of parent-offspring (22 pairs and two trios), monozygotic twins (five pairs) and siblings (192 pairs and five trios). A more thorough confirmatory analysis using a pairwise kinship coefficient estimator (13) as well as the aforementioned method of moments approach was performed separately for African Americans and Hispanics that validated these relationships and identified half-siblings (73 pairs). In most analyses, we only include one of each pairs of relatives, typically the one with the largest call rate.

Admixture and local ancestry: Separately for the African-Americans and the Hispanics we computed eigenvectors using Eigenstrat at 178,101 markers that were in common between our samples and the reference panels and we determined the individual ancestral percentages using Frappe (14) at 656,852 autosomal markers. For both of these calculations we included 475 publically available samples from ancestral populations (YRI, CEU, HGDP East Asian and Native Americans). The Frappe estimates and eigenvectors were concordant. Based on the Frappe estimates, we identified 56 subjects who were self-identified as African American, but who appeared to have less than 10% African ancestry. We also flagged one participant with questionable estimates of both ancestry and relatedness. Since we cannot exclude the possibility of either a sample mishandling or a data entry error, we flagged these 57 samples for exclusion. There were a number of other subjects who identified as African American, but appeared admixed with Native American or Asian ancestry, who are considered in our analyses. Analyses were adjusted for the first four principal components of the African, Native American and East Asian components of the Frappe estimates. Local ancestry was estimated using SABRE (15)

Imputation: Imputation for African Americans was carried out using MACH (16). 829,370 genotyped SNPs were used for imputation. We used Hapmap 2, release 22, 240 phased

haplotypes for CEU and YRI as the reference panel, with 2,203,609 SNPs. We estimated parameters on a subset of 200 WHI subjects, and then imputed all African American subjects. For 2,190,779 SNPs we obtained imputations with minor allele frequency >1% and estimated R-squared >0.3. On a small test sample (2% of the markers on three chromosomes), the average R-squared was 0.88, with an allelic discordance rate of 2.3%.

PAGE MetaboChip. Samples were genotyped using the MetaboChip according to the manufacturer's protocol (Illumina, San Diego, CA, USA). The MetaboChip is a high-density custom content BeadChip array of 196,725 SNPs, which includes densely spaced SNP markers at genome-wide significant loci for cardio-metabolic and anthropometric traits, as well as additional genetic variants to capture ancestral diversity (17). Genotyping quality control, including sample and SNP call rates, and Hardy-Weinberg equilibrium tests have been reported previously (18) and imputation details have been described (19).

Health ABC. Genomic DNA was extracted from buffy coat collected using PUREGENE® DNA Purification Kit during the baseline exam. Genotyping was performed by the Center for Inherited Disease Research (CIDR) using the Illumina Human1M-Duo BeadChip system. Illumina BeadStudio was used to call genotypes. Samples were excluded from the dataset for the reasons of sample failure, genotypic sex mismatch, and first-degree relative of an included individual based on genotype data. Genotyping was successful for 1,151,215 SNPs in 1139 unrelated African Americans.

Principal component analysis (PCA) was performed using Eigenstrat (20). PCA was first performed on genotype data from all Health ABC participants and HapMap samples as anchor points to identify population outliers. PCA was then performed on genotype data from African

American participants that were not genetic outliers, and the resulting eigenvectors were used as covariates in regression models to adjust for population structure. For African Americans, 1,007,948 SNPs with minor allele frequency $\geq 1\%$, call rate $\geq 97\%$ and HWE $P \geq 10^{-6}$ were used for imputation. Imputation was performed for all autosomes using MACH software version 1.0.16. A 1:1 mixture of CEU:YRI HapMap phase II release 22 build 36 phased haplotypes were used as reference panels for imputation. Global ancestry was estimated using STRUCTURE with ancestry informative markers (AIMs) as previously described (21). Local ancestry was estimated using LAMP (22).

HANDLS. 1024 participants were successfully genotyped to 907,763 SNPS at the equivalent of Illumina 1M SNP coverage (709 samples using Illumina 1M and 1Mduo arrays, the remainder using a combination of 550K, 370K, 510S and 240S to equate the million SNP level of coverage), passing inclusion criteria into the genetic component of the study. Initial inclusion criteria for genetic data in HANDLS includes concordance between self reported sex and sex estimated from X chromosome heterogeneity, $> 95\%$ call rate per participant (across all equivalent arrays), concordance between self-reported African ancestry and ancestry confirmed by analyses of genotyped SNPs, and no cryptic relatedness to any other samples at a level of proportional sharing of genotypes $> 12.5\%$ (effectively excluding 1st cousins and closer relatives from the set of probands used in analyses). In addition, SNPs were filtered for HWE P-value $> 10^{-7}$, missing by haplotype P-values $> 10^{-7}$, minor allele frequency > 0.01 , and call rate $> 95\%$. Basic genotype quality control and data management was conducted using PLINKv1.06 (12). Cryptic relatedness was estimated via pairwise identity by descent analyses in PLINK and confirmed using RELPAIR (23).

Ancestry estimates were assessed using both STRUCTUREv2.3 (24-26) and the multidimensional scaling (MDS) function in PLINKv1.06. In the multidimensional scaling analysis, HANDLS participants were clustered with data made available from HapMap Phase 3 for the YRI, ASW, CEU, TSI, JPT and CHB populations, using a set of 36,892 linkage-disequilibrium pruned SNPs common to each population. This set of SNPs was chosen as they are not in $r^2 > 0.20$ with another SNP in overlapping sliding windows of 100 SNPs in the ASW samples. HANDLS participants with component vector estimates consistent with the HapMap ASW samples for the first 4 component vectors were included. In addition, the 1024 quality controlled HANDLS samples were later clustered among themselves using MDS to generate 10 component vectors estimating internal population structure within the HANDLS study. Of the SNPs utilized for MDS clustering, the 2000 SNPs with the most divergent allele frequency estimates between African populations (frequency estimates based on YRI samples) and European populations (frequency estimates based on combined CEU and TSI samples) were utilized as AIMs. These 2000 AIMs were associated with frequency differences on the level of P-values $< 1 \times 10^{-3}$ based on chi-squared tests. A two population model in STRUCTURE was used to estimate percent African and percent European ancestry in the HANDLS samples, for a 10,000 iteration burn-in period, and a 10,000 iteration follow-up of the Markov Chain Monte Carlo model utilized by STRUCTURE. The ancestry estimates from STRUCTURE were highly concordant with the first component vector of the MDS clustering of HANDLS samples, with an r^2 of > 0.82 .

HANDLS participant genotypes were imputed using MACH v1.0.16 (16) based on combined haplotype data for HapMap Phase 2 YRI and CEU samples including SNPs that are monomorphic in either of the reference populations. This process followed two stages, first

estimating recombination and crossover events in a random sample of 200 participants, then based on this data and the reference haplotypes, 200 iterations of the maximum likelihood model were used to estimate genotype dosages for imputed SNPs.

CHS. Genotyping was performed at the General Clinical Research Center's Phenotyping/Genotyping Laboratory at Cedars-Sinai Medical Center using the Illumina HumanOmni1-Quad_v1 BeadChip system. Genotypes were called using the Illumina GenomeStudio software.

Participants were excluded if they had a call rate $\leq 95\%$ or if their genotype was discordant with known sex or prior genotyping (to identify possible sample swaps). Genotyping was attempted in 844 participants, and was successful in 823 persons; the latter constitute the CHS sample for this study. In addition to p10 GC scores of 0.66-0.72, successful samples exhibited greater than 98% call rate, with less than 1% "No Calls" (number of SNPs that were not able to be successfully genotyped per sample). The average p10 GC and average call rate across all samples that genotyped successfully was 0.71 and 99.78%, respectively. A small number of samples were whole genome amplified and performed less optimally than non-amplified samples, with an average p10 GC of 0.69 and average call rate of 99.08%. There was greater than 99.9% concordance rate for nine samples run in duplicate.

SNPs with call frequency < 0.9 were manually re-clustered (approximately 1100 SNPs). 420 of these SNPs were poor performing and could not be optimally clustered and thus were zeroed out. The following SNP exclusions were applied to identify a final set of 963,248 SNPs: call rate $< 97\%$, HWE $P < 10^{-5}$, > 1 duplicate error or Mendelian inconsistency (for reference CEPH trios), and the absence of heterozygotes.

Imputation was performed using BEAGLE version 3.2.1 using the default value of 10 iterations. Imputation was performed in a two-step process. The data were imputed to Hapmap Phase III using reference panels from the ASW, YRI and CEU population. The data was then separately imputed using Hapmap Phase II using the reference panels from the YRI and CEU populations. For each imputation, the observed data was subsetted to only include markers present in the Hapmap reference panel that was used in the imputation. The resulting two sets of imputed data were merged. If a marker was imputed in both the Phase II and Phase III data, the Phase III data was used. Directly-genotyped SNPs that were in the Hapmap samples were not overwritten, but any missing data for a genotyped SNP was filled-in using imputation.

Based on 97,404 genotyped SNPs from the Illumina Omni 1M chip (approximately every 10th SNP on the array), we computed principal components to adjust for admixture among the African-American participants. The first ten components were used in GWAS of African-Americans.

BHS. 1,202 BHS samples were genotyped using the Illumina Human610 Genotyping BeadChip and HumanCVD BeadChip. Genotypes were called using a clustering algorithm in Illumina's BeadStudio software. Three samples on the 610 array gave poor results (call rates <99%) and were discarded from the study. In addition, 3 samples had a different estimated gender from genotype data versus gender provided with the phenotype data and were also discarded. We analyzed the subset of individuals that were unrelated by genotype comparison ($PI_HAT < 0.10$) and had phenotype and covariate information. SNPs with call rates <90% were discarded, and SNPs with call rates between 90-95% or cluster separation score < 0.3 were manually inspected and cluster positions were edited if needed. We removed approximately 30,000 SNP loci (4.9%) due to poor performance. The final average sample call rate was

99.95% for the 610 BeadChip, and 99.32% for the CVD BeadChip. We assessed reproducibility by genotyping 29 samples in duplicate (18 known replicates, 11 blind replicates), and observed >99.99% identical genotype calls on both BeadChips. Finally we observed 99.98% genotype concordance in 12,581 overlapping SNPs between the 610 and CVD BeadChips. Individuals were compared to HapMap3 and verified to be of African-American ancestry based on MDS clustering as carried out using PLINK (12). Genotypes were imputed to HapMap release 22 using the combined set of CEU and YRI haplotypes with MACH v.1.0.16 (16).

BLSA. The analysis was restricted to subjects with African ancestry and each analysis was further adjusted for the top two principal components derived from an EIGENSTRAT analysis utilizing ~10,000 randomly selected SNPs from the 550K SNP panel (20). Genotyping was completed for 282 participants of African ancestry using a call rate of >98.5% without sex discrepancy based on homozygosity rates. 501,704 autosomal SNPs passed quality control (call rate >99%, MAF >1%, HWE >10⁻⁴) and were used for imputation. A 1:1 HapMap YRI:CEU (phase II, release 22) reference panel was used to impute approximately 2.5 million SNPs using MACH (16).

S1 Text References.

- 1 (1989) The Atherosclerosis Risk in Communities (ARIC) Study: design and objectives. *Am. J. Epidemiol.*, **129**, 687-702.
- 2 Redline, S., Tishler, P.V., Tosteson, T.D., Williamson, J., Kump, K., Browner, I., Ferrette, V. and Krejci, P. (1995) The familial aggregation of obstructive sleep apnea. *Am. J. Respir. Crit. Care Med.*, **151**, 682-687.
- 3 Taylor, H.A., Jr., Wilson, J.G., Jones, D.W., Sarpong, D.F., Srinivasan, A., Garrison, R.J., Nelson, C. and Wyatt, S.B. (2005) Toward resolution of cardiovascular health disparities in African Americans: design and methods of the Jackson Heart Study. *Ethn. Dis.*, **15**, S6-4-17.
- 4 Bild, D.E., Bluemke, D.A., Burke, G.L., Detrano, R., Diez Roux, A.V., Folsom, A.R., Greenland, P., Jacob, D.R., Jr., Kronmal, R., Liu, K. *et al.* (2002) Multi-ethnic study of atherosclerosis: objectives and design. *Am. J. Epidemiol.*, **156**, 871-881.
- 5 (1998) Design of the Women's Health Initiative clinical trial and observational study. The Women's Health Initiative Study Group. *Control. Clin. Trials*, **19**, 61-109.
- 6 Fried, L.P., Borhani, N.O., Enright, P., Furberg, C.D., Gardin, J.M., Kronmal, R.A., Kuller, L.H., Manolio, T.A., Mittelmark, M.B., Newman, A. *et al.* (1991) The Cardiovascular Health Study: design and rationale. *Ann. Epidemiol.*, **1**, 263-276.
- 7 Stone, J.L. and Norris, A.H. (1966) Activities and attitudes of participants in the Baltimore longitudinal study. *Journal of gerontology*, **21**, 575-580.
- 8 Josephson, R.A., Shefrin, E., Lakatta, E.G., Brant, L.J. and Fleg, J.L. (1990) Can serial exercise testing improve the prediction of coronary events in asymptomatic individuals? *Circulation*, **81**, 20-24.
- 9 Berenson, G.S. (2001) Bogalusa Heart Study: a long-term community study of a rural biracial (Black/White) population. *Am. J. Med. Sci.*, **322**, 293-300.

- 10 Lettre, G., Palmer, C.D., Young, T., Ejebe, K.G., Allayee, H., Benjamin, E.J., Bennett, F., Bowden, D.W., Chakravarti, A., Dreisbach, A. *et al.* (2011) Genome-wide association study of coronary heart disease and its risk factors in 8,090 African Americans: the NHLBI CARE Project. *PLoS Genet.*, **7**, e1001300.
- 11 Musunuru, K., Lettre, G., Young, T., Farlow, D.N., Pirruccello, J.P., Ejebe, K.G., Keating, B.J., Yang, Q., Chen, M.H., Lapchyk, N. *et al.* (2010) Candidate gene association resource (CARE): design, methods, and proof of concept. *Circ. Cardiovasc. Genet.*, **3**, 267-275.
- 12 Purcell, S., Neale, B., Todd-Brown, K., Thomas, L., Ferreira, M.A., Bender, D., Maller, J., Sklar, P., de Bakker, P.I., Daly, M.J. *et al.* (2007) PLINK: a tool set for whole-genome association and population-based linkage analyses. *Am. J. Hum. Genet.*, **81**, 559-575.
- 13 Thornton, T. and McPeck, M.S. (2010) ROADTRIPS: case-control association testing with partially or completely unknown population and pedigree structure. *Am. J. Hum. Genet.*, **86**, 172-184.
- 14 Tang, H., Peng, J., Wang, P. and Risch, N.J. (2005) Estimation of individual admixture: analytical and study design considerations. *Genet. Epidemiol.*, **28**, 289-301.
- 15 Tang, H., Coram, M., Wang, P., Zhu, X. and Risch, N. (2006) Reconstructing genetic ancestry blocks in admixed individuals. *Am. J. Hum. Genet.*, **79**, 1-12.
- 16 Li, Y., Willer, C.J., Ding, J., Scheet, P. and Abecasis, G.R. (2010) MaCH: using sequence and genotype data to estimate haplotypes and unobserved genotypes. *Genet. Epidemiol.*, **34**, 816-834.
- 17 Voight, B.F., Kang, H.M., Ding, J., Palmer, C.D., Sidore, C., Chines, P.S., Burt, N.P., Fuchsberger, C., Li, Y., Erdmann, J. *et al.* (2012) The metabochip, a custom genotyping array for

genetic studies of metabolic, cardiovascular, and anthropometric traits. *PLoS Genet.*, **8**, e1002793.

18 Buyske, S., Wu, Y., Carty, C.L., Cheng, I., Assimes, T.L., Dumitrescu, L., Hindorff, L.A., Mitchell, S., Ambite, J.L., Boerwinkle, E. *et al.* (2012) Evaluation of the metabochip genotyping array in African Americans and implications for fine mapping of GWAS-identified loci: the PAGE study. *PLoS One*, **7**, e35651.

19 Liu, E.Y., Buyske, S., Aragaki, A.K., Peters, U., Boerwinkle, E., Carlson, C., Carty, C., Crawford, D.C., Haessler, J., Hindorff, L.A. *et al.* (2012) Genotype imputation of Metabochip SNPs using a study-specific reference panel of ~4,000 haplotypes in African Americans from the Women's Health Initiative. *Genet. Epidemiol.*, **36**, 107-117.

20 Price, A.L., Patterson, N.J., Plenge, R.M., Weinblatt, M.E., Shadick, N.A. and Reich, D. (2006) Principal components analysis corrects for stratification in genome-wide association studies. *Nat. Genet.*, **38**, 904-909.

21 Nalls, M.A., Wilson, J.G., Patterson, N.J., Tandon, A., Zmuda, J.M., Huntsman, S., Garcia, M., Hu, D., Li, R., Beamer, B.A. *et al.* (2008) Admixture mapping of white cell count: genetic locus responsible for lower white blood cell count in the Health ABC and Jackson Heart studies. *Am. J. Hum. Genet.*, **82**, 81-87.

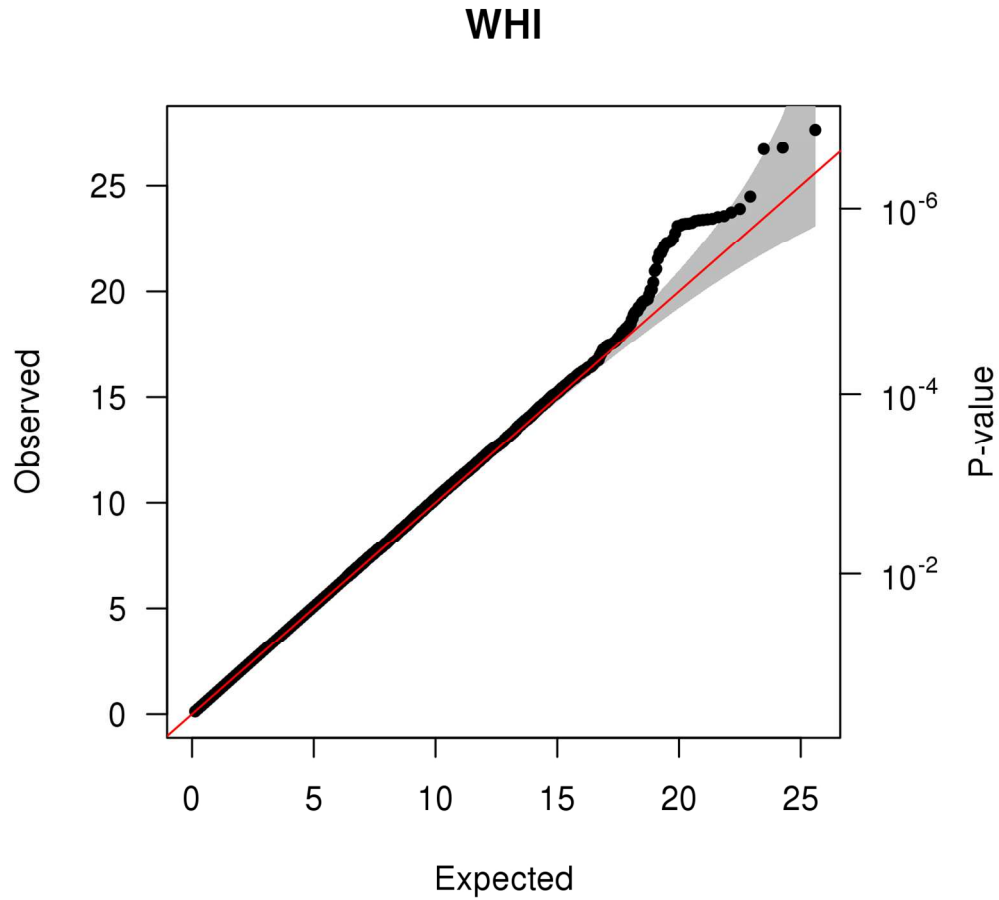
22 Pasaniuc, B., Sankararaman, S., Kimmel, G. and Halperin, E. (2009) Inference of locus-specific ancestry in closely related populations. *Bioinformatics*, **25**, i213-221.

23 Epstein, M.P., Duren, W.L. and Boehnke, M. (2000) Improved inference of relationship for pairs of individuals. *Am. J. Hum. Genet.*, **67**, 1219-1231.

24 Pritchard, J.K., Stephens, M. and Donnelly, P. (2000) Inference of population structure using multilocus genotype data. *Genetics*, **155**, 945-959.

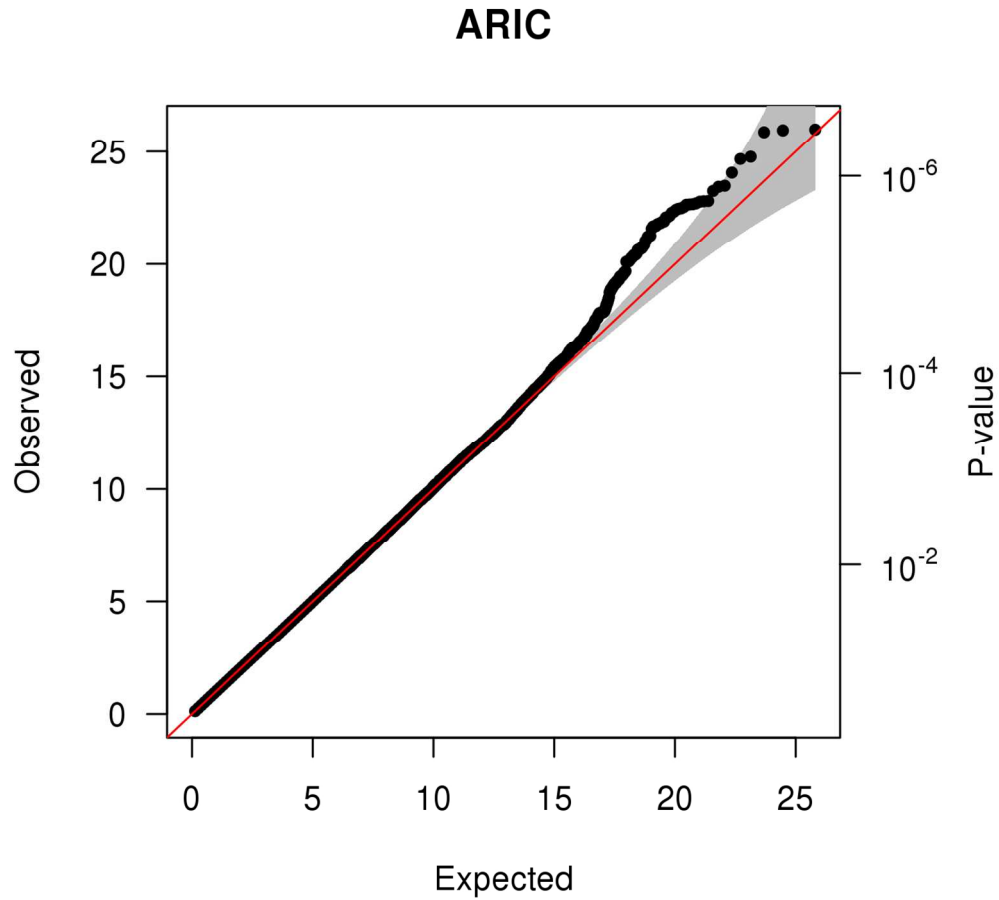
25 Falush, D., Stephens, M. and Pritchard, J.K. (2003) Inference of population structure using multilocus genotype data: linked loci and correlated allele frequencies. *Genetics*, **164**, 1567-1587.

26 Falush, D., Stephens, M. and Pritchard, J.K. (2007) Inference of population structure using multilocus genotype data: dominant markers and null alleles. *Mol. Ecol. Notes*, **7**, 574-578.



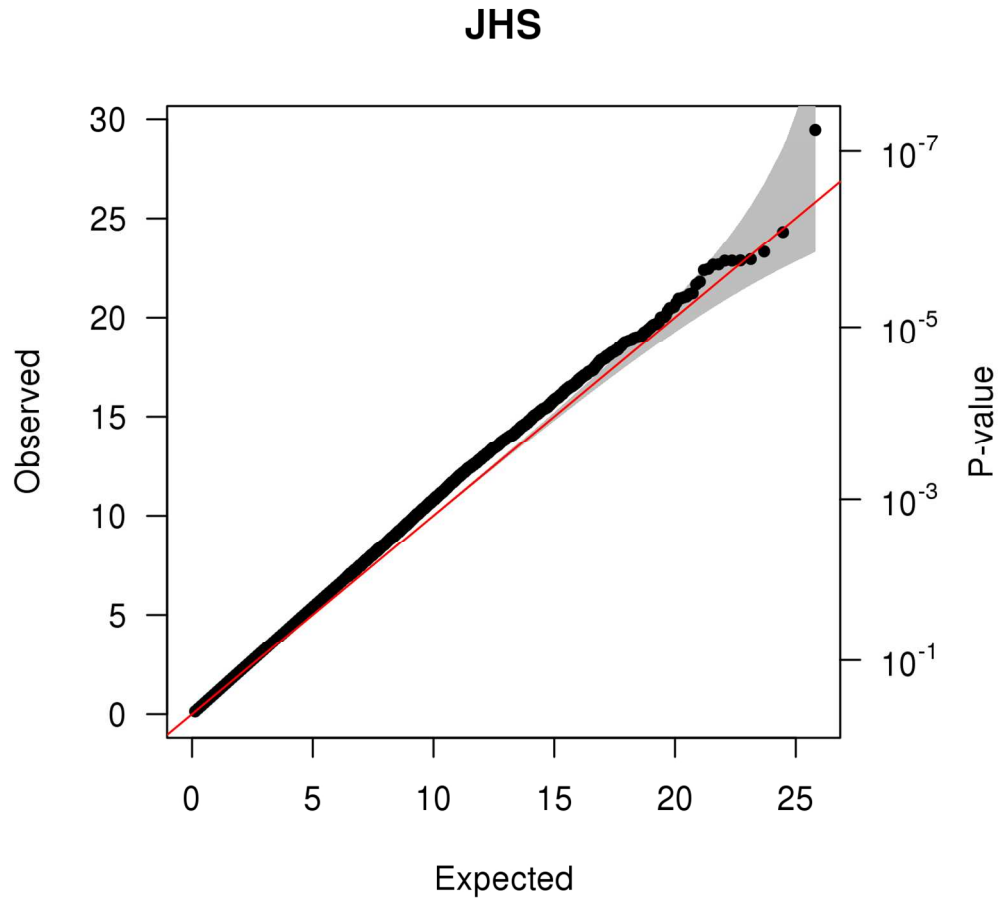
S1 Fig. QQ plot of P-values from WHI data unadjusted for genomic control. The X-axis marks the expected quantiles, the left-hand Y-axis marks the observed quantiles, and the right-hand Y-axis marks the P-values corresponding to the observed quantiles. A line originating from the origin and having a slope of 1 is shown in red. The 95% probability bounds for each order statistic are shaded in gray.

S1 Fig.
127x127mm (300 x 300 DPI)



S2 Fig. QQ plot of P-values from ARIC data unadjusted for genomic control. The X-axis marks the expected quantiles, the left-hand Y-axis marks the observed quantiles, and the right-hand Y-axis marks the P-values corresponding to the observed quantiles. A line originating from the origin and having a slope of 1 is shown in red. The 95% probability bounds for each order statistic are shaded in gray.

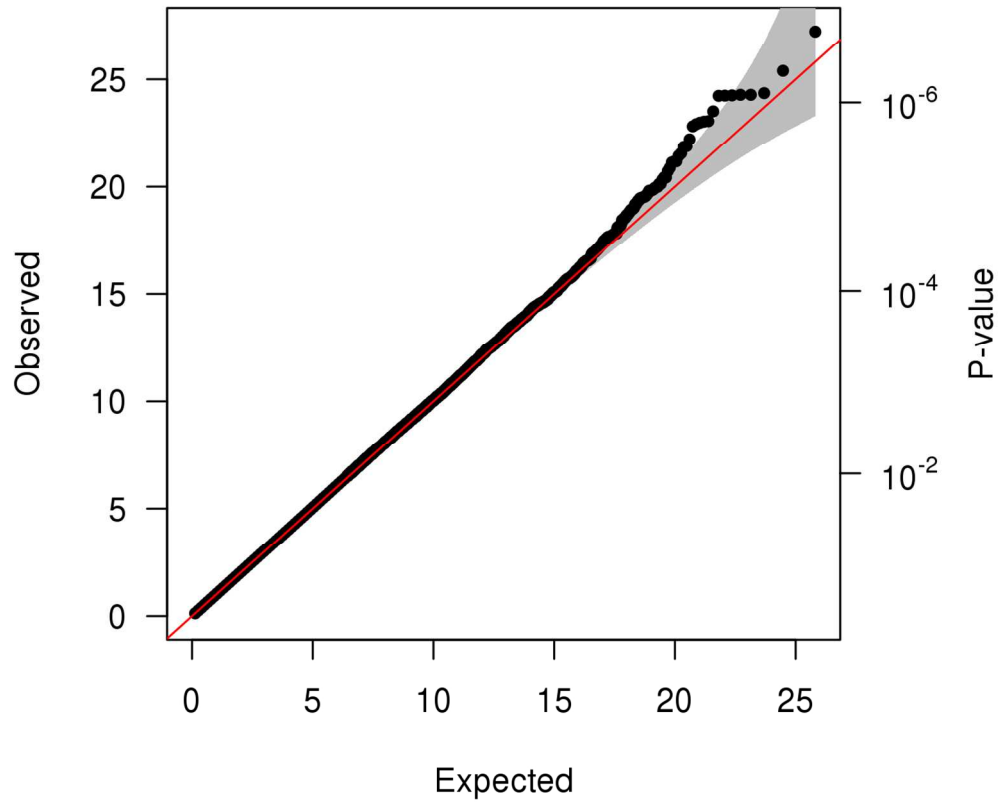
S2 Fig.
127x127mm (300 x 300 DPI)



S3 Fig. QQ plot of P-values from JHS data unadjusted for genomic control. The X-axis marks the expected quantiles, the left-hand Y-axis marks the observed quantiles, and the right-hand Y-axis marks the P-values corresponding to the observed quantiles. A line originating from the origin and having a slope of 1 is shown in red. The 95% probability bounds for each order statistic are shaded in gray.

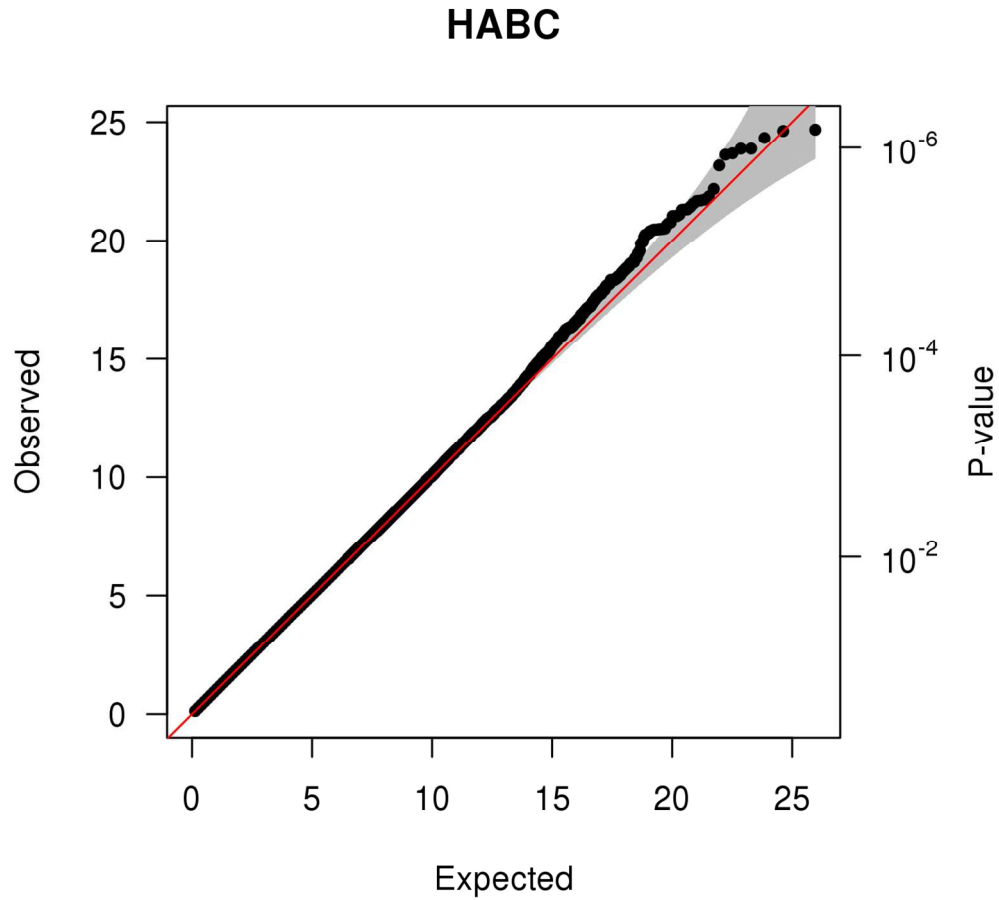
S3 Fig.
127x127mm (300 x 300 DPI)

MESA



S4 Fig. QQ plot of P-values from MESA data unadjusted for genomic control. The X-axis marks the expected quantiles, the left-hand Y-axis marks the observed quantiles, and the right-hand Y-axis marks the P-values corresponding to the observed quantiles. A line originating from the origin and having a slope of 1 is shown in red. The 95% probability bounds for each order statistic are shaded in gray.

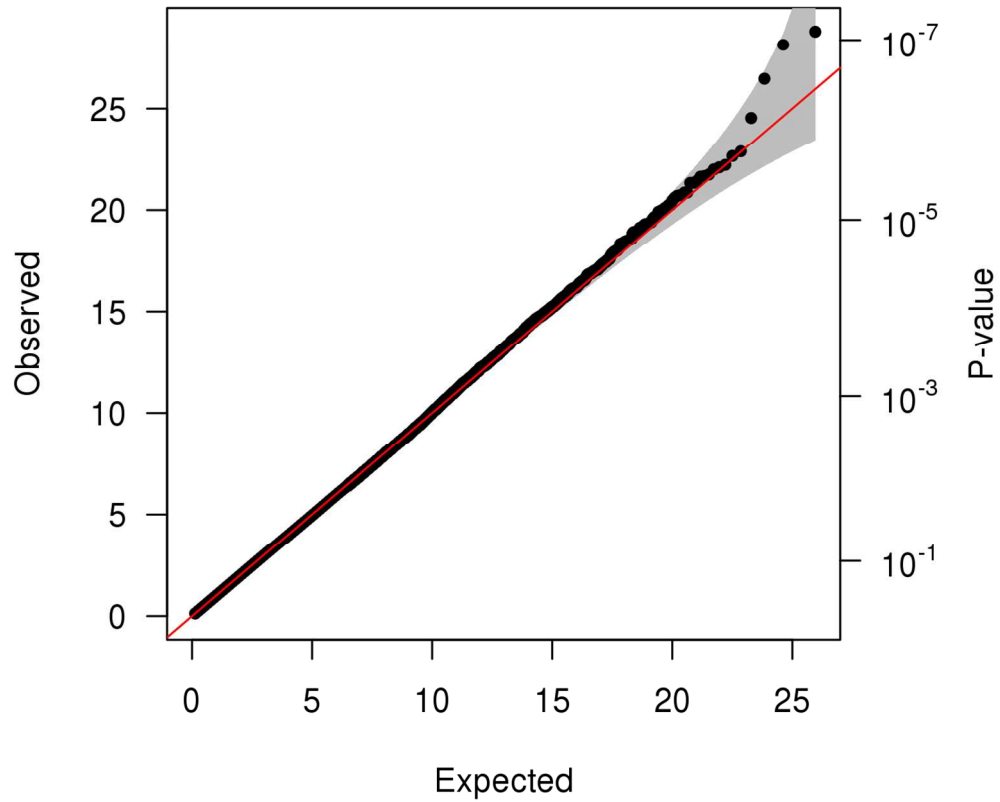
S4 Fig.
127x127mm (300 x 300 DPI)



S5 Fig. QQ plot of P-values from HABC data unadjusted for genomic control. The X-axis marks the expected quantiles, the left-hand Y-axis marks the observed quantiles, and the right-hand Y-axis marks the P-values corresponding to the observed quantiles. A line originating from the origin and having a slope of 1 is shown in red. The 95% probability bounds for each order statistic are shaded in gray.

S5 Fig.
127x127mm (300 x 300 DPI)

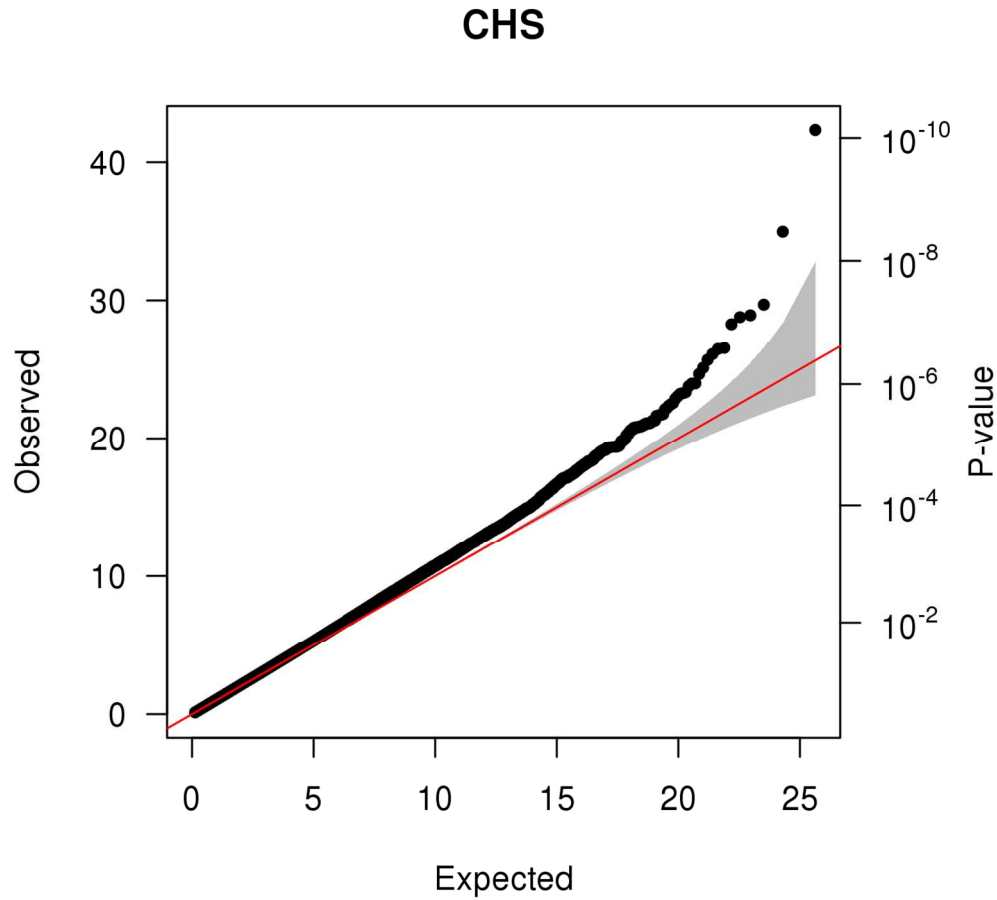
HANDLS



S6 Fig. QQ plot of P-values from HANDLS data unadjusted for genomic control. The X-axis marks the expected quantiles, the left-hand Y-axis marks the observed quantiles, and the right-hand Y-axis marks the P-values corresponding to the observed quantiles. A line originating from the origin and having a slope of 1 is shown in red. The 95% probability bounds for each order statistic are shaded in gray.

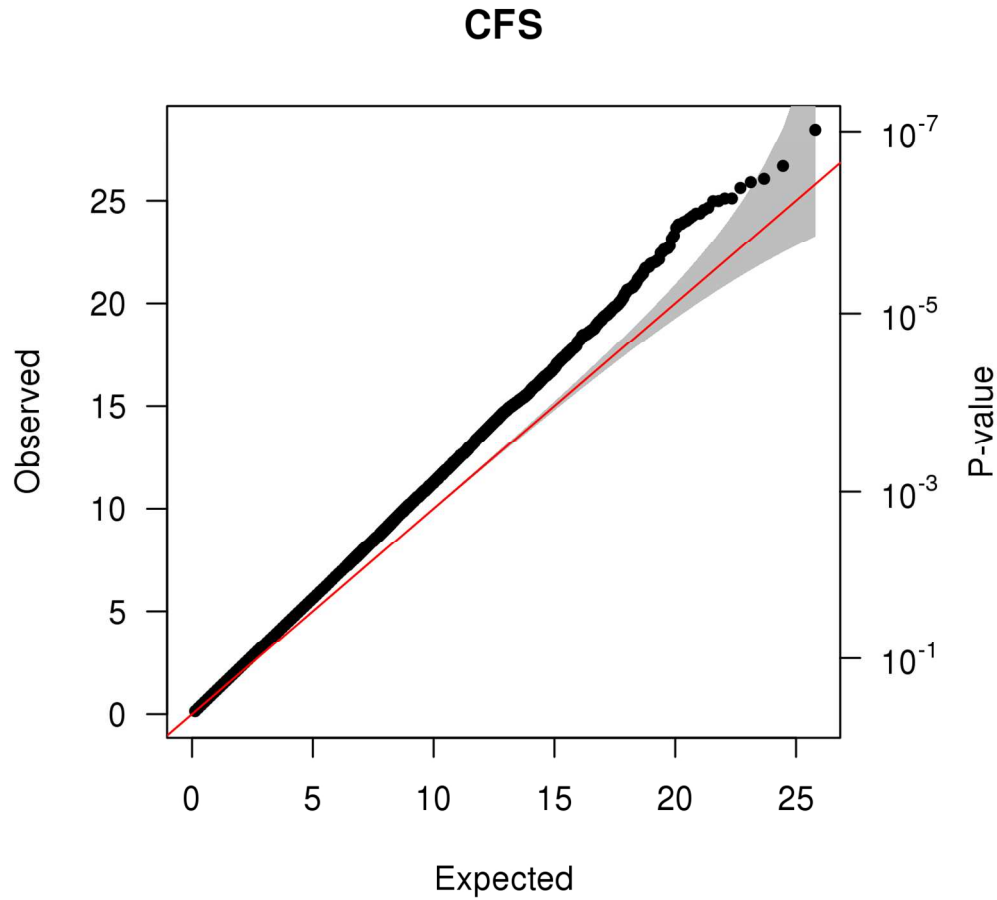
S6 Fig.

127x127mm (300 x 300 DPI)



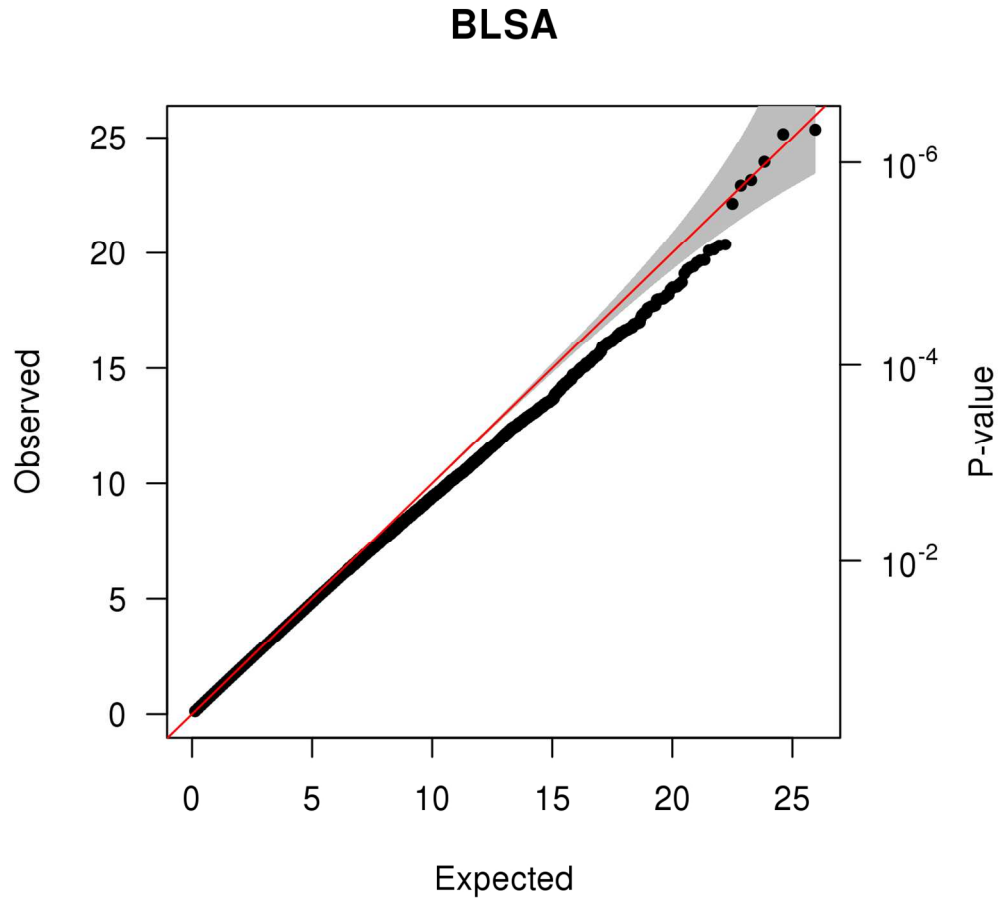
S7 Fig. QQ plot of P-values from CHS data unadjusted for genomic control. The X-axis marks the expected quantiles, the left-hand Y-axis marks the observed quantiles, and the right-hand Y-axis marks the P-values corresponding to the observed quantiles. A line originating from the origin and having a slope of 1 is shown in red. The 95% probability bounds for each order statistic are shaded in gray.

S7 Fig.
127x127mm (300 x 300 DPI)



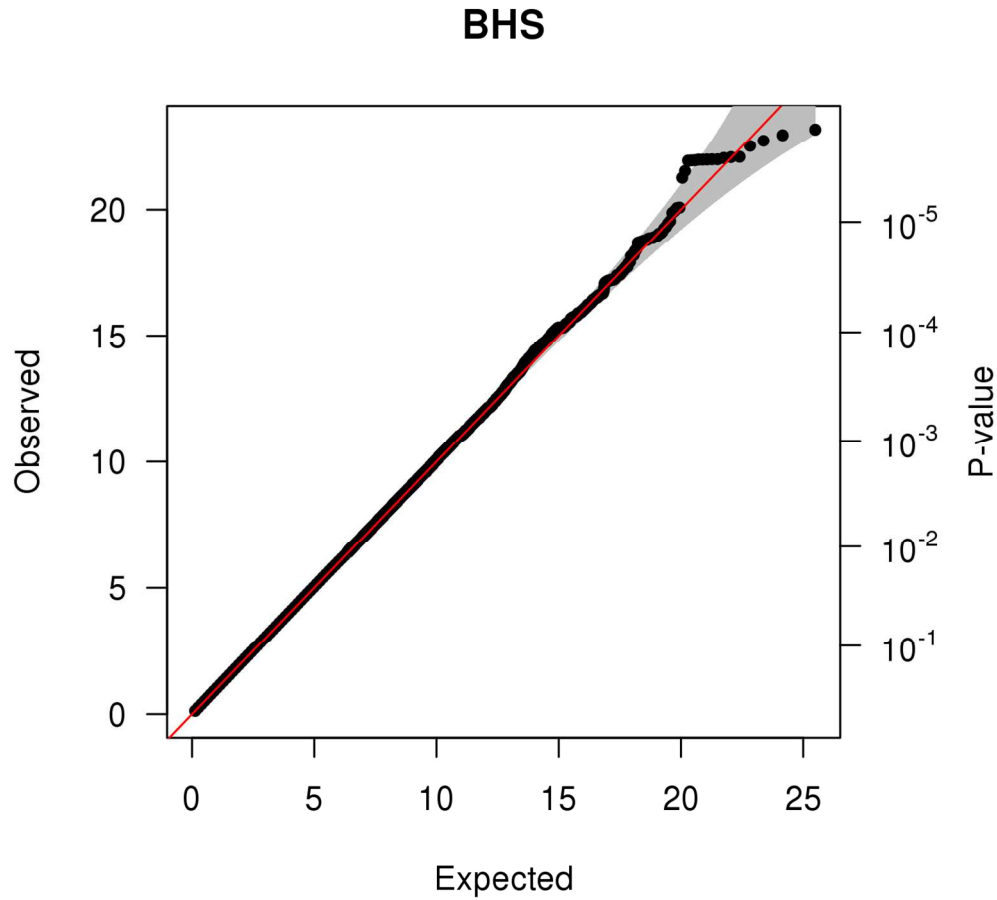
S8 Fig. QQ plot of P-values from CFS data unadjusted for genomic control. The X-axis marks the expected quantiles, the left-hand Y-axis marks the observed quantiles, and the right-hand Y-axis marks the P-values corresponding to the observed quantiles. A line originating from the origin and having a slope of 1 is shown in red. The 95% probability bounds for each order statistic are shaded in gray.

S8 Fig.
127x127mm (300 x 300 DPI)



S9 Fig. QQ plot of P-values from BLSA data unadjusted for genomic control. The X-axis marks the expected quantiles, the left-hand Y-axis marks the observed quantiles, and the right-hand Y-axis marks the P-values corresponding to the observed quantiles. A line originating from the origin and having a slope of 1 is shown in red. The 95% probability bounds for each order statistic are shaded in gray.

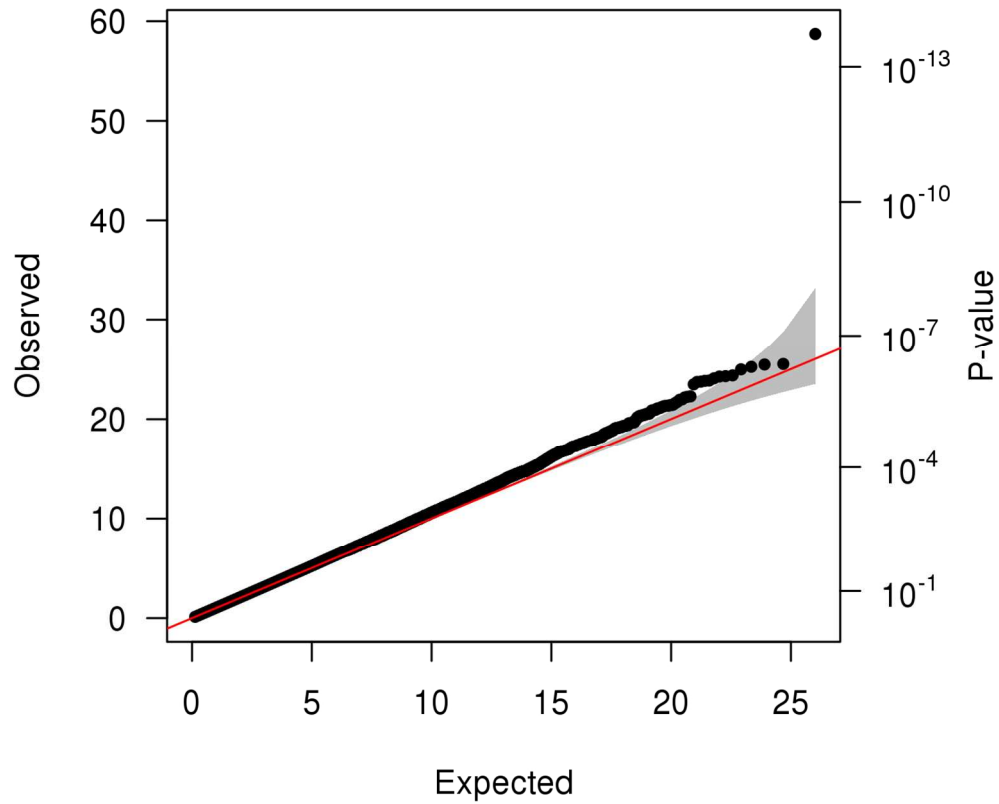
S9 Fig.
127x127mm (300 x 300 DPI)



S10 Fig. QQ plot of P-values from BHS data unadjusted for genomic control. The X-axis marks the expected quantiles, the left-hand Y-axis marks the observed quantiles, and the right-hand Y-axis marks the P-values corresponding to the observed quantiles. A line originating from the origin and having a slope of 1 is shown in red. The 95% probability bounds for each order statistic are shaded in gray.

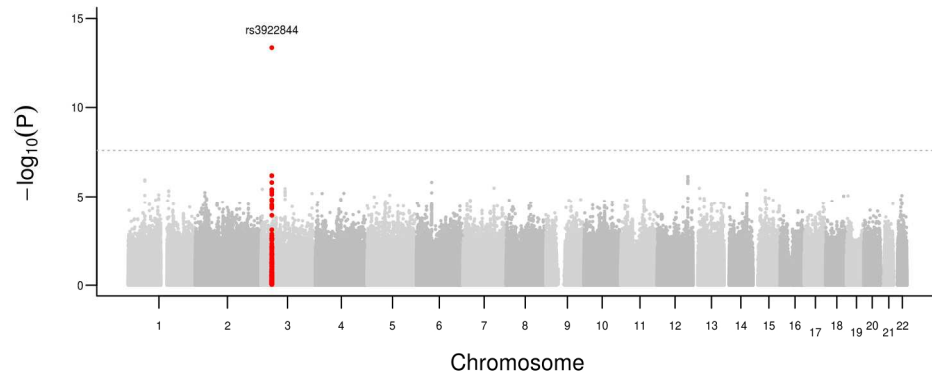
S10 Fig.
127x127mm (300 x 300 DPI)

Meta-analysis



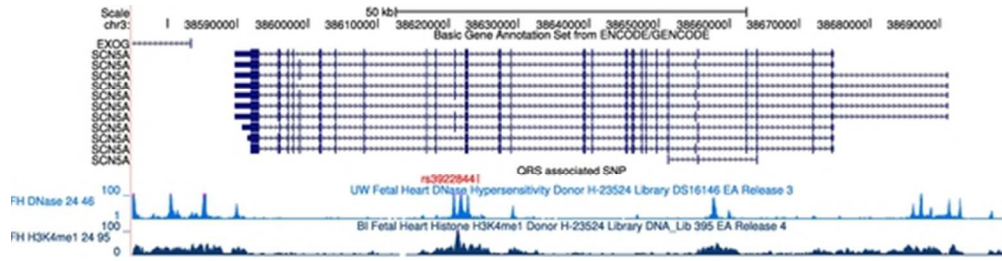
S11 Fig. QQ plot of meta-analysis P-values from African Americans. P-values adjusted for genomic control at the study level but not at the meta-analysis level. The X-axis marks the expected quantiles, the left-hand Y-axis marks the observed quantiles, and the right-hand Y-axis marks the P-values corresponding to the observed quantiles. A line originating from the origin and having a slope of 1 is shown in red. The 95% probability bounds for each order statistic are shaded in gray.

S11 Fig.
127x127mm (300 x 300 DPI)



S12 Fig. Manhattan plot of GWAS meta-analysis in African Americans. Plotted P-values are genomic control-corrected at the level of the study and the meta-analysis. Red points mark the region harboring a genome-wide significant association ($P \leq 2.5 \times 10^{-8}$). Genome-wide significant SNP ID indicated.

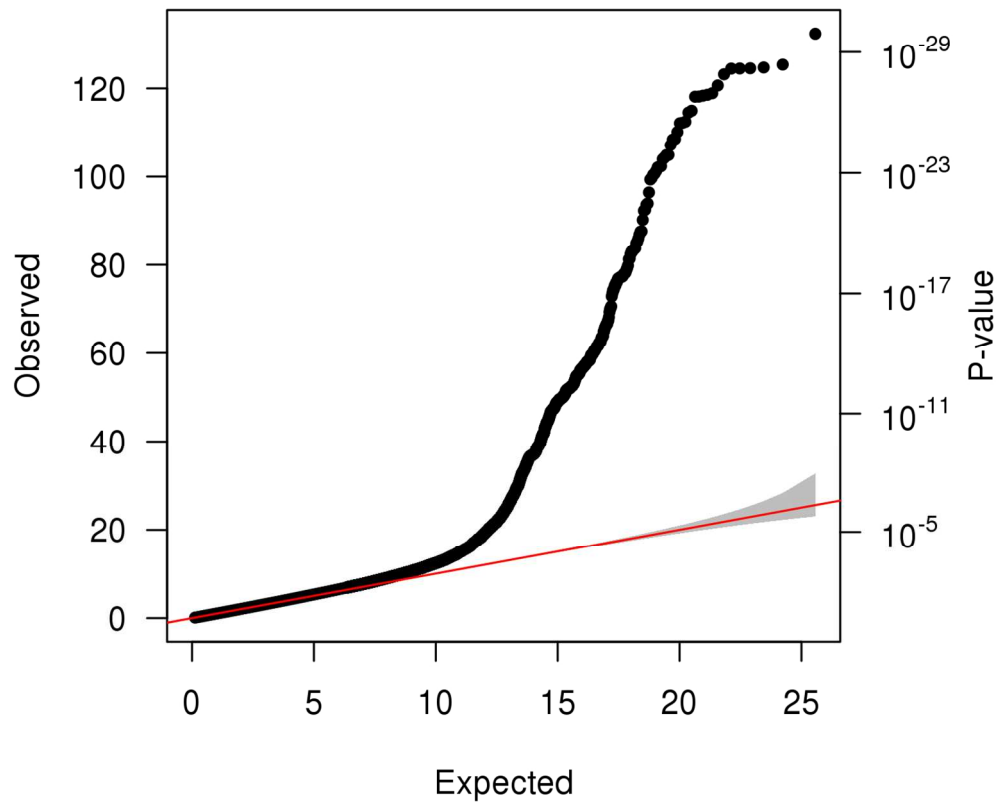
S12 Fig.
190x95mm (300 x 300 DPI)



S14 Fig. Functional annotation of SCN5A region using data from a Roadmap Epigenomics heart sample. Gene annotations from GENCODE version 7, and genomic coordinates based on hg 19. Location of rs3922844 indicated in red. DNase I hypersensitive sites (DHS) and Histone H3 Lysine 4 mono-methylation from the same male fetal heart donor (H-23524).

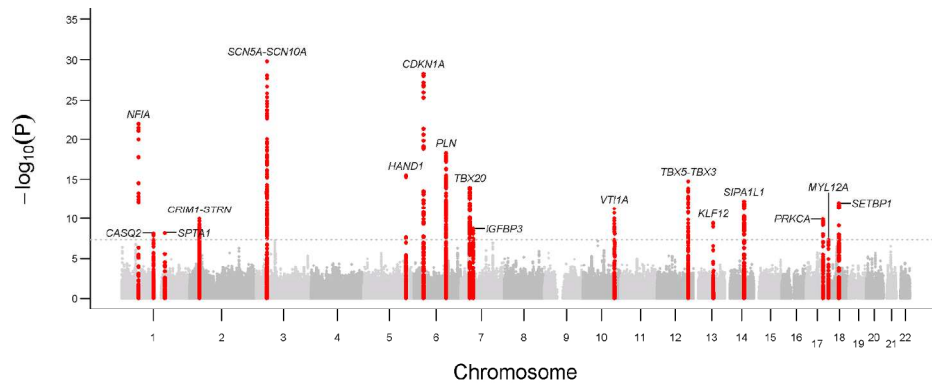
S14 Fig.
48x12mm (300 x 300 DPI)

Meta-analysis EA and AA



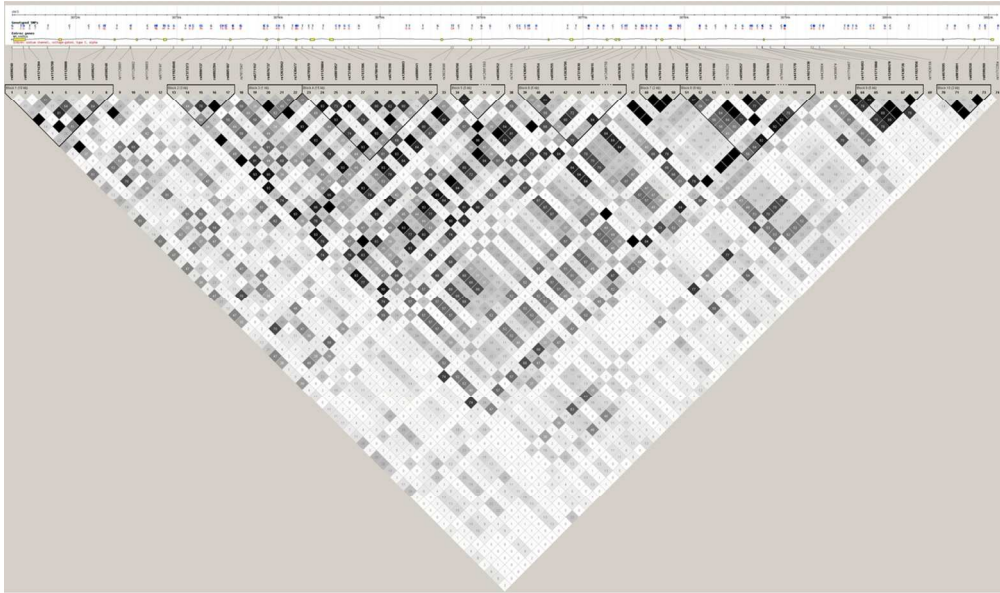
S15 Fig. QQ plot of transethnic meta-analysis P-values. P-values adjusted for genomic control at the study level but not at the meta-analysis level. The X-axis marks the expected quantiles, the left-hand Y-axis marks the observed quantiles, and the right-hand Y-axis marks the P-values corresponding to the observed quantiles. A line originating from the origin and having a slope of 1 is shown in red. The 95% probability bounds for each order statistic are shaded in gray.

S15 Fig.
127x127mm (300 x 300 DPI)

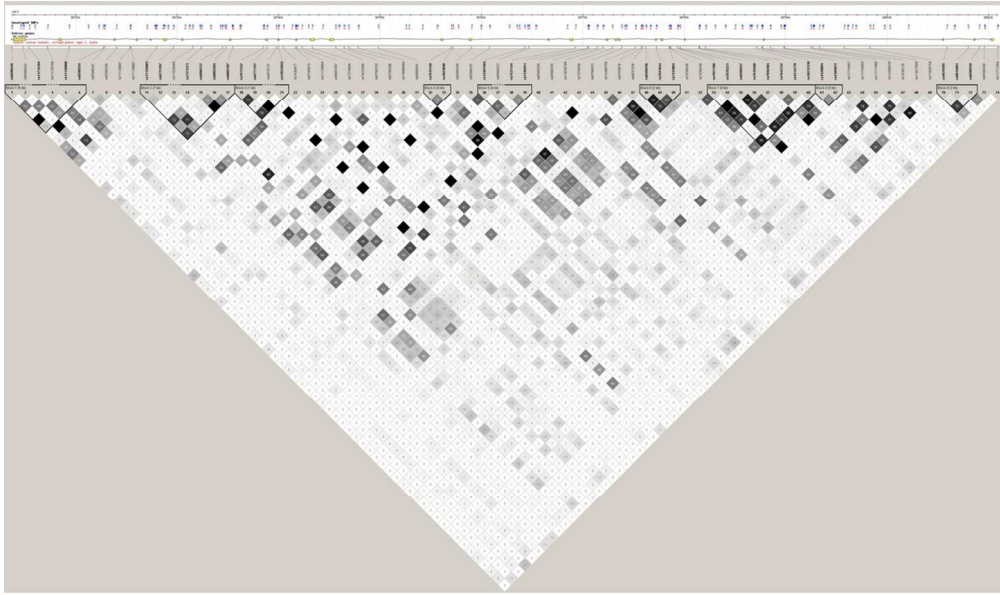


S16 Fig. Manhattan plot of transethnic meta-analysis results. Plotted P-values are double genomic control-corrected. Red points mark regions harboring genome-wide significant associations ($P \leq 5 \times 10^{-8}$). Candidate genes are indicated at each genome-wide significant locus.

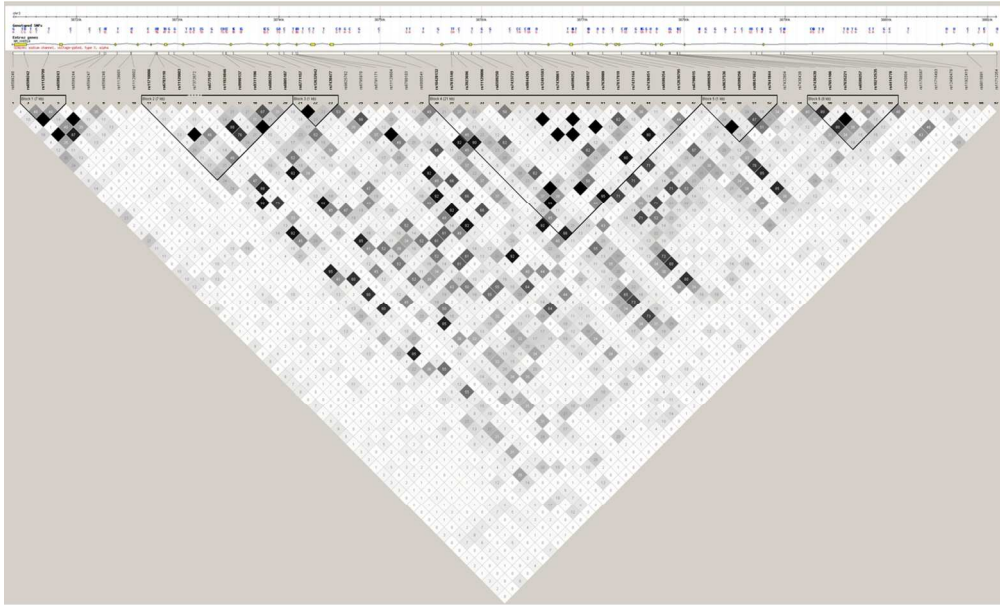
S16 Fig.
190x95mm (300 x 300 DPI)



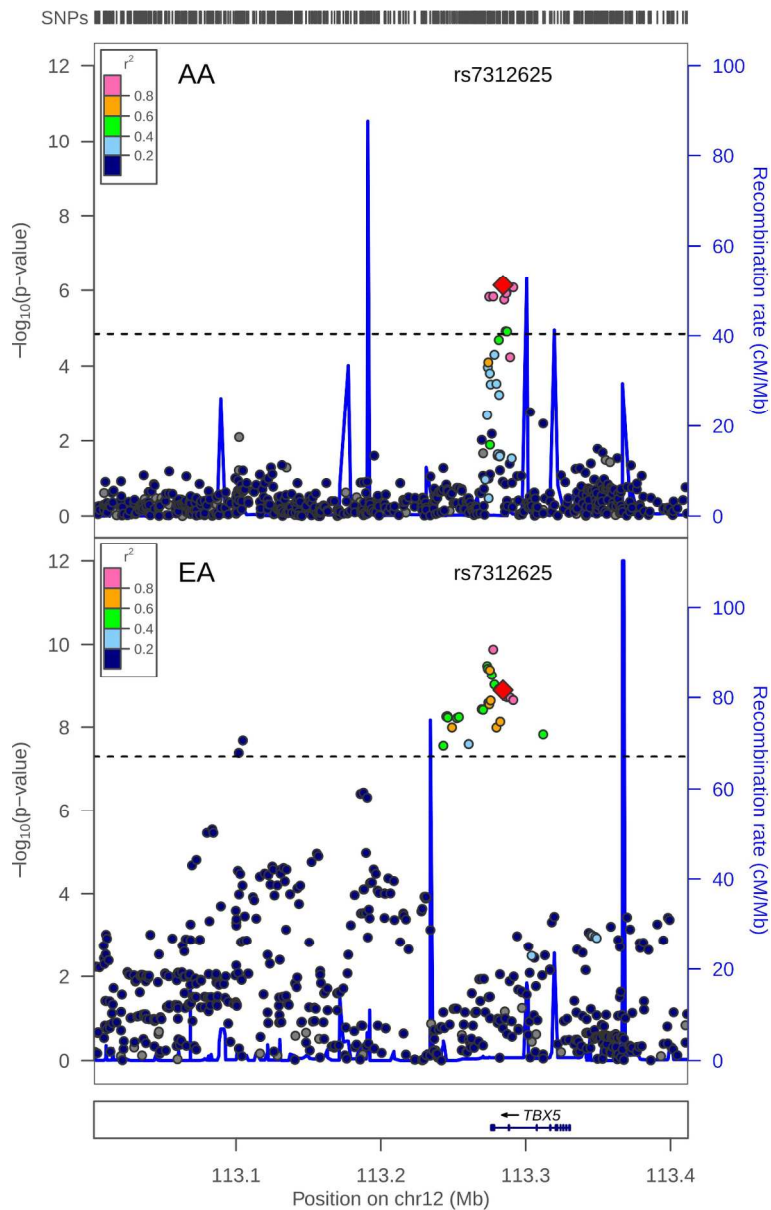
S17 Fig. LD plot of SCN10A based on HapMap phase II CEU. LD measured in r^2 is displayed.
S17 Fig.
112x66mm (300 x 300 DPI)



S18 Fig. LD plot of SCN10A based on HapMap phase II YRI. LD measured in r^2 is displayed.
S18 Fig.
112x66mm (300 x 300 DPI)



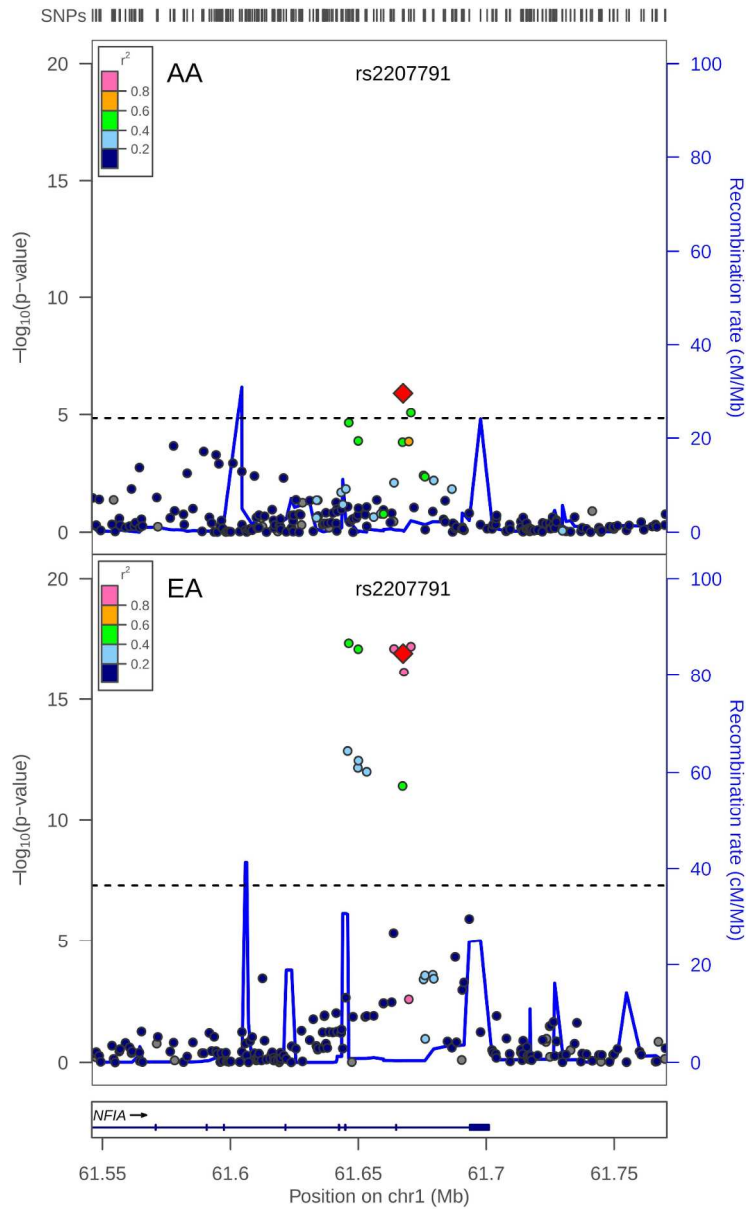
S19 Fig. LD plot of SCN10A based on HapMap phase III ASW. LD measured in r^2 is displayed.
S19 Fig.
114x69mm (300 x 300 DPI)



S20 Fig. Regional association plot at TBX5 locus. African American SNP association meta-analysis results are plotted in the top panel, and meta-analysis results from cohorts of European ancestry are plotted in the bottom panel. The AA index SNP (rs7312625) is designated by a red diamond in both panels. The LD (r^2) shown is relative to the AA index SNP and is based on HapMap YRI in the top panel and HapMap CEU in the bottom panel. Gray circles are SNPs without HapMap LD data. The X-axis marks the chromosomal position. Recombination rates estimated from African Americans and HapMap CEU individuals are shown in the top and bottom panels, respectively. The dashed horizontal line in the top panel marks the discovery significance threshold for the 22 previously discovered loci (1.4×10^{-5}) and in the bottom panel marks the GWAS significance level (5.0×10^{-8}) for European ancestry.

S20 Fig.

182x289mm (300 x 300 DPI)



S21 Fig. Regional association plot at NFIA locus. African American SNP association meta-analysis results are plotted in the top panel, and meta-analysis results from cohorts of European ancestry are plotted in the bottom panel. The AA index SNP (rs2207791) is designated by a red diamond in both panels. The LD (r^2) shown is relative to the AA index SNP and is based on HapMap YRI in the top panel and HapMap CEU in the bottom panel. Gray circles are SNPs without HapMap LD data. The X-axis marks the chromosomal position. Recombination rates estimated from African Americans and HapMap CEU individuals are shown in the top and bottom panels, respectively. The dashed horizontal line in the top panel marks the discovery significance threshold for the 22 previously discovered loci (1.4×10^{-5}) and in the bottom panel marks the GWAS significance level (5.0×10^{-8}) for European ancestry.

S21 Fig.
188x308mm (300 x 300 DPI)